STUDY OF THE USE OF NON-TRACKING EARTH STATION ANTENNAS FOR COMMUNICATING TO NEAR SYNCHRONOUS SATELLITES

Prepared for

DEPARTMENT OF COMMUNICATIONS
Communications Research Centre
Shirley Bay, Ontario

by

RCA LIMITED
Government & Commercial Systems Division
Antenna Laboratories
1001 Lenoir Street
Montreal 207, Quebec.

Contract: PL.36001-2-3599, Serial No. OPL2-0118
Date: July 1973.

2

STUDY OF THE USE OF NON-TRACKING EARTH STATION ANTENNAS FOR COMMUNICATING TO NEAR SYNCHRONOUS SATELLITES

Prepared for

DEPARTMENT OF COMMUNICATIONS
Communications Research Centre
Shirley Bay, Ontario

by

RCA LIMITED
Government & Commercial Systems Division
Antenna Laboratories
1001 Lenoir Street
Montreal 207, Quebec.

Prepared by: Rezso Csongor
R. J. Csongor
1

Chun Chen Huang
C. C. Huang

Approved by: P. Foldes
P. Foldes

J. A. Stovman
J. A. Stovman, Eng.

Contract: PL.36001-2-3599, Serial No. OPL2-0118
Date: July 1973.

TABLE OF CONTENT

LIST OF FIGURES

LIST OF TABLES

1.0 INTRODUCTION

1.1 General

The present study was initiated by the Communications Research Centre of the Department of Communications and of the Department of Supply and Services. Its basic aim was to investigate the feasibility of using antennas having beams of elliptical cross-section for CTS ground communications terminals. Such antennas may be used for communications experiments without ground terminal tracking. The elliptical cross-section beam is to provide the coverage of the rectangular angular region that represents the possible locations of the CTS relative to any of the ground terminal locations.

According to the work statement, the scope of the present study was relatively limited. The investigation was restricted to theoretical analysis, survey of potentially usable type of antennas and preliminary cost study. The original statement of work was further refined as the work progressed on the basis of the close liaison between the CRC Design Authority and the study group at RCA Limited.

In the following report, the most interesting results of the study program are summarized. The report first provides an analysis of the general relationships between the various parameters of the required radiated patterns (Sec. 2). This section is aimed to understand the basic problem of area coverage for the present geometry. In the second part of the report, the problems of practical realizations are analysed for non-circular aperture paraboloids (Sec. 3), for cylindrical paraboloids (Sec. 4), and for antenna combinations using array techniques (Sec. 5). In Section 6, the possible use of the pillbox antenna is investigated.

For the two most important basic types of realization described in Sections 3 and 4, full mathematical treatment is presented as the base of an RCA developed vector field computer program. Patterns and pattern characteristics are calculated for these cases to cover the presently necessary details.

No numerical analysis is presented for the array type of antennas, however, the characteristics of these systems are discussed on the basis of the previous results or data published in the literature.

The cost and availability of the above types of antennas are only discussed briefly in Section 8. Unfortunately, the limited scope of the present program did not allow more detailed investigation of this aspect, but nevertheless, first cut cost figures were established.

1.2 Recommendations

1. Elliptically contoured parabolic reflector antennas are recommended for ground terminals in the 3 ft. to 6 ft. equivalent diameter range, unless the aspect ratios exceed about 3:1.

2. Fiberglass construction of antenna reflectors could be considered. Commercially procured circular contoured reflectors can be relatively easily cut to a different contour This would be a difficult procedure for spun metal reflectors, but their deicing is easier.

3. The larger diameter ($\gtrsim$ 4 ft.) combined with aspect ratios ($\gtrsim$ 3:1) may require multiple feed configurations and would therefore be more complex and costly. Limited tracking systems using more conventional circular antenna reflectors are also applicable (Ref.6). The choice between the two depends upon some factors beyond the scope of this report and therefore a specific recommendation is difficult to make, but in the opinion of the authors, a limited tracking system would be more cost effective, as well as minimizing usable gain from a given aperture.

4. A brief experimental program to refine the detailed feed dimensions and the antenna characteristics is recommended. Such a program would take about 3 months to perform and would cost about $25,000. (at cost). The results of this program would verify calculations and take into consideration all the practical aspects dealing with construction of a breadboard model of a 3 ft. equivalent diameter antenna with low aspect ratio and a 6 ft. equivalent diameter with high aspect ratio.

Tentative dimensions for selected antenna sizes are given in Tables 7.1 and 7.2.

2.0 CONSIDERATIONS OF BEAM PARAMETERS

2.1 Relationship of the Required Coverage Area and the Beam Parameters of Circular Paraboloids

In the following, some basic considerations will be presented with respect to the selection of the principal antenna beam characteristics. The coverage of the angular area will be any possible location of the Communications Technology Satellite (CTS) and any earth station location considered in connection with the planned communications experiments.

Coverage of the slightly moving satellite is to be achieved by a stationary beam.

The coverage area or satellite motion box (MB) initially considered will correspond to a solid angle of $\alpha_1 \times \alpha_2 = 0.46^\circ \times 2.2^\circ$ (MB_1, Fig. 2.1). Following this study, consideration will be given to an MB of $\alpha_1 \times \alpha_2 = 0.46^\circ \times 1.43^\circ$. ($MB_2$, Fig. 2.2). The asymmetry of these MB's are characterized by their aspect ratio $\Omega_0 = \frac{\alpha_2}{\alpha_1}$, which for the studied cases is 4.783 and 3.109.

The antennas considered for this part of the communications experiments were originally assumed to be equivalent in terms of gain and other major electrical parameters to circular paraboloidal reflectors with diameters ranging from 2 to 6 feet. As the planning of the program progressed two major equivalent diameter ranges emerged as most suitably satisfying the systems requirements: diameters around 3 feet and around 8 feet. (Ref. 1) Assuming 55% antenna efficiency the gain, beamwidth and some other characteristics of circular paraboloids with 2, 3 and 8 ft. diameters are shown in Table 2.1.

The numbers in Table 2.1 were calculated by assuming an aperture distribution in the form (Ref. 2) of

$$f(\rho) = \bar{A} + \bar{B}\left[1 - \left(\frac{\rho}{a}\right)^2\right]^P \qquad (1)$$

where ρ is the radial coordinate in the aperture and $\rho_{max} = a$.

With A = 0.3 and P = 2 the above formula results in a 10 db taper at the edge of the reflector. The corresponding 3 db beamwidth is

$$\Theta_3 = 1.172\,\frac{\lambda}{D} \quad \text{Radian} \qquad (2)$$

The 3 db contours of the beams at the receive and transmit frequencies are superimposed on the MB_1 and MB_2 contours in Figures 2.1 and 2.2. It is clear that because of the difference of shape of the cross-section of the beams and the MB's considered, the gain at the edge regions of the elongated MB's are lower than that at the edge of a ficticious circular MB having identical coverage area. On the other hand in the direction of the centre of the MB the gain is higher. The gain potential of the selected reflector areas are not fully utilized for the given MB's. Obviously with a nearly elliptical or dumpbell shaped beam

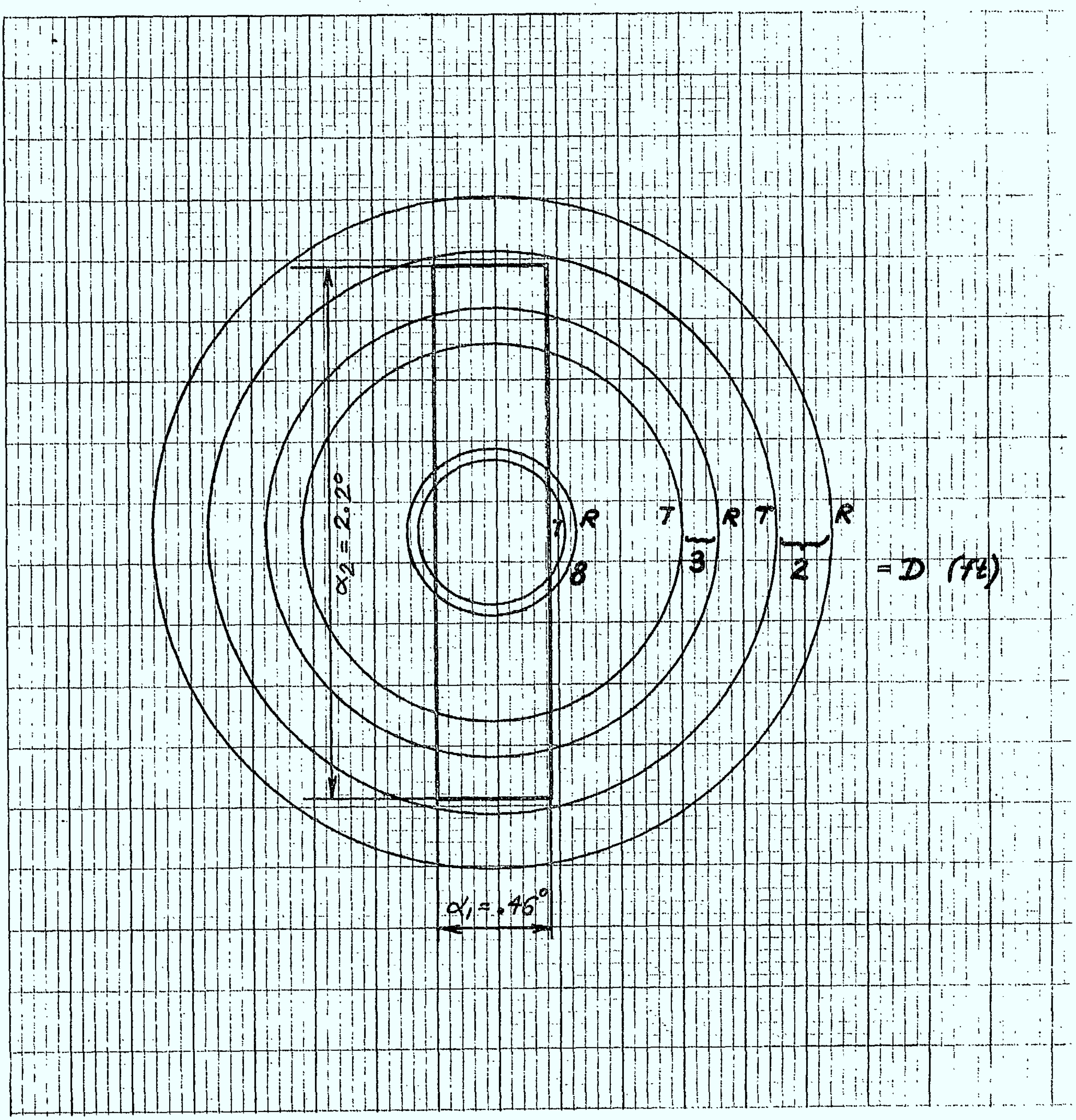

Fig. 2.1 Satellite motion box of 2.2° x .46° and 3 db contours of patterns of circular paraboloids. (Ideal sector beam gain of motion box: G_{MB_2} = 46.16 db)

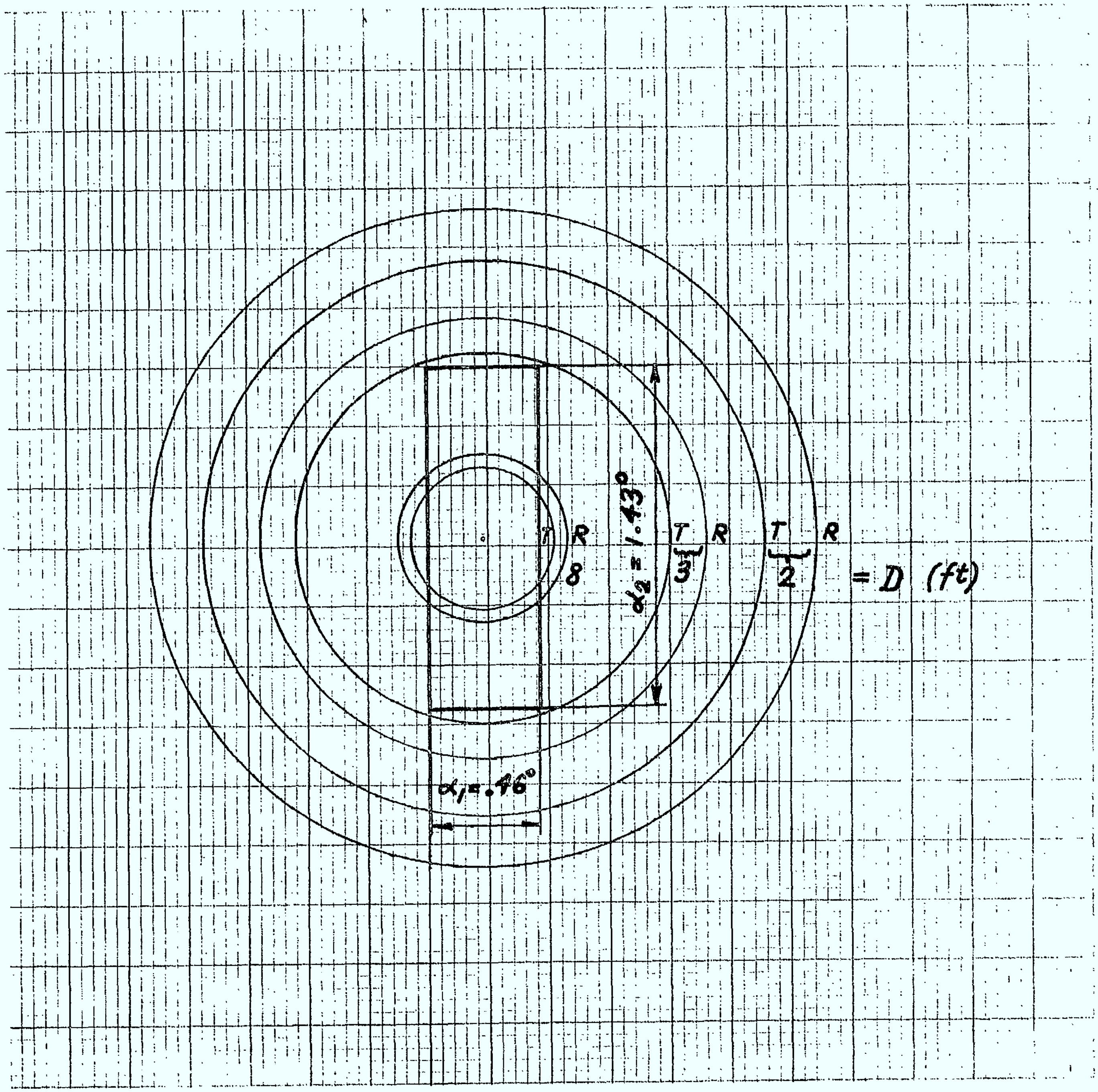

Fig. 2.2 Satellite motion box of $1.43° \times .46°$ and 3 db contour of patterns of circular paraboloids. (Ideal sector beam gain of motion box: $G_{MB_1} = 47.98$ db)

TABLE 2.1

Calculated Pattern Characteristics of a Centre Fed Circular Aperture

Beamwidth factor: 1.172
First sidelobe K_1 (db): 27.5
Aperture efficiency: 86.72%
(0.62 db)

Diameter (ft.)	Area $(ft)^2$	Frequency: 11.947 GHz (λ = 0.9886 in.) 3 db Beamwidth Θ_3^o	$G = \frac{27,000}{\Theta_3^2}$ (db)	$G_o = \pi^2 \left(\frac{D}{\lambda}\right)^2$ (db)	G_o (η = 55%)	Frequency: 14.248 GHz (λ = 0.8290 in.) 3 db Beamwidth Θ_3^o	$G = \frac{27,000}{\Theta_3^2}$ (db)	$G_o = \pi^2 \left(\frac{D}{\lambda}\right)^2$ (db)	G_o (η = 55%) (db)
2	3.14	2.77	35.46	37.65	35.05	2.32	37.00	39.18	36.58
3	7.07	1.84	39.81	41.17	38.57	1.55	40.51	42.70	40.1
8	50.3	0.69	47.54	49.69	47.09	.58	49.01	51.22	48.62

cross-section the gain over the edge of the MB could be made more uniform. The purpose of the following study in short, is to determine the parameters of such beams. Moreover, by considering the physical structure of antennas capable to produce these beams the improvements in edge gain should be evaluated in terms of the penalties suffered in size, complexity, weight, tolerance requirements, cost, difficulties of installation and operation. Thus, the selection of optimum antenna must reflect these as well as the purely technical constraints. The overall problem can be solved in two steps. First, the optimum beam cross-section for a given MB and on-axis gain can be determined, yielding the diameter of an equivalent circular paraboloid with the given gain. Second, the antenna structure that is, capable of producing the required beam can be established. In doing so part of the required beam characteristics may be traded off for increased operational simplicity and reduced costs.

To establish the effectiveness of various beam cross-sections for a given MB, a relationship must be developed between the worst case edge gain and the on-axis gain. Assuming an elliptical beam cross-section with a major axis to minor axis ratio, or beam aspect ratio of Ω_b (Figure 2.3)

$$\Omega_b = \frac{\Theta_{3B}}{\Theta_{3A}} \tag{3}$$

where Θ_{3A} and Θ_{3B} are the 3 db beamwidth values in the orthogonal planes corresponding to aperture dimensions A and B and $\Theta_{3B} \geq \Theta_{3A}$.

For an axially symmetric beam $\Omega_b = 1$. It will be also assumed that the far-field pattern of the beam (in decibels) near to its maximum may be approximated by a quadratic function of the angle. The error associated to this assumption for the presently considered 0 - 10 db range is small.

The relationship between beamwidth and aperture distribution geometry

$$\Theta^{o}_{3B} = k_B \frac{\lambda}{B} \frac{180}{\pi} \tag{4}$$

and

$$\Theta^{o}_{3A} = k_A \frac{\lambda}{A} \frac{180}{\pi} \tag{5}$$

where A and B are the major and minor dimensions of the aperture and k_A and k_B are the corresponding beamwidth factors. The value of k_A and k_B depend on the aperture field distribution. It is quite reasonable to expect that the aperture tapering would be maintained at about the same level ($\simeq$ 10 db) at least in the planes of the major and minor aperture dimensions over the range of aperture aspect ratios considered. Using the above formulas:

$$\Omega_b = \frac{k_B}{k_A} \frac{A}{B} \tag{6}$$

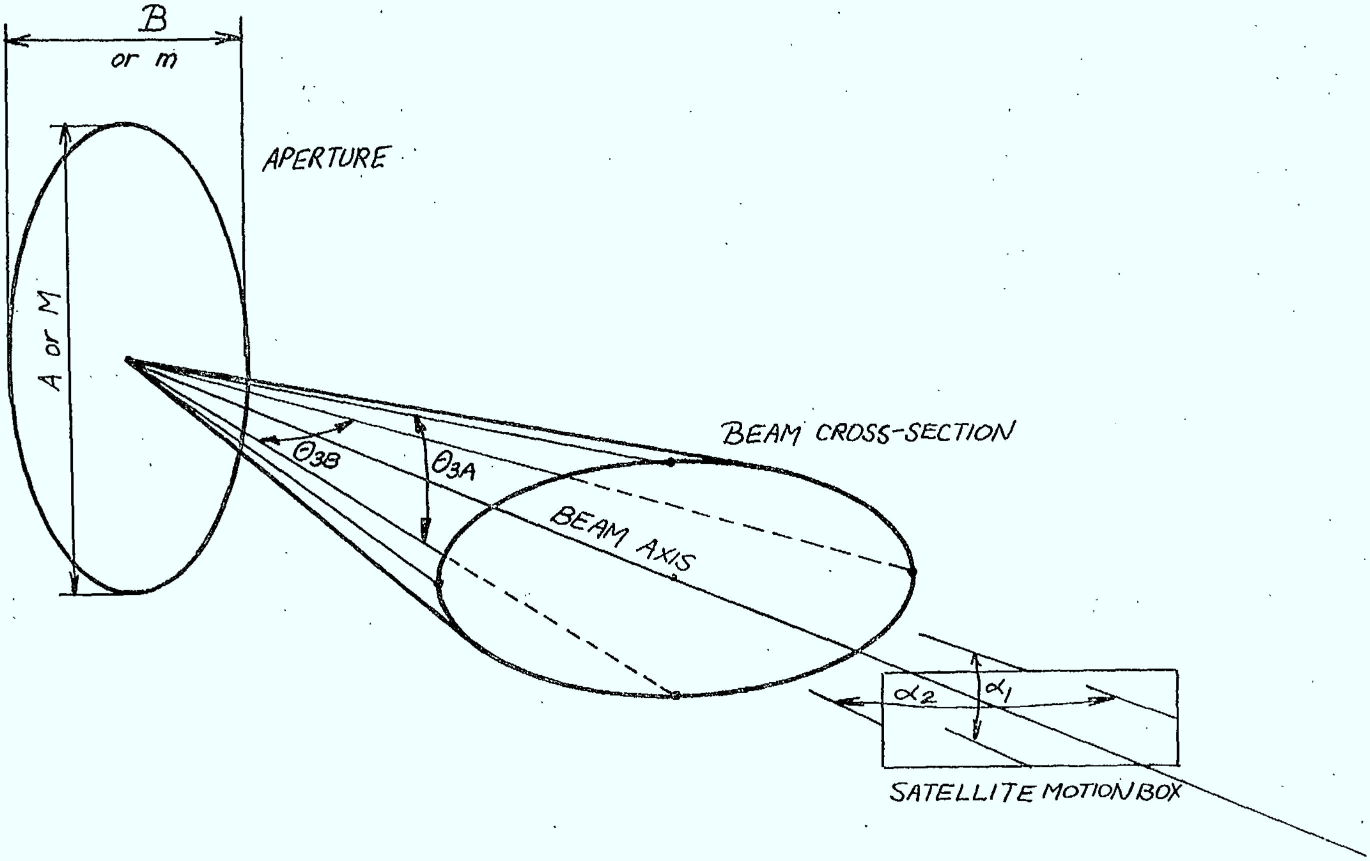

2.3 Geometry and designations of an elliptical beam.

The beamwidth factor for the assumed edge taper of about 10 db which represents a common compromise between aperture efficiency and spillover loss depends also on the shape of the aperture illumination function. This dependence however is not great. For the assumed type of aperture field distribution type the values of k for various P values and 10 db taper are

P = 1	1.2	2	2.5	3	4
k = 1.14	1.162	1.172	1.176	1.176	1.170

indicating a spread of only about 3%. The representative value of $k_A = k_B = 1.17$ may be adopted for most calculations. With this choice the aperture aspect ratio defined by and beam aspect ratio have the same numerical value

$$\Omega_a = \Omega_b \qquad (7)$$

2.2 The Edge Gain

For the assumptions stated previously, it is possible to express the worst case gain drop in MB relative to the on-axis gain. The relative gain drop at an angle $\frac{\alpha_2^o}{2}$ in the plane of the long dimension

$$\Delta G_{edge} = -3\left(\frac{\alpha_2^o}{k_B \frac{\lambda}{B} \frac{180}{\pi}}\right)^2 \quad db \qquad (8)$$

It is more convenient to express ΔG_{edge} for the case when the peak gain remains unchanged while the aperture aspect ratio is varied. This requires a constant aperture area. In order to convert (8) for more convenient use, it is better to express the minor axis of the elliptical aperture in terms of equivalent diameter D and Ω_a, i.e.,

$$D^2 = AB \qquad (9)$$

and

$$\frac{A}{B} = \Omega_a \qquad (10)$$

from which

$$B = \frac{D}{\sqrt{\Omega_a}} \qquad (11)$$

Inserting (11) into (8)

$$\Delta G_{edge} = -3\left(\frac{\alpha_2^o}{k_B \frac{\lambda}{D}\sqrt{\Omega_a}\, \frac{180}{\pi}}\right)^2 \quad db \qquad (12)$$

or

$$\Delta G_{edge} = -3\left(\frac{\alpha_2^o \pi}{180}\right)^2 \left(\frac{D}{\lambda}\right)^2 \frac{1}{k_B^2 \Omega_a} \quad db \qquad (13)$$

(12 is plotted for $\alpha_2 = 2.2^o$ in Figure 2.4 and for $\alpha_2 = 1.43^o$ in Figure 2.5. with the as parameter. The beam width factor in both cases is $k_B = 1.2$. It should be noted that along the shorter dimension of the MB characterized by α_1 a similar expression describes the edge gain. However, as long as

$$\Omega_b > \Omega_o \qquad (14)$$

the minimum edge gain will occur in the plane of the long dimension of the MB. Thus, when considering minimum edge gain one should consider only $\Omega_b < \Omega_o$ curves. For the longer of the analyzed MB $\Omega_o = \frac{2.2}{.46} = 4.783$ and for the shorter it is $\Omega_o = \frac{1.43}{.46} = 3.11$.

The actual value of the ege gain in decibels is

$$G^{db}_{edge} = G^{db}_{peak} - |\Delta G_{edge}| \qquad (15)$$

In general for an antenna efficiency of

$$G = \eta G_o$$
$$= \eta \pi^2 \frac{AB}{\lambda^2}$$

thus

$$= \eta \pi^2 (D/\lambda)^2 \qquad (16)$$

$$G^{db}_{edge} = 10 \log \eta + 10 \log \pi^2 \left(\frac{D}{\lambda}\right)^2 - 3 \left(\frac{\alpha_2^o}{180} \pi\right)^2 \left(\frac{D}{\lambda}\right)^2 \frac{1}{k_B^2 \Omega_a} \qquad (17)$$

In Figures 2.6 and 2.7, G^{db}_{edge} is plotted for $\eta = 1$ and for any value of η the corresponding efficiency value has to be subtracted. Figure 2.6 shows G^{db}_{edge} for $\alpha_2 = 2.2^o$ and Figure 2.7 for $\alpha_2 = 1.43^o$. The beamwidth factor was 1.2 and the wavelength 0.9886 in. in both cases. The parameter of the families of curves is the aperture aspect ratio Ω_a.

2.3 General Observations About the Edge Gain

2.3.1 Edge Gain Maximums

For a given satellite motion box defined for example by α_2 and α_1 and for a given aperture aspect ratio Ω_a there is a maximum edge gain value as a function of D. It may be expressed as:

$$\left(G^{db}_{edge}\right)_{max} = 10 \log \eta + 10 \log \left[3.33 \left(\frac{180}{\alpha_2^o}\right)^2 k_B^2 \Omega_a\right]$$

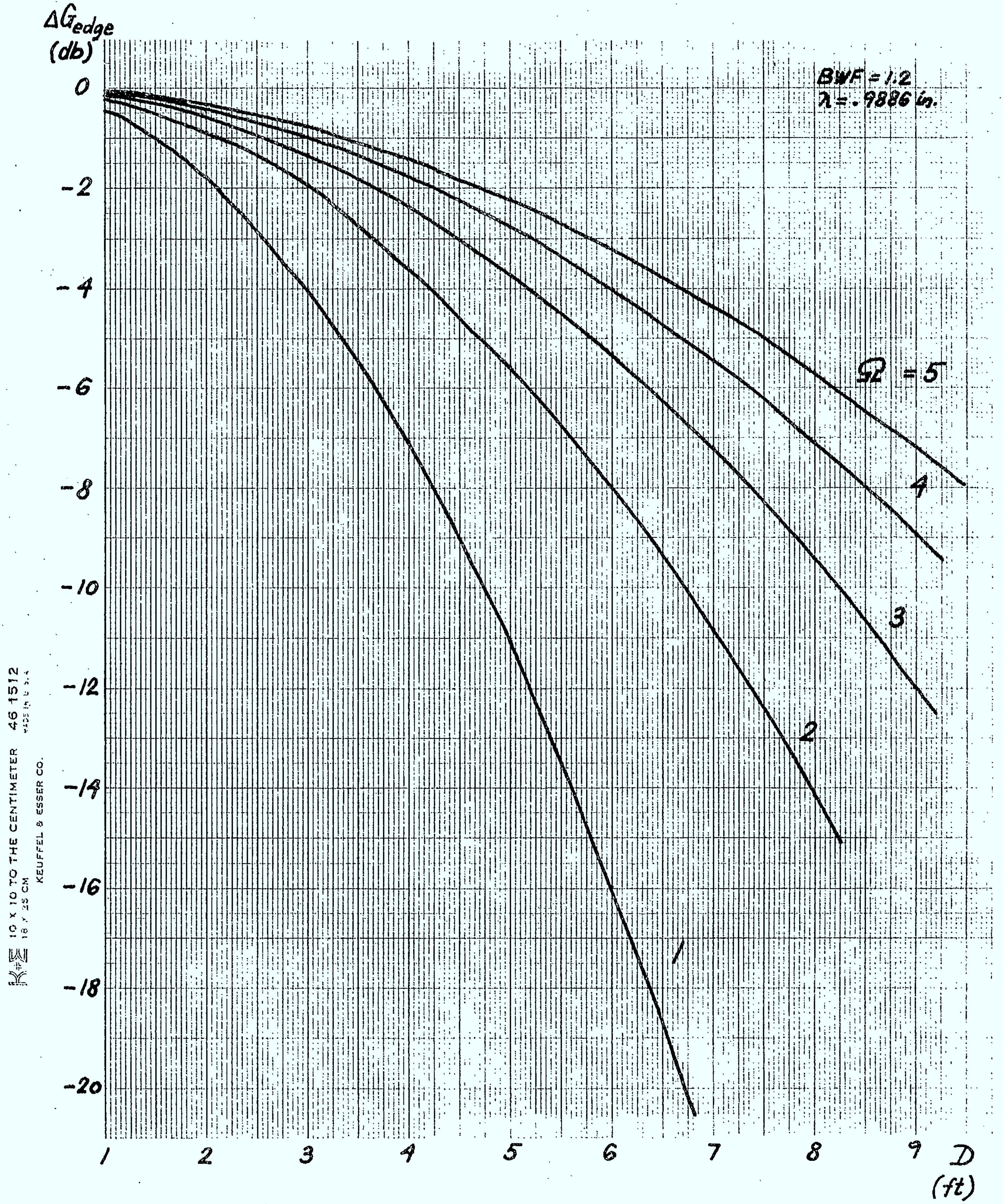

Fig. 2.4 Edge gain to on-axis gain ratio in the plane corresponding to α_2 vs. the diameter D of equivalent gain circular aperture ($\alpha_2 = 2.2°$).

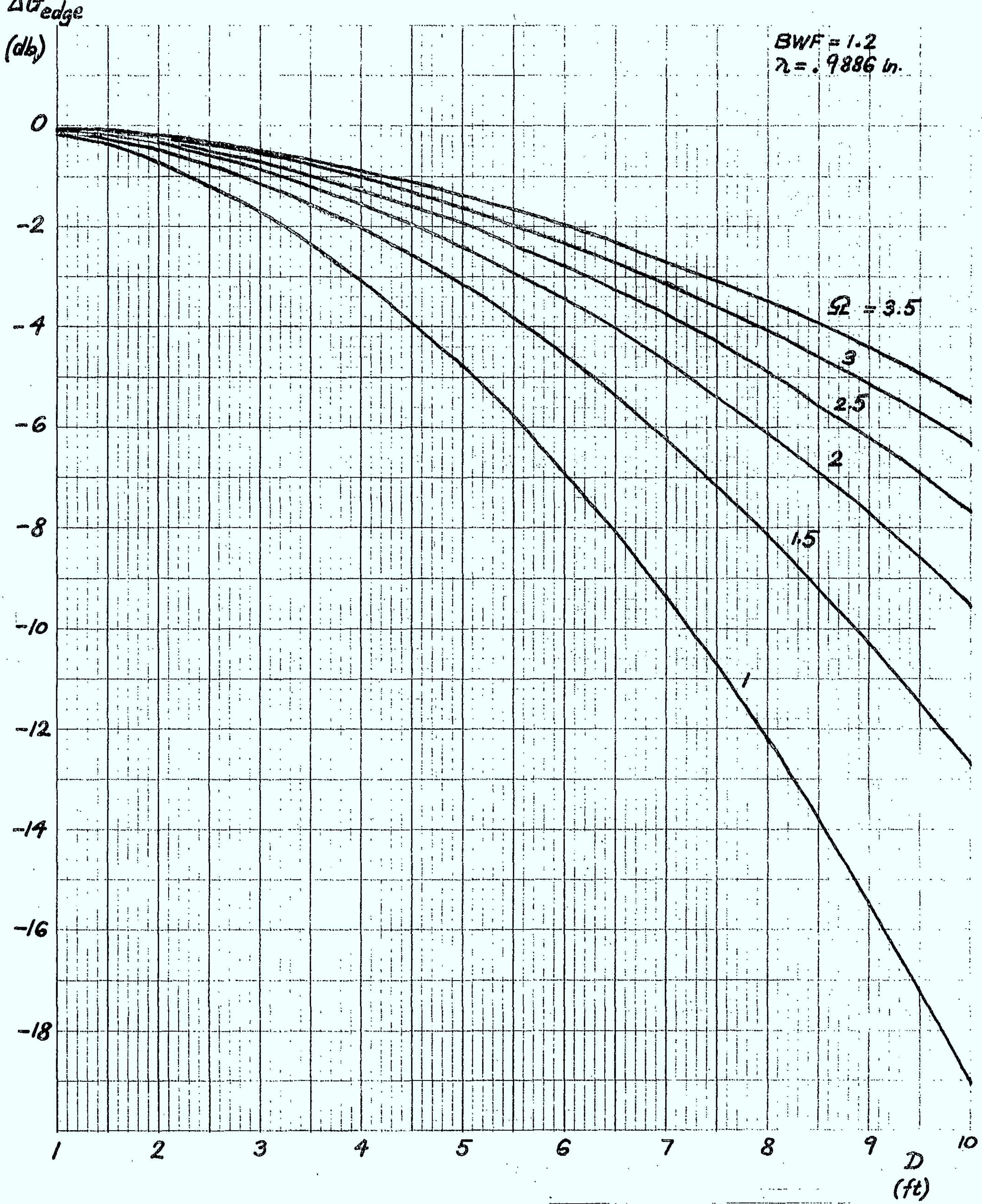

Fig. 2.5 Edge gain to on-axis gain ratio in the plane corresponding to α_2 vs. the diameter D of equivalent gain circular aperture ($\alpha_2 = 1.43^{\circ}$).

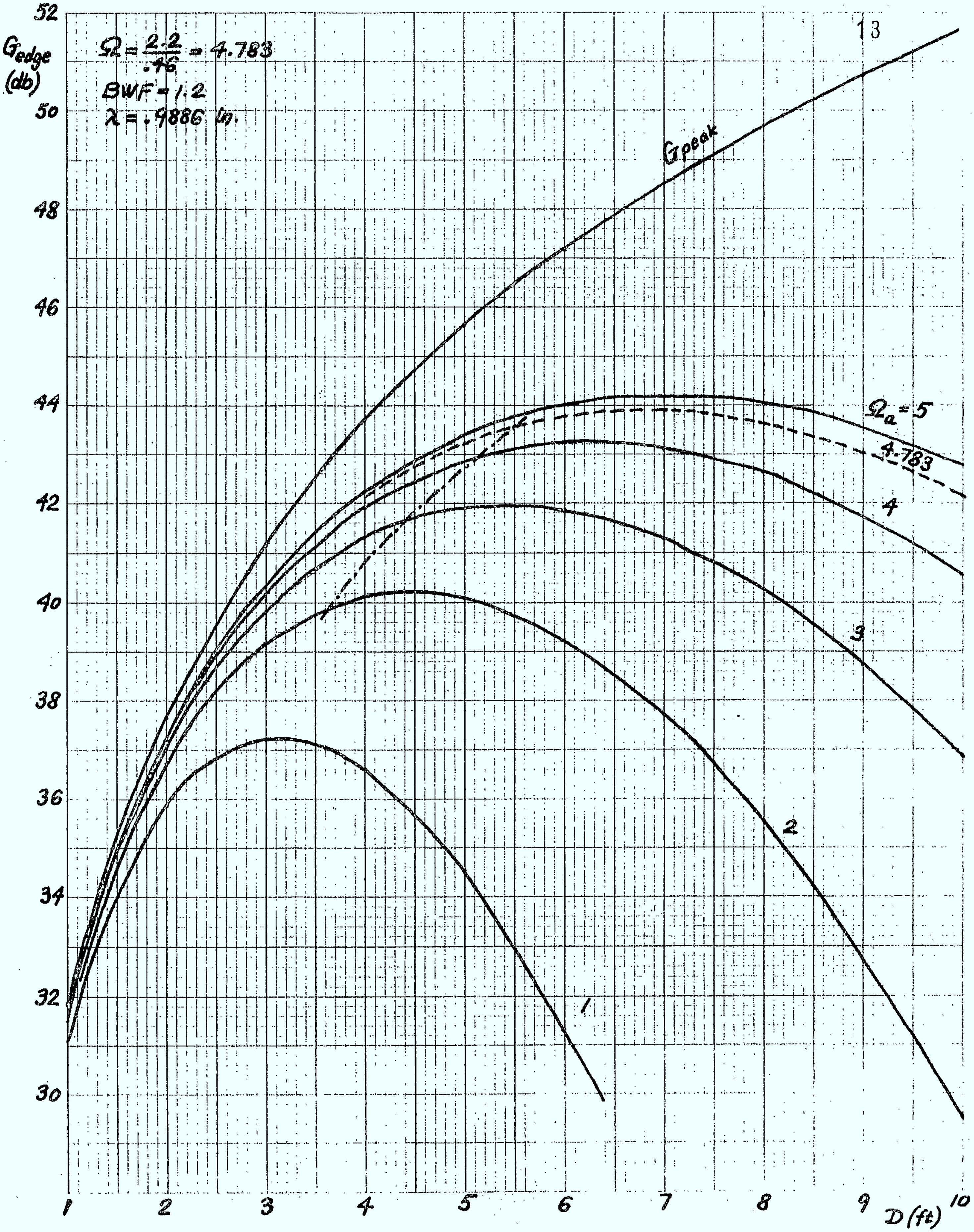

Fig. 2.6 Edge gain of elliptical apertures with aspect ratio Ω_a at the edge of $2.2° \times 0.46°$ coverage area vs. the diameter D of equivalent gain circular apertures.

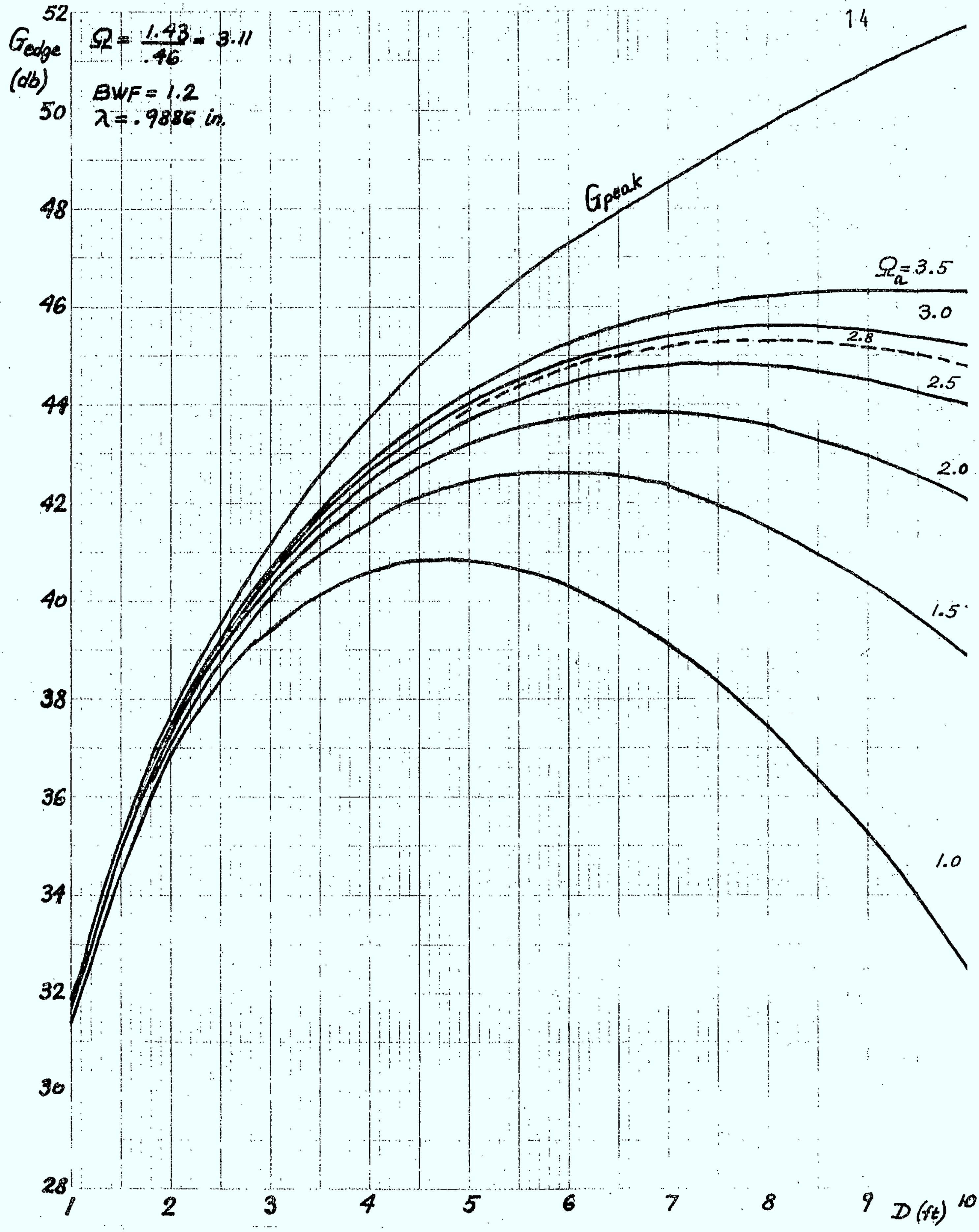

Fig. 2.7 Edge gain of elliptical apertures with aspect ratio Ω_a at the edge of $1.43^\circ \times .46^\circ$ coverage area vs. the diameter D of equivalent gain circular apertures.

For the two MB's considered (G_{edge}) max. is shown in Figure 2.8 vs Ω_a. Again the curves should be considered only for $\Omega_a \leq \Omega$ shown by dashed lines. The gain values correspond to $\eta = 1$ and $10 \log \eta$ should be added to the readings for $\eta < 1$.

2.3.2. Equivalent Circular Aperture Diameter for Maximum Edge Gain

The edge gain maxima occur at particular D_M values. These are the solution of the equation

$$\frac{dG^{db}_{edge}}{dD} \equiv 0 \tag{19}$$

$$D_M = \frac{\sqrt{20 \log e}}{\sqrt{6}} \; \frac{180}{\pi} \; \frac{\lambda \, k_B}{\alpha_2^o} \sqrt{\Omega_a} \tag{20}$$

D_M and λ should be expressed in the same units. This equation is depicted in Figure 2.9 for $\alpha_2{}^o = 2.2^o$ and for $\alpha_2{}^o = 1.43^o$.

2.3.3. Difference Between Gain and Edge Gain for Maxium Edge Gain

It is of some interest to determine the maximum edge gain for the various aperture aspect ratios with respect to the on-axis or peak gain. This can be determined from Figures 2.4 and 2.5 at the values of D_M read-off from the curves in Figure 2.9. It can be found that this quantity is independent of the dimensions of the satellite motion box and the aperture aspect ratio. Its value is:

$$G^{db}_{peak}\Big/_{D=D_M} = \left(G^{db}_{edge}\right)_{max} = 4.3 \; db \tag{21}$$

This is the same value which Duncan (Ref. 3) derived for the maximum off-axis gain of apencil beam assuming a Gaussian function power pattern.

2.3.4. Edge Gain Versus Aperture Aspect Ratio

For an elliptical antenna aperture of a given area, i.e. for a given equivalent gain circular aperture diameter D the edge gain increases with increasing aperture aspect ratio. The rate of increase is higher

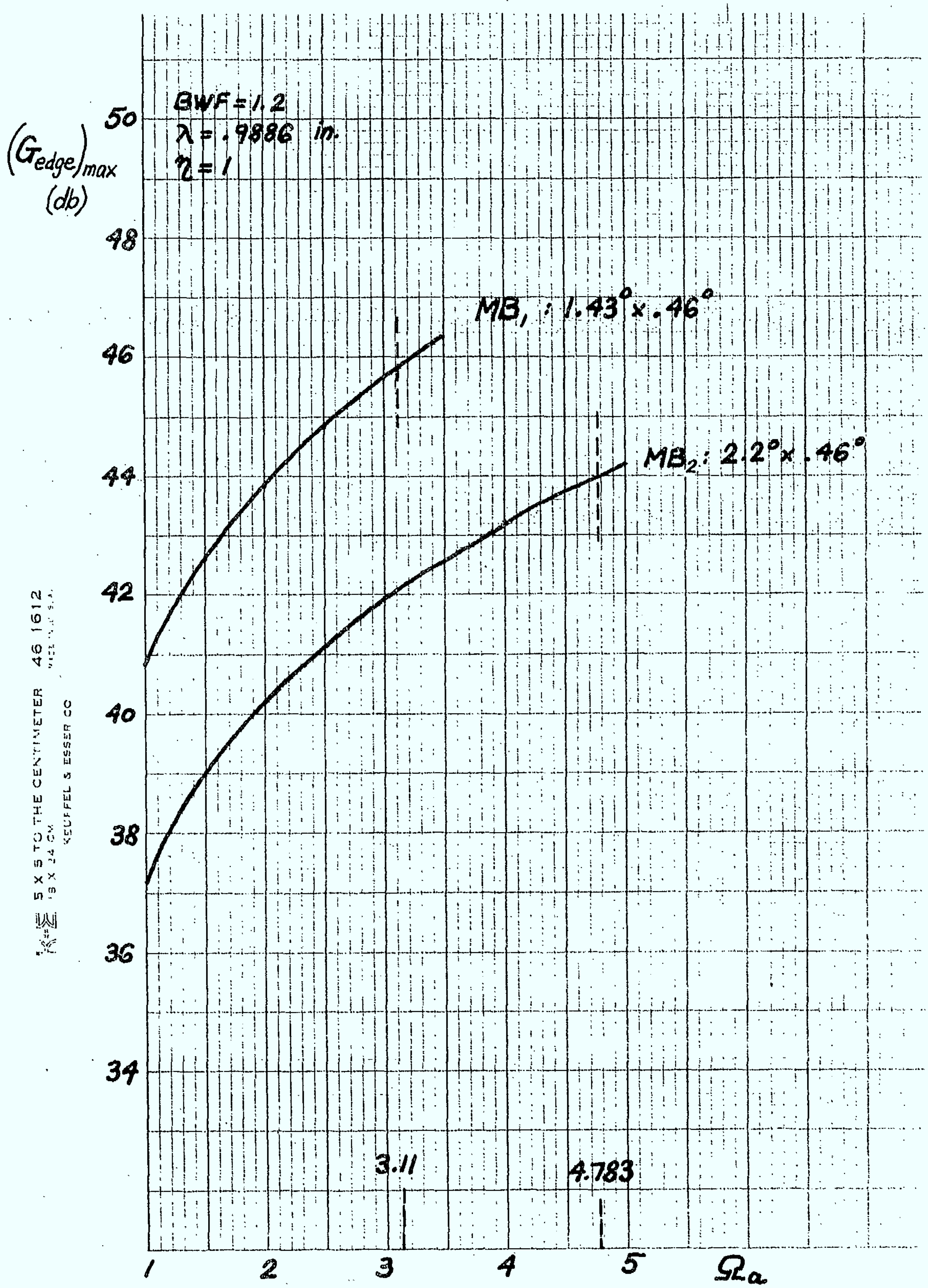

2.8 Maximum edge gain vs. aperture aspect ratio.

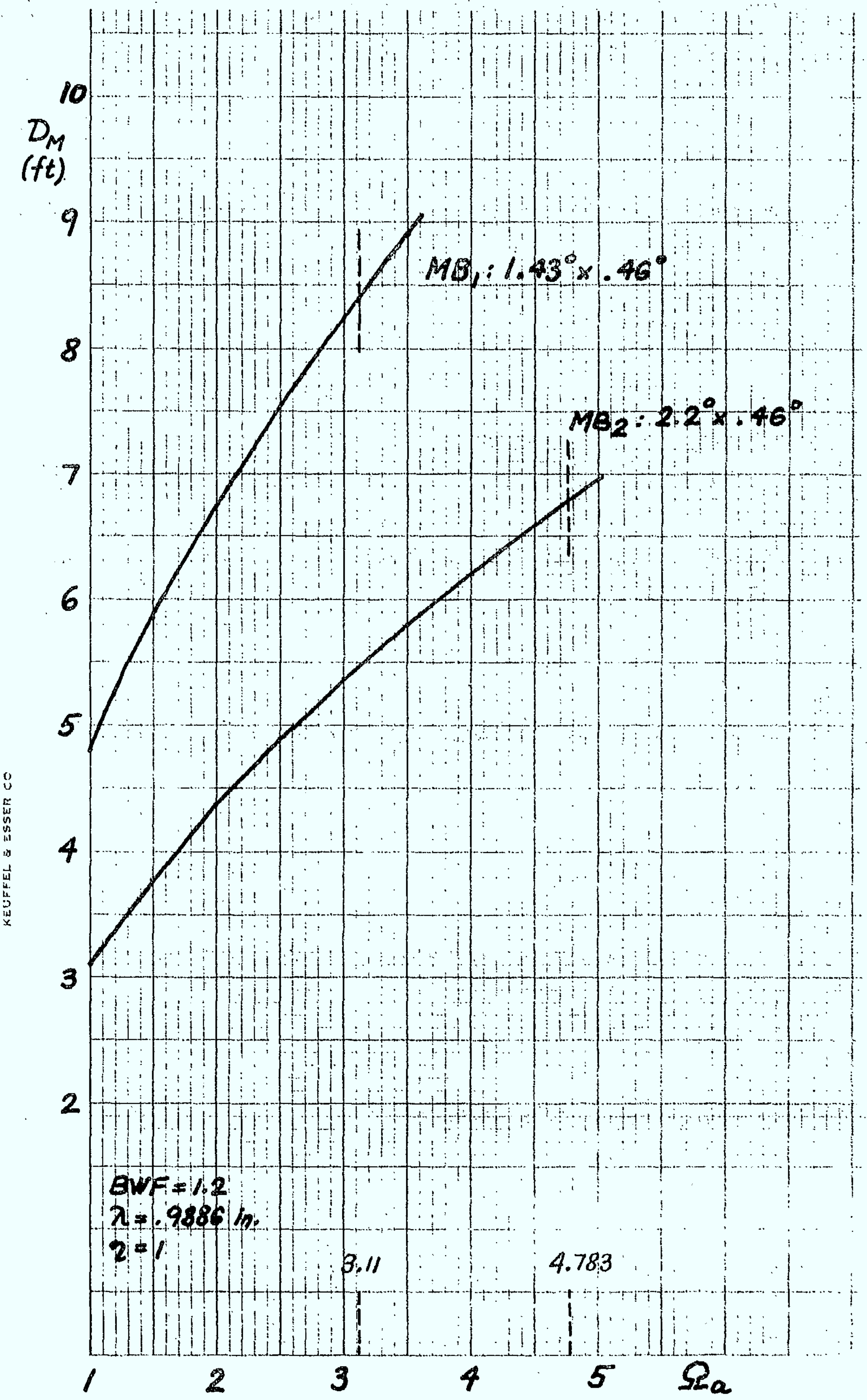

Fig. 2.9 Diameter of circular aperture with equivalent gain for maximum edge gain versus aperture aspect ratio.

at low aperture aspect ratios. The rate of increase also varies with D. The family of curves in Figure 2.10 shows the change of edge gain versus aperture aspect ratio for values of $D = D_M$ corresponding to several values of Ω_a. The change in edge gain for each D_M is measured from the value of (G^{db}_{edge}) max. corresponding to these D_M values

$$G^{db} - \left(G^{db}_{edge}\right)_{max}\Big|_{D=D_M(\Omega_a)} = \Delta g_{edge}(\Omega_a)\Big|_{D=D_M(\Omega_a)} \qquad (22)$$

The MB is $2.2^\circ \times .46^\circ$. A similar family of curves for the MB: $1.43^\circ \times 0.46^\circ$ is shown in Figure 2.11.

2.3.5. Frequency Dependency of Edge Gain

The curves in Figures 2.4 to 2.11 were drawn for λ_{Ro} = .9886 inches which corresponds to $f_{Ro} = \sqrt{11.7 \times 12.2} = 11.947$ GHz, the centre of the extended receive frequency band. For simultaneous transmit and receive operation the investigation has to be extended to the transmit frequency band. The centre frequency of this band is $f_{To} = \sqrt{14.0 \times 14.5} = 14.248$ GHz corresponding to a wave-length of $\lambda_{To} = 0.8290$ inches.

Examining the expressions of edge gain a change in frequency may be interpreted as a proportional change in D. Thus

$$\frac{D}{\lambda_{To}} = k\frac{D}{\lambda_{Ro}} = \frac{\lambda_{Ro}}{\lambda_{To}}\frac{D}{\lambda_{Ro}} = \frac{D^*}{\lambda_{Ro}} \qquad (23)$$

Thus D at the new wavelength λ_{To} is equivalent to $D^* = \frac{\lambda_{Ro}}{\lambda_{To}} D = \frac{.9886}{.8290} D = 1.1925\, D$ at the old wavelength of λ_{Ro}. Figures 2.4, 2.5 2.6, 2.7, 2.12, 2.13 and 2.14 are directly useable at λ_{To} or at any other wavelength λ if the D scale on the abscissa is multiplied by the factor $k = \frac{\lambda_{Ro}}{\lambda}$.

It can be seen from the curves that for the assumed conditions of frequency independent aperture illumination, the edge gain deteriorates with the square of the increasing frequency. For such a case and wideband operation the frequency of optimum operation has to be selected <u>above</u> the geometrical mean centre of the band.

2.3.6. Pointing Error Sensitivity of Edge Gain

The rate of change of the relative edge gain with respect to the 3 db beamwidth Θ_3° of the beam may be written as

TABLE 2.2

Frequencies and Dimension Scaling Factors

Designation	Freq. (GHz)	Wavelength	Scale Factor	Notes
Receive f_1	11.7	1.009	.98	
f_2	12.2	0.9681	1.02	Extended band
f_{Ro}	11.947*	0.9886	1.0	
Transmit f_3	14.0	0.8436	1.17	
f_4	14.5	0.8146	1.21	Extended band
f_{To}	14.248	0.8290	1.19	
f_R - .15 GHz	11.833	0.9981	.99	
f_R	11.983	0.9856	1.00	Receive frequency
f_R + .15 GHz	12.133	0.9735	1.016	
f_T - .15 GHz	14.00	0.8436	1.17	
f_T	14.15	0.8347	1.184	Transmit frequency
f_T + .15 GHz	14.30	0.8259	1.197	

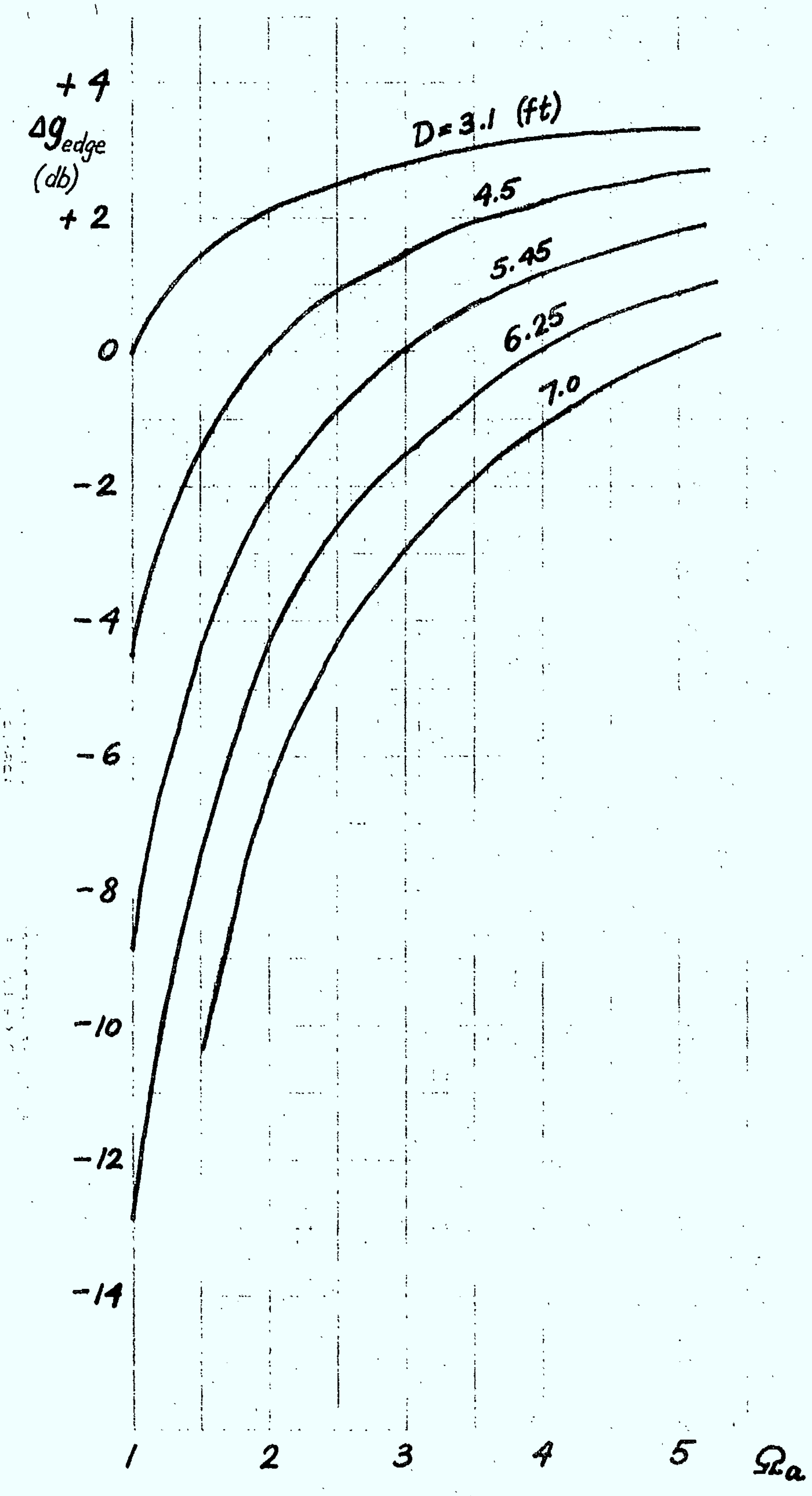

2.10 Change of edge gain versus aperture aspect ratio. Parameter is the diameter of the circular aperture whose edge gain is maximum at the Ω_a value where $\Delta g_{edge} = 0$ (MB: 2.2° x .46°).

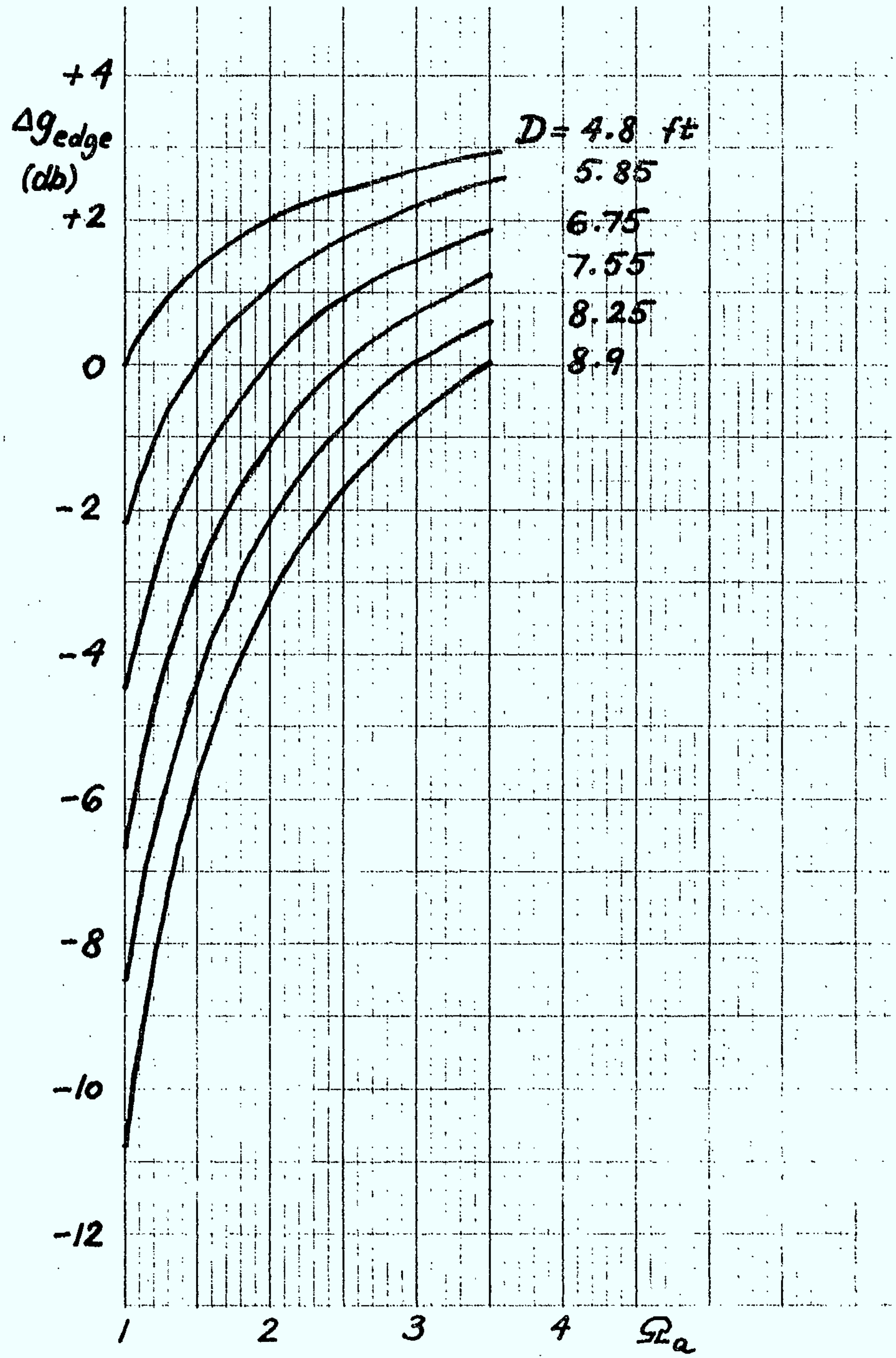

2.11 Change of edge gain versus aperture aspect ratio. Parameter is the diameter of the circular aperture whose edge gain is maximum at the Ω_a value where $\Delta g_{edge} = 0$ (MB: 1.43° x .46°).

$$\frac{\partial(\Delta G_{edge})}{\partial \Theta^{\circ}_{3B}} = 6\,\frac{(\alpha^{\circ}_{2})^{2}}{(\Theta_{3B})^{3}} = 6\,\frac{(\alpha^{\circ}_{2})^{2}}{k_B^{3}\left(\frac{\lambda}{D}\right)^{3}\Omega_a^{2}\left(\frac{180}{\pi}\right)^{3}} =$$

$$= 6\left(\frac{D}{\lambda}\right)^{3}\frac{1}{k_B^{3}\left(\frac{180}{\pi}\right)^{3}}\,\frac{(\alpha^{\circ}_{2})^{2}}{\Omega_a^{2}} \qquad (24)$$

Assumingthat all other parameters are constant the change in edge gain is:

$$\Delta\left(\Delta G_{edge}\right) = \frac{\partial(\Delta G_{edge})}{\partial \Theta^{\circ}_{3B}}\,\Delta\Theta^{\circ}_{3B} \qquad (25)$$

A pointing error of β° has the same effect on edge gain as an increased value of $\Theta^{\circ\prime}_{3B} = \Theta^{\circ}_{3B} + 2\beta^{\circ}$. (See Sketch)

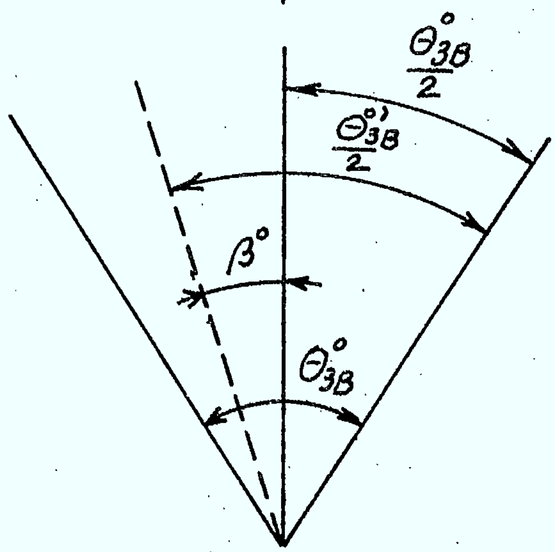

$$\Delta\Theta^{\circ}_{3B} = \Theta^{\circ\prime}_{3B} - \Theta^{\circ}_{3B} = 2\beta^{\circ} \qquad (26)$$

Thus

$$\delta\left(\Delta G_{edge}\right) = 12\left(\frac{\pi}{180}\right)^{2}\left(\frac{D}{\lambda}\right)^{3}\left(\frac{\alpha^{\circ}_{2}}{\Omega_a}\right)\beta^{\circ}$$

$$= 6.38\times10^{-5}\left(\frac{D}{\lambda}\right)^{3}\left(\frac{\alpha^{\circ}_{2}}{\Omega_a}\right)^{2}\beta^{\circ} \qquad (27)$$

The change in relative edge gain for given α_2, Ω_a and $\beta°$ is increasing with the third power of D/λ. Besides weight, cost etc. this is one more reason why the smallest possible dish area should be used for portable not too accurately aligned antennas. The function $\delta(\Delta G_{edge})/\beta$ is shown in Figure 2.12 for a MB: 1.43° x .46° and in Figure 2.13 for MB: 2.2° x .46°.

2.4 Beam Parameters for MB1 (1.43° x .46°)

Looking at Figures 2.7 and 2.9 one may note that a circular paraboloid reflector (curve $\Omega_a = 1$) provides maximum edge gain at a diameter of 4.7 ft. The theoretical value of this maximum is 40.85 db. At the convenient D of 3 ft. the gain is 39.45 db i.e. 1.4 db lower. Increasing the aperture aspect ratio at D = 3 ft will give very moderate edge gain increase only. At D = 4.7 ft however, using an elliptical aperture with an aspect ratio of $\Omega_a = 1.5$ provides an edge gain increase of 1.4 db to 42.25 db. An aperture aspect ratio of 1.5 is not excessive to realize the 1.4 db potential gain increase. Increasing Ω_a to 2 would provide an other 0.6 db edge gain. This 33% increase of Ω_a to 2 might not allow the full realization of the predicted increase of 0.8 db. It seems that at D = 4.7 ft, $\Omega_a = 1.5$ might be a reasonable limit of aperture aspect ratio in this case. The gain variation over the MB is 2.8 db maximum. The sensitivity of the edge gain to pointing error may be determined from Figure 2.12. At D = 3 ft. and $\Omega_a = 1$ the edge gainchange is $\Delta(G_{edge})$ = 6.3 db for $\beta = 1°$ of pointing error. At D = 4.7 it is 24 db/deg. still with $\Omega_a = 1$. With $\Omega_a = 1.5$ it is 10.8 db/deg. For the value of $\Omega_a = 2$ it drops to 6 db/deg. It seems that although the increase of edge gain in going from $\Omega_a = 1.5$ to 2 might not be very significant this Ω_a may still be useful for it reduces the gain loss due to pointing error. Taking pointing error considerations into account the combination of D = 4.7 ft and $\Omega_a = 2$ may be quite desirable.

If the 4.7 ft diameter is too large and the 36% smaller D = 3 ft is preferred because of other operational requirements an aperture aspect ratio of $\Omega_a = 1.5$ would give about 0.5 db edge gain increase over a circular aperture but would reduce the edge gain sensitivity with pointing error from 6.3 db/deg. to 2.8 db/deg. If pointing error is one of the prime considerations then it seems that the aspect ratio might have to be increased somewhat beyond the value that would be indicated by considering only a reasonable return in edge gain increase for the added complexity of higher Ω_a.

Turning now to the higher gain antenna category of the order of 8 ft diameter the first glance at Figure 2.7 would indicate a higher aperture aspect ratio. From Figure 2.9 we find that at a diameter of 8 ft edge gain maximum is achieved by $\Omega_a \cong 2.8$. This maximum edge gain is 45.3 db (See Figure 2.8) The size of this aperture is quite considerable: its dimensions are

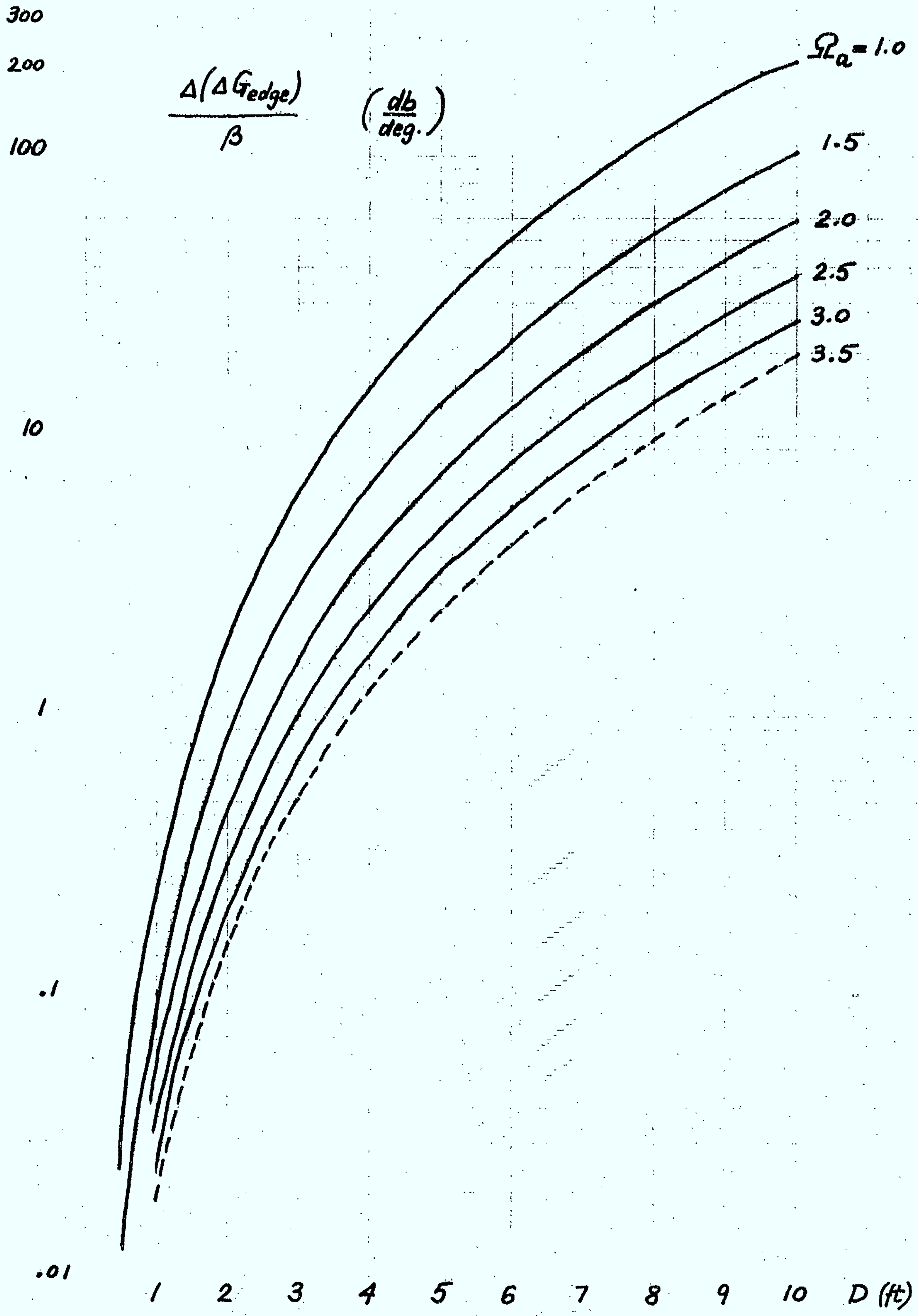

2.12 Change in relative edge gain per degree of pointing error (MB: $1.43^\circ \times .46^\circ$, λ =.9886 in., BWF = 1.2).

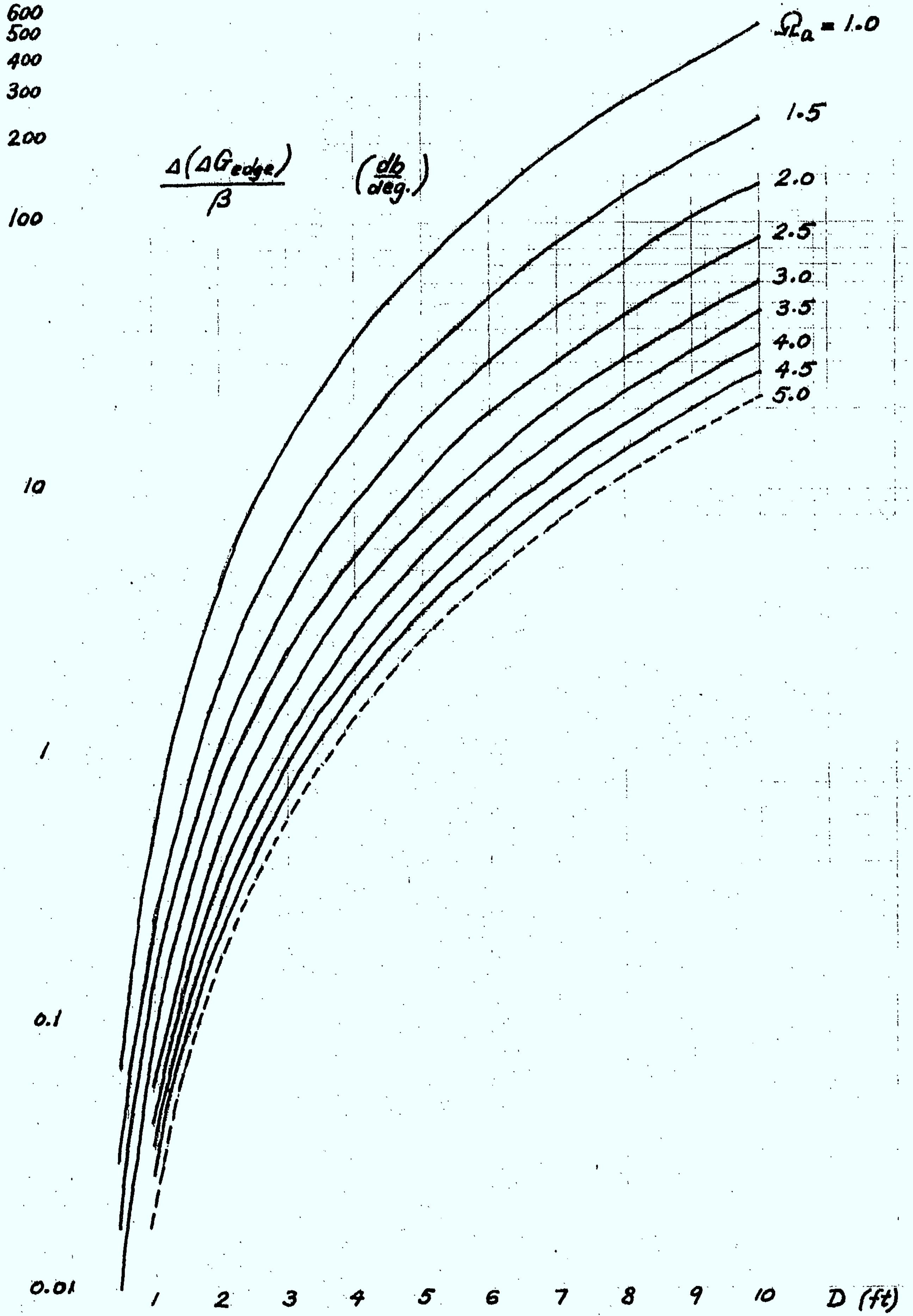

2.13 Change in relative edge gain per degree of pointing error ($MB: 2.2^\circ \times .46^\circ$, $\lambda = .9886$ in., $BWF = 1.2$).

$A = \sqrt{\Omega_a}\, D = 13.39$ ft and $B = D/\sqrt{\Omega_a} = 4.87$ ft. Its pointing error sensitivity from Figure 2.12 is about 15 db per degree. It will be of some practical importance to investigate how some of the undesirable characteristics of this aperture may be improved.

a) Because of the flat maximum of G_{edge} versus D one gains very little by using a D value exactly corresponding to the maximum instead of a reduced D. In Figure 2.7 $\Omega_a = 2.8$ is drawn with dashed line. It shows that at the expense of losing 0.3 db edge gain one could use a D = 6.5ft. i.e. an 18.8% smaller diameter. From Figure 2.12 the corresponding change in pointing error is from 15 db per degree to about 8 db/deg. In this case essentially an 18.8% reduction of D was achieved at the expense of 0.3 db edge gain. At the same time the pointing error sensitivity was reduced by about 50%. The gain value is 45 db.

b) Near the optimum Ω_a G^{db}_{edge} is a slowly varying function of Ω_a. At D = 8 ft reducing Ω_a from the optimum 2.8 value to 2.5 the drop in gain is about 0.5 db from 45.3 db to 44.8 db. This can actually be increased by reducing the diameter slightly, or maintained at the same level even at a diameter of 7 ft. The gain at this point is 44.8 db and the pointing sensitivity is 12.8 db/deg. It seems that the steps taken in a) are more effective.

The figures obtained for the various cases discussed are summarized in Table 2.3. Those marked with an asterisk represent an optimum within the category in the context of the discussion above.

It seems that consideration should also be given to the 3 ft diameter circular paraboloid. When compared to D = 3, $\Omega_a = 1.5$ its gain is about .55 db lower and its pointing sensitivity is greater by a factor of 2.25. On the other hand it is a commercially readily available off the shelf item.

When the 4.7 ft diameter $\Omega_a = 2$ case is compared to the D = 3, $\Omega_a = 1$ case it is clearly a larger aperture area, higher edge gain solution. What is interesting about this is that the increase in edge gain 42.9 - 39.45 = 3.45 db is almost as high as the theoretical on-axis gain increase corresponding to the increase in aperture area:

$10 \log \left(\frac{4.7}{3}\right)^2 = 3.9$ db

Looking at the cases listed belonging to the 8 ft diameter category it would seem that the expected increase in gain over that of the 3 ft category could only be realized with a considerably higher (Ω_a = 2.5 to 2.8) aperture aspect ratio. At these Ω_a's however the edge gain is a very slowly varying function of D and a considerable reduction in diameter is possible at the expense of a small gain reduction. Thus considering the accompanying reduction of weight, cost, alignment difficulties etc. it seems that a D = 6.5 to 7.0 ft represent the best compromise. The decrease in aperture area is $-10 \log(6.5/8)^2 = 1.8$ db while the decrease in gain is only 45.3 - 45.0 = .3 db.

An other interesting observation may be made by examining Figure 2.14. It shows the upper bound of the edge gain for the two MB's. These are the edge gains corresponding to aperture aspect ratios equal to those of the MB's, i.e. $\Omega_a = \Omega_o$. The curve marked G_1 corresponds to the MB of 1.43° x .46° . It has its maximum ≈ 45.8 db at D ≈ 8.5 ft beyond which the edge gain drops again. Thus the approximately 8 ft diameter considered for one of the two antenna categories represents the maximum antenna size in a theoretical sense that is useable for the given MB. The gain figure of about 46 db is similarly a theoretical maximum under the given conditions.

2.5 Beam Parameters for MB2 (2.2° x .46°)

This MB has a considerably greater aspect ratio and its efficient coverage will require a more a symmetrical beam. The edge gain curves corresponding to this case are shown in Figure 2.6. A circular paraboloidal aperture provides maximum edge gain at the diameter of 3 ft. This gain is 37.2 db which is 2.25 ft. lower than this aperture could provide for MB_1. By making the aperture elliptical to the extent of Ω_a = 2 the edge gain increased from 2 to 3 the corresponding improvement is only 0.6 db. If only a part of this can be realized due to feed problems, phase error etc., it would then seem reasonable to keep Ω_a at 2. On the other hand a 0.7 db increase may be achieved by increasing D to 3.6 ft. The pointing sensitivity is 15 db/deg. at Ω_a = 1 and 3.7 db/deg. at Ω_a = 2. (Figures 2.13).

Considering now the 8 ft diameter category one would suspect that this size is "Too large" since already for MB_1 it represented a maximum. Indeed from Figure 2.9 one can see that 8 ft. is greater than the diameter corresponding to maximum edge gain even for the optimum value of Ω_a = 4.783. It seems that there are basically two ways of approaching the problem.

a) Assuming that the antenna structure is suitable to provide a great beam aspect ratio say even up to the optimum of about 4.8 the diameter should be reduced considerably. At D = 5.5 ft the edge gain is the same as at 8 ft. At 6.5 ft it is actually higher by .3 db

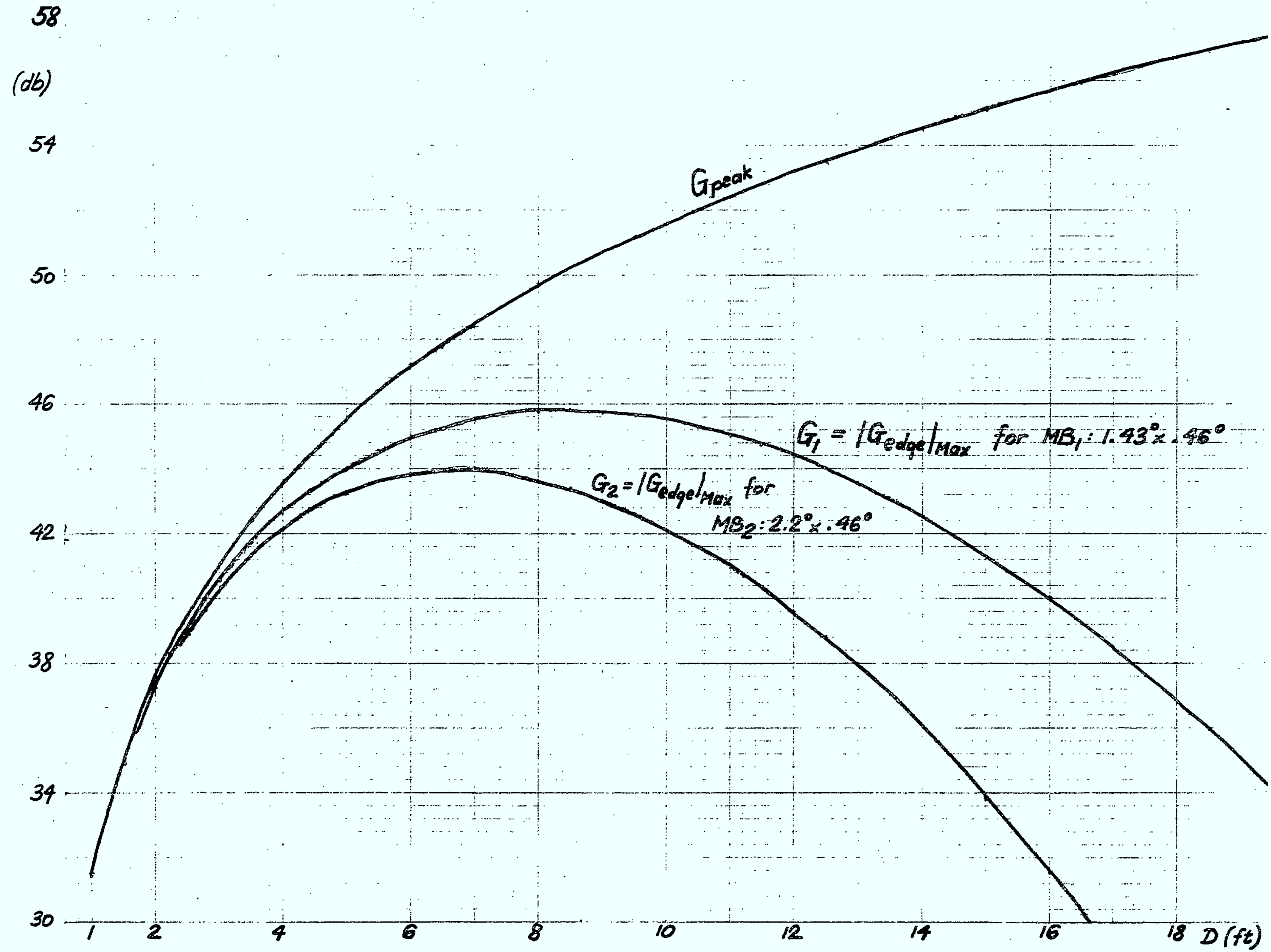

2.14 Upper bound of edge gain vs D for 2.2° x .46° and for 1.43° x .46° MB's.

reaching the maximum of 43.9 db. Since an 18% increase in D is considered too high a price for a 0.3 db gain improvement $D = 5.5$ is the preferable size. The major and minor dimensions of this aperture are 12.03 ft. and 2.51 ft. (At $D = 8$ ft they are 17.5 ft and 3.66 ft). The pointing error sensitivity at $D = 5.5$ ft is 4 db/degree.

b) If for reasons of practical realization, the beam aspect ratio is limited to values considerably lower then the optimum 4.8, the gain values that may be achieved will also drop at a fairly fast rate (D is reduced at the same time to optimize G_{edge} for the particular Ω_a). Keeping the edge gain about 0.3 db below the maximum by selecting $D < D_M$ corresponding to the particular Ω_a the dash dot curve in Figure 2.6 indicates reasonable intermediate cases between the 3 ft and 8 ft diameter categories. Table 2.4 summarizes the basic properties of the apertures considered for MB_2.

The maximum theoretical edge gain possible with sector beams for MB_1 is 49.79 db and for MB_2 is 47.92 db. Relative to these limiting values, considerably less can be achieved with the type of aperture distributions presently considered.

The upper bound of the edge gain for MB_2 is shown in Figure 2.14 by curve G_2.

Considering the upper bounds of the edge gain for the two MB's depicted in Figure 2.14 one may make the following general observation. If by the designation of "3 ft. diameter category" we consider antennas that can provide an edge gain as high as a 3 ft. diameter circular aperture can on its axis (at the given frequency) then one can clearly provide this for both MB_1 and MB_2. The theoretical maximum value of this gain is 41.2 db. This can be achieved with $D = 3.25$ ft. for MB_1 and with $D = 3.45$ ft for MB_2. No 8 ft. diameter category exists however for these MB's, i.e. the 49.7 db edge gain is unattainable without tracking. The maximum is 45.3 db for MB_1 and 43.9 db for MB_2 corresponding to 4.8 ft and 4.1 ft diameter "categories" respectively. In Tables 2.3 and 2.4 ΔG_{edge} indicates how far down

TABLE 2.3

Comparison of Elliptical Apertures, MB: $1.43^{\circ} \times .46^{\circ}$

D (ft)	Ω_a	ΔG_{edge} (db)	G_{edge} (db)	G_{edge} (db) ($\eta = 55\%$)	Pointing Sensitivity db/deg.	Notes
(*) 3	1	-1.7	39.45	36.85	6.3	3 ft. diameter category
* 3	1.5	-1.1	40.0	37.4	2.8	
4.7	1	-4.25	40.85	38.25	24.0	
4.7	1.5	-2.8	42.25	39.65	10.8	Intermediate
* 4.7	2	-2.1	42.9	40.3	6.0	
8	2.8	-4.4	45.3	42.7	15.0	8 ft. diameter category
* 6.5	2.8	-2.9	45.0	42.4	8.0	
8	2.5	-4.9	44.8	42.2	19.0	
7	2.5	-3.7	44.8	42.2	12.8	

TABLE 2.4

Comparison of Elliptical Apertures, MB: $2.2^{\circ} \times .46^{\circ}$

D (ft)	Ω_a	ΔG_{edge} (db)	G_{edge} (db)	G_{edge} db (η =55%)	Pointing Sensitivity db/deg.	Notes
3	1	-3.95	37.2	34.6	15.0	
* 3	2	-1.95	39.15	36.55	3.7	3 ft. diameter category
3.6	2	-2.9	39.85	37.25	6.6	
* 5.5	4.8	-2.9	43.6	41.00	4	8 ft. diameter category
4.4	3	-2.9	41.6	39.00	7.5	Intermediate

the edge gain is with respect to the theoretical maximum on-axis gain (See also Figures 2.4 and 2.5) corresponding to the given diameter.

For the sake of simplicity all absolute gain values shown assumed an antenna efficiency of 100%. In Tables 2.3 and 2.4 they are also given for an efficiency of η = 55% for easier comparison with realistic, practical values. With the aid of Figure 2.15 gain figures may be obtained for any other η value.

2.6 Considerations of Basic Antenna Concepts

In Sections 2.4 and 2.5 the characteristics of elliptical beams suitable for covering two different satellite motion boxes were determined. Some useful alternatives were provided taking into account the originally planned two gain (and size) categories. The aperture sizes and shapes selected for both MB's are summarized in Table 2.5 together with their edge gain for 55% overall efficiency and with their pointing error sensitivity. In Figure 2.16 the scaled down envelopes of thes apertures are shown. From an initial review of this table one can say that for (MB_1) the first and second case may be realized by a cut paraboloidal reflector. The third case may also be a paraboloid or a parabolic cylinder structure. For MB_2 the fourth aperture could probably be a cut paraboloid while the last aperture having an aspect ratio of about 4.8 should be a parabolic cylinder or a paraboloid fed by an array of horns. If the satellite motion box MB_2 is not to be considered then the requirements for MB_1 may be realized with the same concept changing only the size and geometry to achieve the different beam parameters.

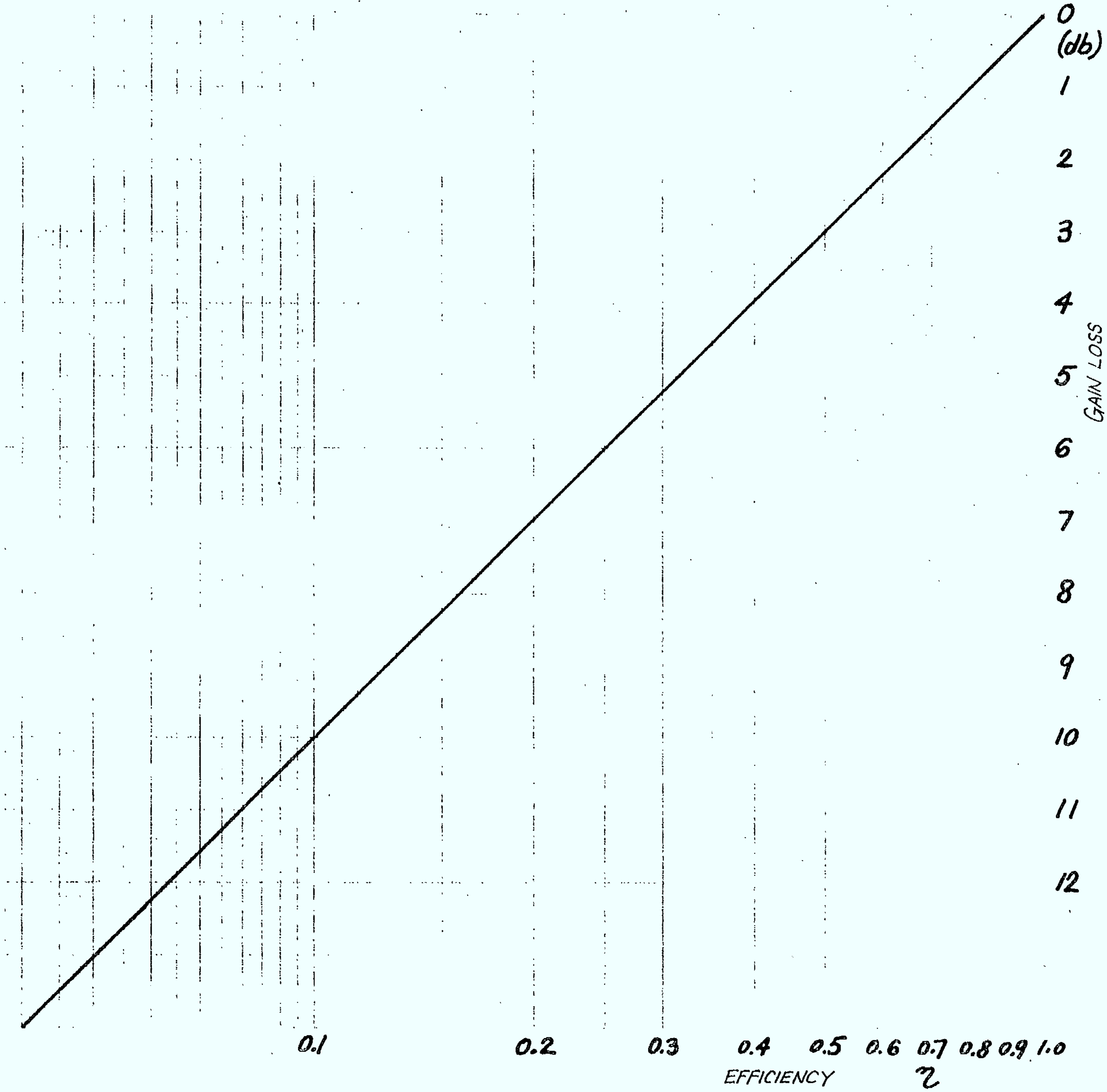

2.15 Gain loss versus efficiency.

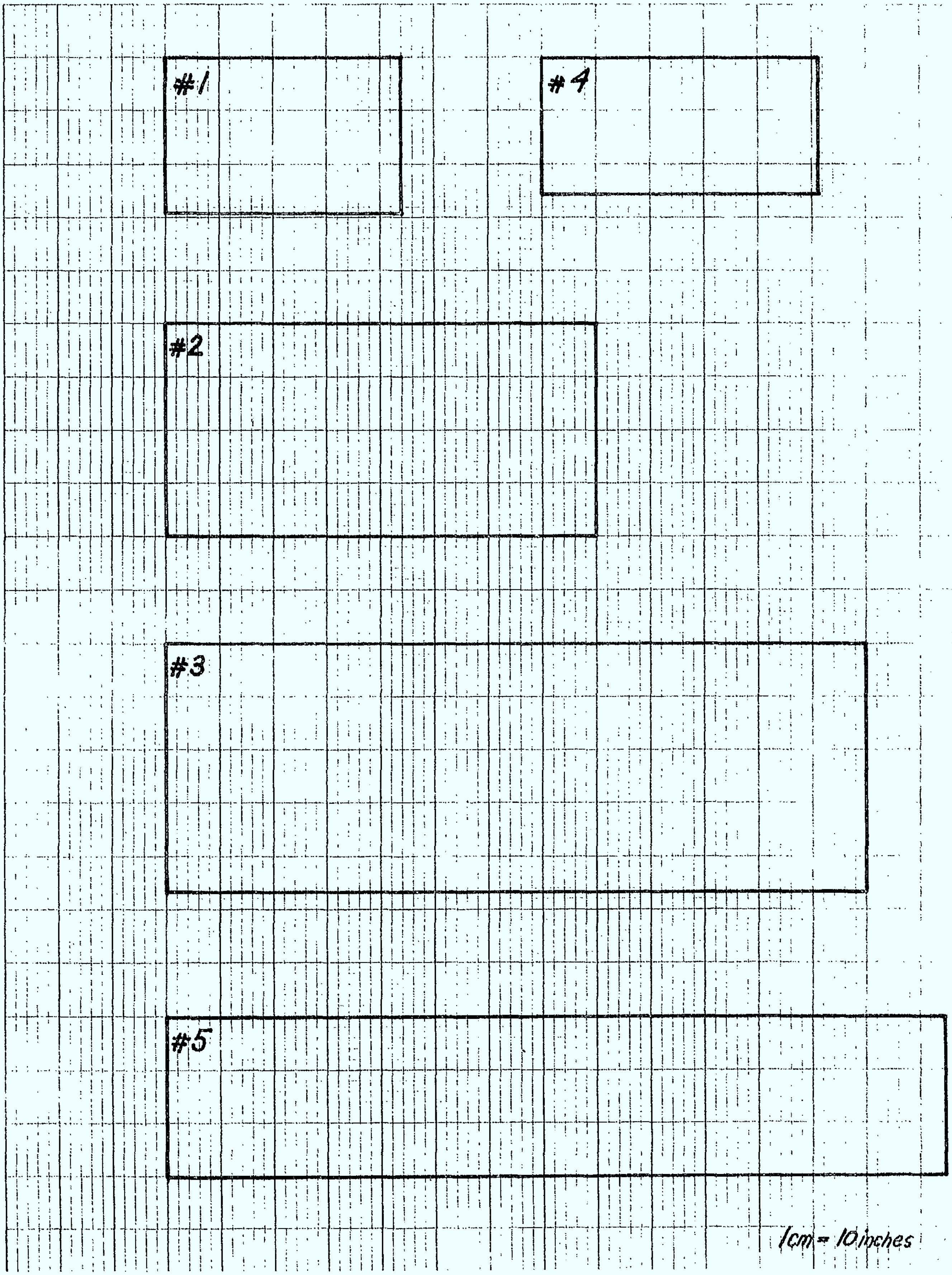

Fig. 2.16 Scaled down envelopes of the selected elliptical apertures (Nos. refer to Table 2.5)

TABLE 2.5

Summary of Selected Elliptical Aperture Parameters

	#	D (ft)	Ω_a	$G_{edge}/\eta=55\%$	Pointing Error Sensitivity (db/deg)	A (ft)	B (ft)	A (in)	B (in)	Area $(ft)^2$
MB1: $1.43^{\circ} \times .46^{\circ}$	1	3	1.5	37.4	2.8	3.67	2.45	44	29.4	7.1
	2	4.7	2.0	40.3	6.0	6.65	3.32	79.8	39.84	17.3
	3	6.5	2.8	42.4	8.0	10.88	3.88	130.56	46.56	33.2
MB2 $2.2^{\circ} \times .46^{\circ}$	4	3	2	36.55	3.7	4.24	2.12	50.91	25.46	7.1
	5	5.5	4.8	41.0	4	12.05	2.51	144.6	30.12	23.7

#	$G_{on\text{-}axis}$ db ($\eta = 55\%$)	ΔG_{edge} db	11.947 GHz $\Theta_{3M}{}^{\circ}$	11.947 GHz $\Theta_{3M}{}^{\circ}$	14.248 GHz $\Theta_{3M}{}^{\circ}$	14.248 GHz $\Theta_{3M}{}^{\circ}$
1	38.5	1.1	2.3	1.54	1.94	1.3
2	42.4	2.1	1.71	.85	1.43	.71
3	45.3	2.9	1.46	.52	1.22	.44
4	38.5	1.95	2.67	1.33	2.2	1.12
5	43.9	2.9	2.26	.47	1.89	.394

3.0 NON-CIRCULAR APERTURE PARABOLOID ANTENNAS

3.1 Introduction

Probably the simplest possible way to realize a high gain, elliptical beam cross-section is by the use of an elliptically contoured section of a paraboloid reflector. The required beam cross-section can be provided by selecting the aperture aspect ratio approximately equal to the beam aspect ratio. The shape of the aperture contour may be elliptical, follow a constant field intensity contour provided by the source, or may be some intermediate form.

To illuminate elliptical apertures efficiently the radiating source aperture must have a high major to minor dimension ratio. Simple sectoral or piramidal horns having such apertures have considerably separated phase centres in the E- and H-planes. The location of these points are also frequency dependent. In the present case the problem is made more difficult by the fact that two orthogonal polarizations have to be accomodated simultaneously, one in the receive the other one in the transmit frequency band.

The effects of these phase centre differences can be partly corrected by a slight deformation of the curvature of the paraboloid in the two main planes. Such a correction improves the sidelobe levels, but has very small effect on peak gain and even smaller effect on edge gain. Thus the added structural complexity is not warranted for the present problem.

If the reflector is centre fed one major limitation will be blockage by the feed, particularly for larger feeds (arrays).

The feed may be offset to reduce blockage. However, for such a case the major problem is that the displaced phase centres will cause a frequency dependent beam squint between the orthogonally polarized beams (Transmit and Receive). This squint reduces the effective edge gain over the MB.

The primary problem for the offset fed antenna is the development of a suitable feed system. This might incorporate some methods of reducing the phase centre separation. One such method could be the application of a lens over the horn. Another one can be a hoghorn with orthogonally uni-polarized parabolic cylinder surfaces of differing curvatures. The detrimental effects of beam squint is less in the plane of the shorter dimension of the MB where there is usually sufficient gain reserve. Figure 3.1 shows that this can be achieved by offsetting the feed in the plane of the major dimension of the aperture.

In this section the characteristics of various paraboloid reflectors will be examined. To facilitate calculations a model is used containing some simplifications. The calculated results in some cases will be compared with measured data available from other programs. It is assumed that accurate prediction of performance depends largely on experimental optimization of the required feed.

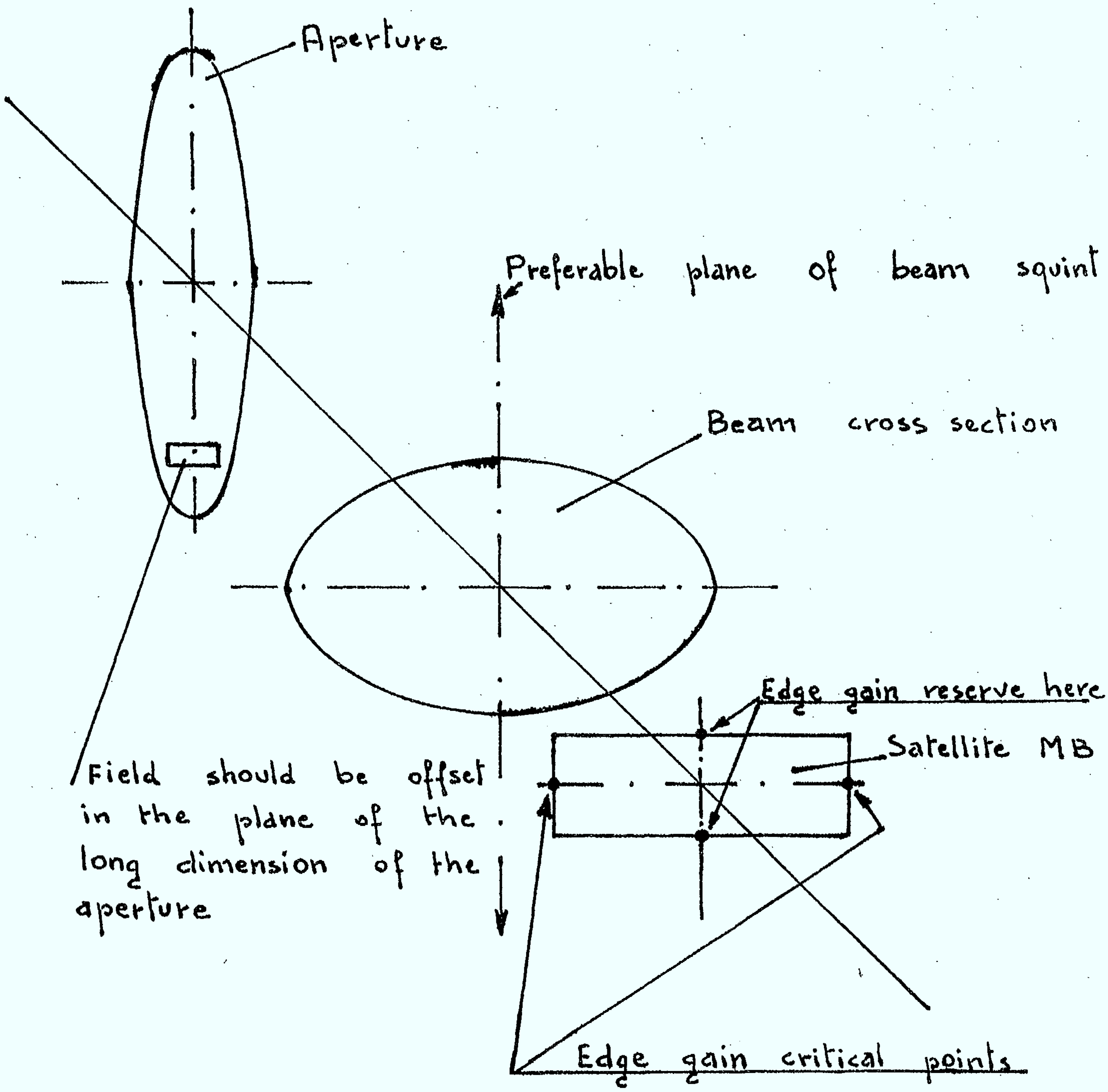

Fig. 3.1 Relationship between feed offset and edge gain

3.2 Computer Program for the Calculation of Radiation Characteristics

The theoretical computations have been made using the computer program "ANTENNA" developed by RCA Ltd. This program is a generalized algorithm for computing the radiation patterns and gain characteristics of reflector antennas by means of the vector surface current method. The program has been steadily developed to allow greater and greater flexibility and while the computations in this report have used idealized feeds with unique point phase centres and idealized elliptical or rectangular contours for the reflectors, minor changes to the algorithm can include arbitrary reflector shapes and feed radiation characteristics.

The program is limited by the usual simplifications:

(1) the reflector surface is in the far-field of the primary point source

(2) the surface currents are continuous at the reflector edge

(3) currents flowing on the shadowed side of the reflector are neglected

(4) edge effects are ignored

(5) only the critical scattered field is considered interaction of surface elements being ignored

(6) each ray from a point on the reflector is reflected from a tangent plane at the point

(The first simplification may be overcome by substituting the appropriate near-field pattern of the feed, or by using an internally generated sub-programme to give the coupled field at each surface point).

The program may be used to compute patterns from elliptical or rectangular apertures, where the contour is defined by the projection of the reflecting surface into the focal plane. Furthermore, by inserting additional cards into the source deck, elliptical contours can be generated. The contour is determined by the computation of a discriminant whose sign determines whether the ray strikes the reflector or not.

Blockage effects can be included by reading in the focal plane coordinates of the feed and supports in the data deck. Each ray is traced after striking the reflector surface and if it passes through the blocking region, its amplitude is set equal to zero. The gain reduction effects of such obstacles is also computed on two components, that due to scattering and that due to directivity, or area loss. Both components are printed in the output.

The feed is assumed to be a rectangular TE_{10} feed where 'a' and 'b' dimensions are included in the input data. Later versions of the program include the feed cross-polarized component in the total far-field cross-polarized pattern (i.e. the vector sum of the feed and reflector cross-polarized components). However, for the present report the feed was assumed to be uni-polarized with the cross-polarized component suppressed. Hence, the computed cross-polarized field is that of the reflector alone.

Feed offset (i.e. separation of the reflector aperture centre from the focus) can be included by appropriate input data. The program computer, the optimum feed tilt point the feed axis at the projected aperture centre. In addition, outside control is available to tilt the feed angle (to control gain and beam symmetry) in the plane of offset.

Feed displacements in the x, y, and z directions can be included, with optional rotation of the feed to keep the feed axis pointed at the centre of the reflector/as determined by the feed offset).

The surface current integration is carried out in a spherical coordinate system with the angular integration intervals adjusted to yield approximately constant size surface cells. That is, the solid angle subtended at the feed is approximately constant for all surface points. It may be noted that this is not the most efficient integration technique but the necessity of including the blockage at all far-field angles makes a sufficiently small cell size unavoidable.

The program computes the co- and cross-polarized patterns in three planes, the first of which must contain the peak of the beam. If the beam has been scanned by a feed displacement, the $\emptyset = 0$ pattern is that through the peak and in the plane defined by the feed displacement vector and the reflector axis. The remaining two planes are optional, taken in this report and 90° to the $\emptyset = 0$ plane, through the beam peak. It is, of course, necessary to estimate the position of the beam peak in order to ensure 45° and 90° plane patterns which do indeed pass through the beam peak, and more than one run may be necessary to determine the beam deviation factor of a specific geometry.

Output is available on tables of gain characteristics and the three patterns in the 0°, 45° and 90° planes.

3.3 Elliptical Aperture of Aspect Ratio 1.8

In Table 2.5 of the previous chapter the potentially desirable D and Ω_a combinations were shown. It was found that aperture aspect ratios of 1.5 and 2.0 with D = 3 ft. represented the low gain category of suitable fixed beam antennas. It was also stated that such antennas might be of the paraboloid reflector type.

Figure 3.2 and 3.3 shows the calculated E and H plane patterns of an elliptical aperture paraboloid antenna scaled to the frequency of 11.95 GHz. The major and minor axis of the aperture are A = 37.17 in. and B = 20.66 in. The aspect ratio is thus

$$\Omega_a = \frac{A}{B} = \frac{37.17}{20.66} = 1.8$$

The focal length is F = 35.7 in. With this

$$\frac{F}{B} = 1.73 \qquad \text{and} \qquad \frac{F}{A} = .96$$

The maximum gain of this aperture is G = 38.89 db which is equal to the maximum gain of a D = 2.31 ft. diameter circular aperture. The quantities Ω_a = 1.8 and D = 2.31 ft. are very close the required Ω = 1.5 and 2.0 with D = 3 ft. They are considered here because for this case measured patterns are available from a development program currently under way. The aperture was fed by a TE_{10} mode horn offset by Δ = 9.3 in. The horn dimensions are a = 3.26 in. and b = 1.44 in. These result in a 10 db taper in the primary pattern in the direction of the reflector edges. The field is polarized in parallel with the long dimension of the elliptical reflector. The offset is also in this plane. (Fig. 3.4) Offset in this plane reduces its effect on the edge gain.

Figures 3.5 and 3.6 show the measured E and H-plane patterns of the antenna. The major electrical parameters of the calculated and measured patterns are summarized in Table 3.1 There is an excellent agreement between measured and calculated patterns and also between the major electrical parameters derived from calculation. This could be easily accounted for by random and systematic phase error and feed losses. The overall efficiency for the calculated case is η = 61% and for the measured is 55.5%.

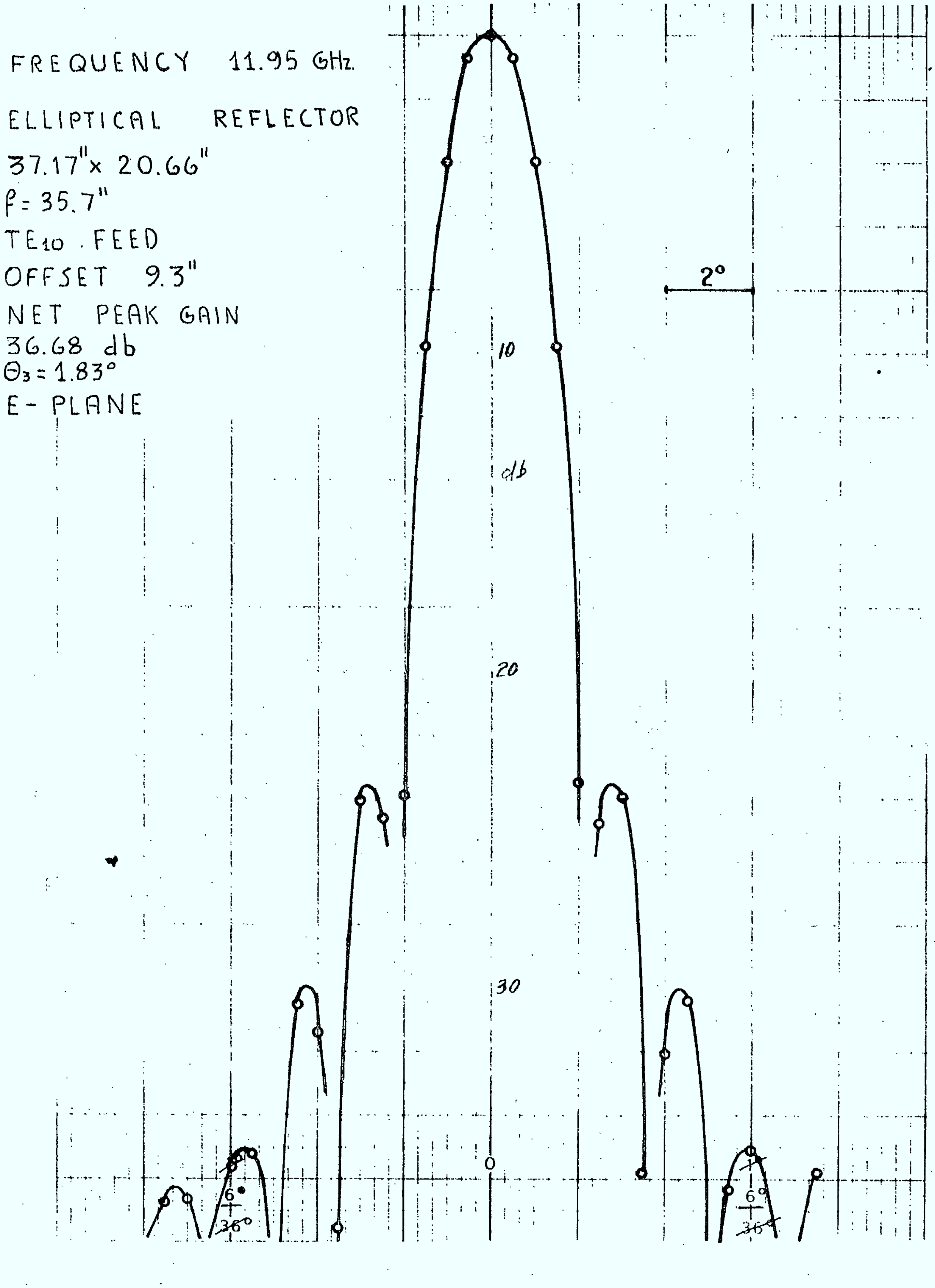

Fig. 3.2 Computed pattern at 11.95 GHz in the E-plane

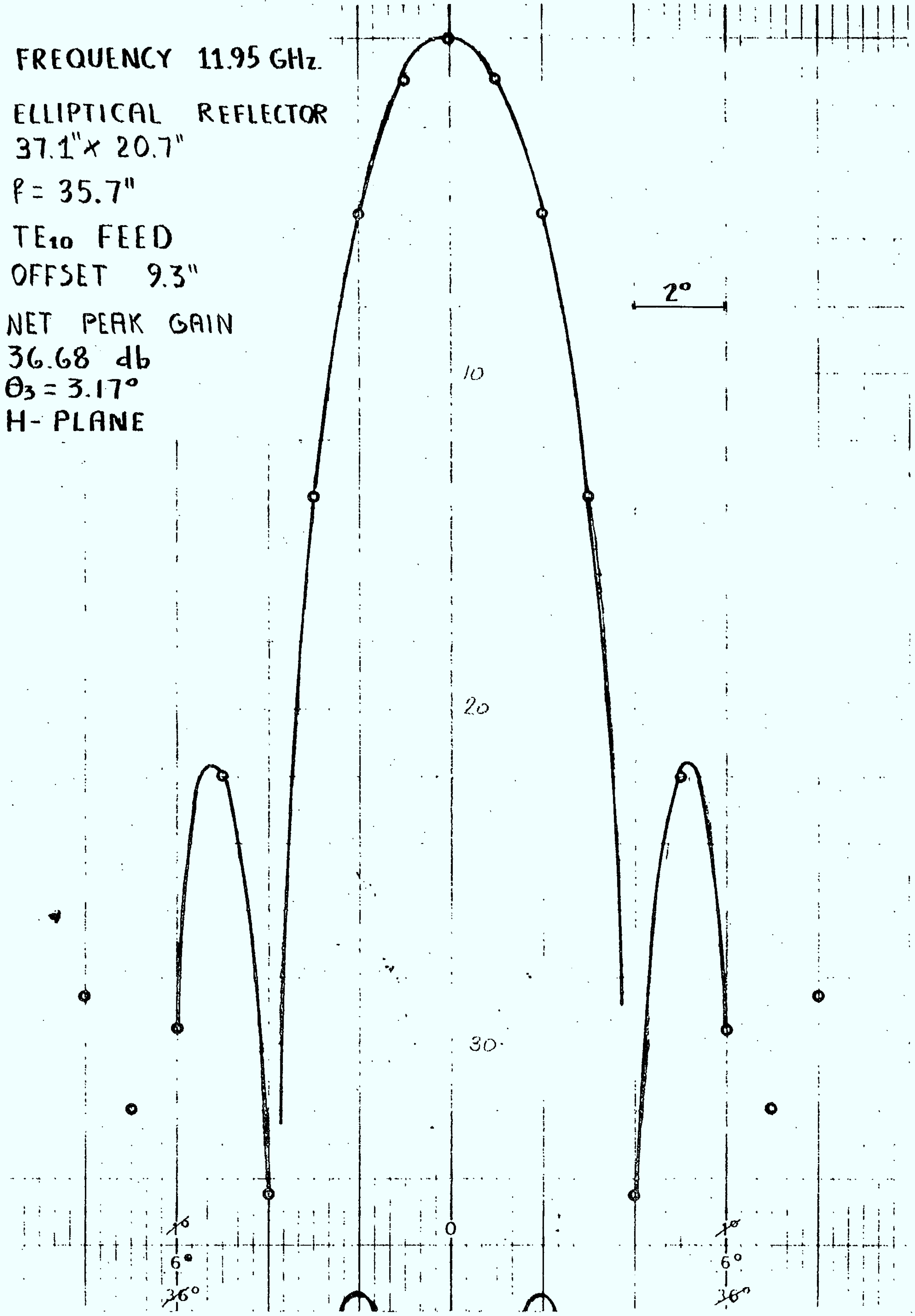

Fig. 3.3 Computed pattern at 11.95 GHz in the H-plane

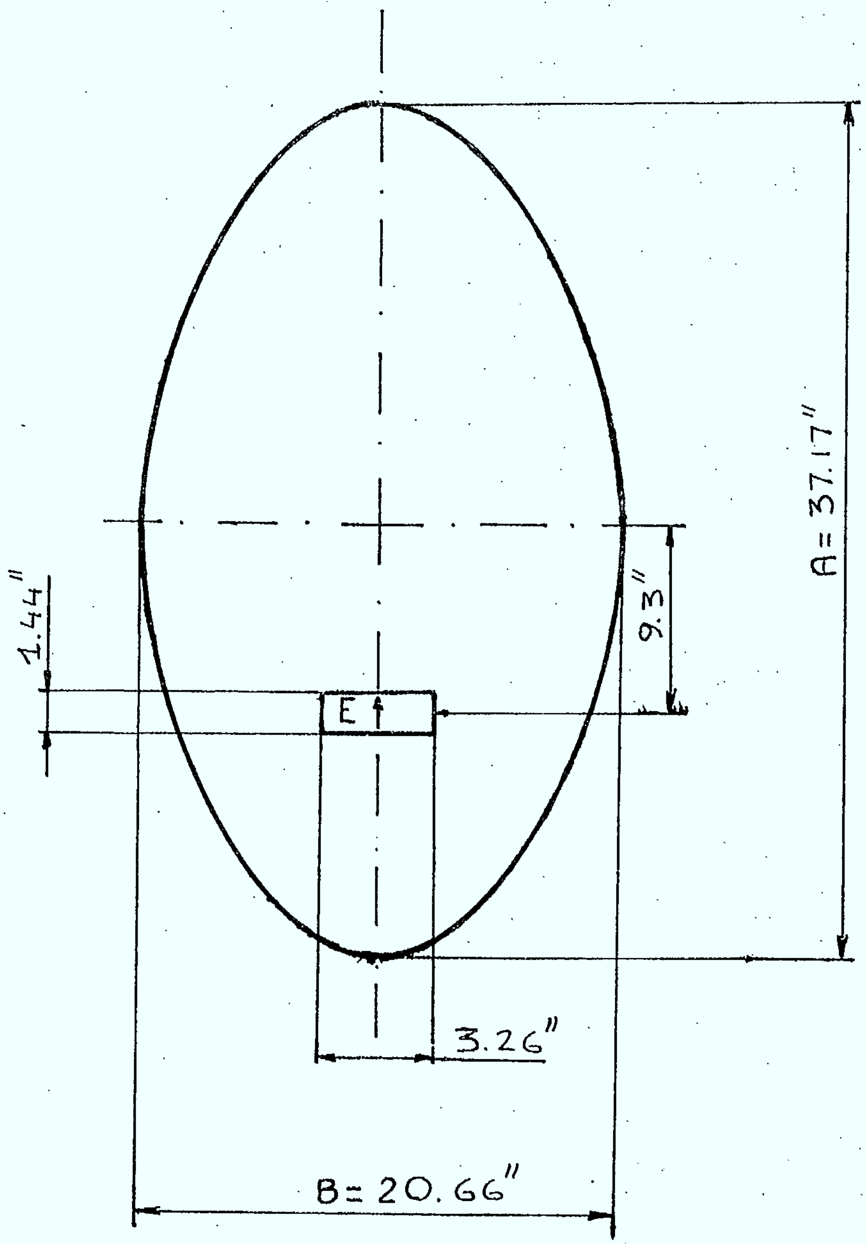

Fig. 3.4 Geometry of the 1.8 aspect ratio elliptical aperture paraboloidal reflector

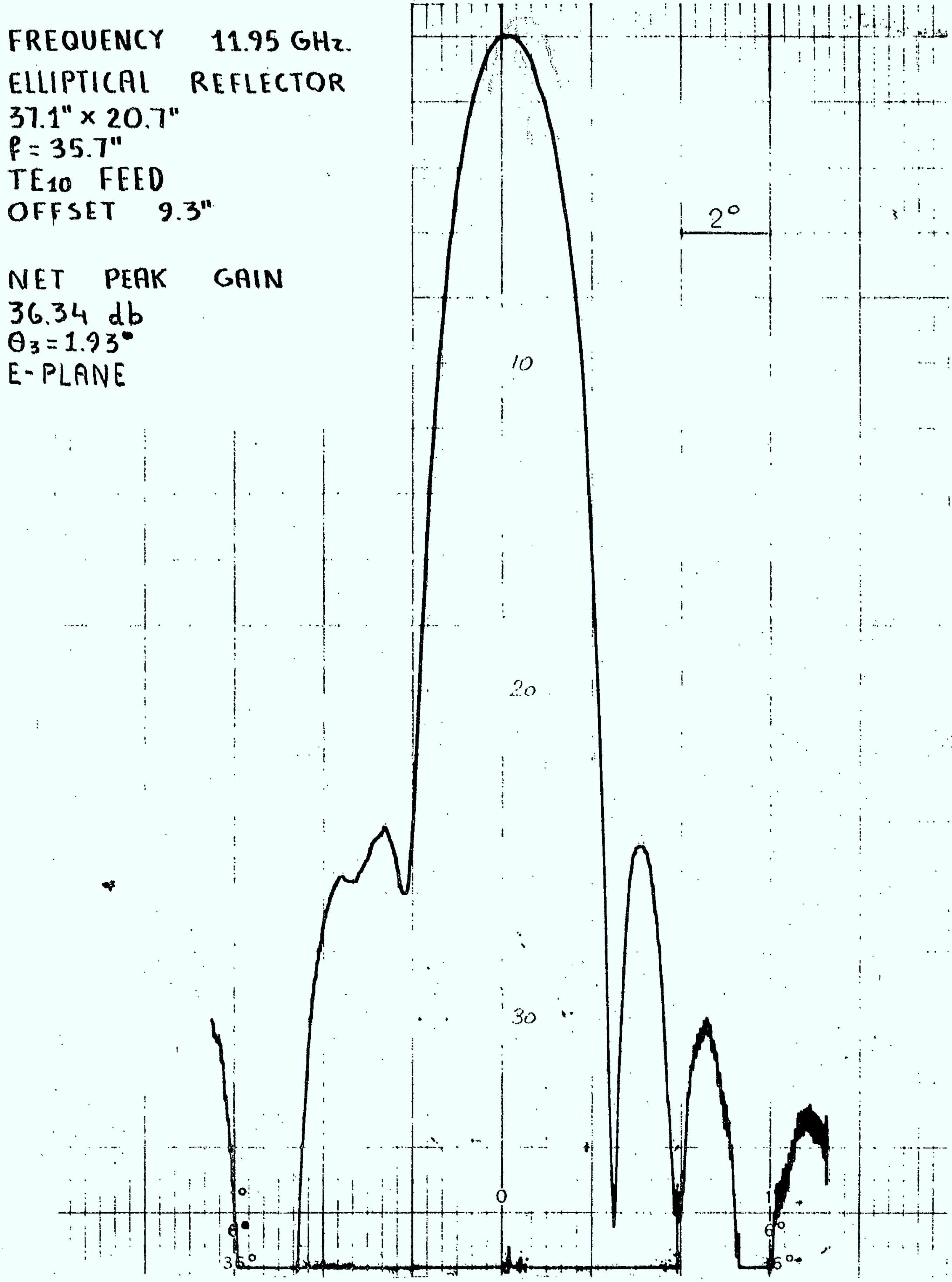

Fig. 3.5 Measured E-plane pattern of the 1.8 aspect ratio elliptical aperture fed by a 3.26 x 1.44 in. rectangular horn.

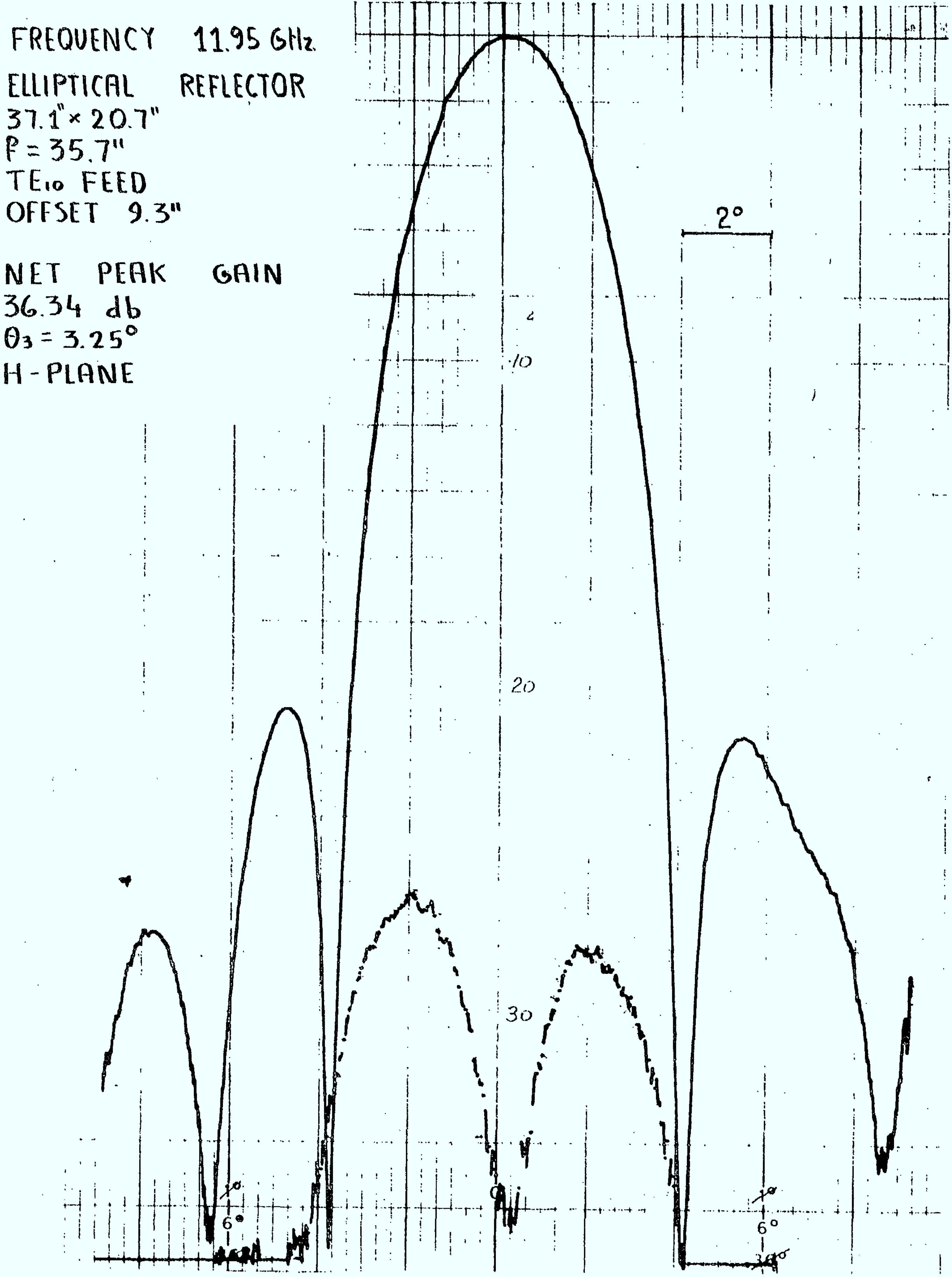

Fig. 3.6 Measured H-plane pattern of the 1.8 aspect ratio elliptical aperture fed by a 3.26 x 1.44 in. rectangular horn

TABLE 3.1

Calculated and Measured Pattern Characteristics of an Offset Fed Elliptical Aperture of Aspect Ratio 1.8

Identification	Offset (in)	3 db Beamwidth (deg.)		Highest Sidelobe Level (db)		Beamwidth Factor		Beam Cross-Section Aspect Ratio	$G = \frac{27000}{\Theta_{3E}\Theta_{3H}}$ (db)	Overall Cross-polarized feed (db below peak)	
		E-plane Θ_{3E}	H-plane Θ_{3H}	E-plane	H-plane	E-plane k_E	H-plane k_H			E-plane	H-plane
Calculated	9.3	1.83	3.17	23.5	21.5	1.20	1.16	1.73	36.68		
Measured	9.3	1.93	3.25	24.0	20.5	1.27	1.19	1.68	36.34	35	26

3.4 Elliptical Aperture of Aspect Ratio 2.5

The elliptical aperture of the aspect ratio 2.8 and an equivalent circular aperture diameter of 6.5 feet was selected for the high gain category for MB_1 (Table 2.5). To avoid excessive computation costs the D = 2 ft. case was calculated with $\mathcal{R}_a = 2.5$ and the results for D = 6.5 ft. were obtained by scaling. The geometry is shown in Figure 3.7. The aperture is defined by A = 49.3 in., B = 123.3 in. and F = 52.3 in. It is fed by a rectangular (horn) aperture of a 0.87 in. and b= 1.57 in. offset by Δ = 12.3 in. The polarization assumed is along the A dimension and the offset is in this plane too. The principal and 45° plane patterns are shown in Figures 3.8 to 3.10. Its calculated characteristics are summarized in Table 3.2

Since the maximum gain of the aperture is Go = 47.9 db the calculated efficiency of the antenna is 2.0 db i.e. 62.5%.

3.5 Aperture Having an Aspect Ratio of 4.78

This high aspect ratio with an equivalent D of 5.5 ft. represents the requirement for the high gain antenna category for the long 2.2° x .46° satellite motion box. Although current systems consideration might favour the shorter 1.43° x .46° motion box, the above mentioned requirement was also investigated. An aspect ratio of 5 would preferably require a different antenna concept nevertheless such paraboloidal reflector characteristics were also calculated for comparative purposes.

For this large aspect ratio aperture a centrally located feed was considered. The dimensions of the aperture are 144.37 in and 30.17 in.

3.5.1 Elliptically Contoured Aperture

The geometry of this aperture and feed layout is shown in Figure 3.11 with designations used in the computer program for two orthogonal polarizations. The primary illumination is provided by a TE_{10} mode feed. Its dimensions were selected for about optimum trade-off between aperture efficiency and spillover efficiency. The primary pattern was to have a 10 db taper at the reflector edge along the major and minor axes of the ellipse. The focal length was selected with the constraint in mind that the waveguide must be above cut-off when the polarization is along the minor axis of the ellipse. (Figure 3.11 (i)) In this case to have

$$\frac{a}{\lambda} > 0.5$$

F/D_H must be $$\frac{F}{D_H} = \frac{F}{B} > \frac{0.5}{2.09} = .239$$

The chosen value of $\frac{F}{B}$ = .3135 (i.e. $\frac{F}{A}$ = 1.5) corresponds to $\frac{a}{\lambda}$ = 0.66

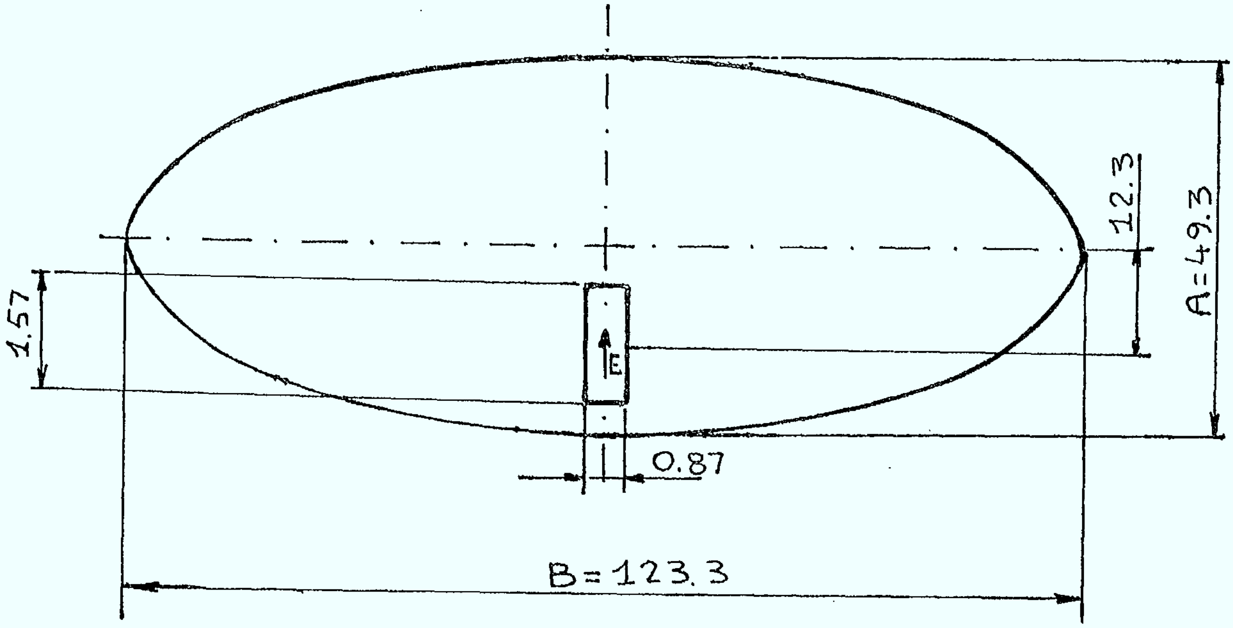

All dimensions are in inches

Fig. 3.7 Geometry of 2.5 aspect ratio elliptical aperture paraboloidal reflector

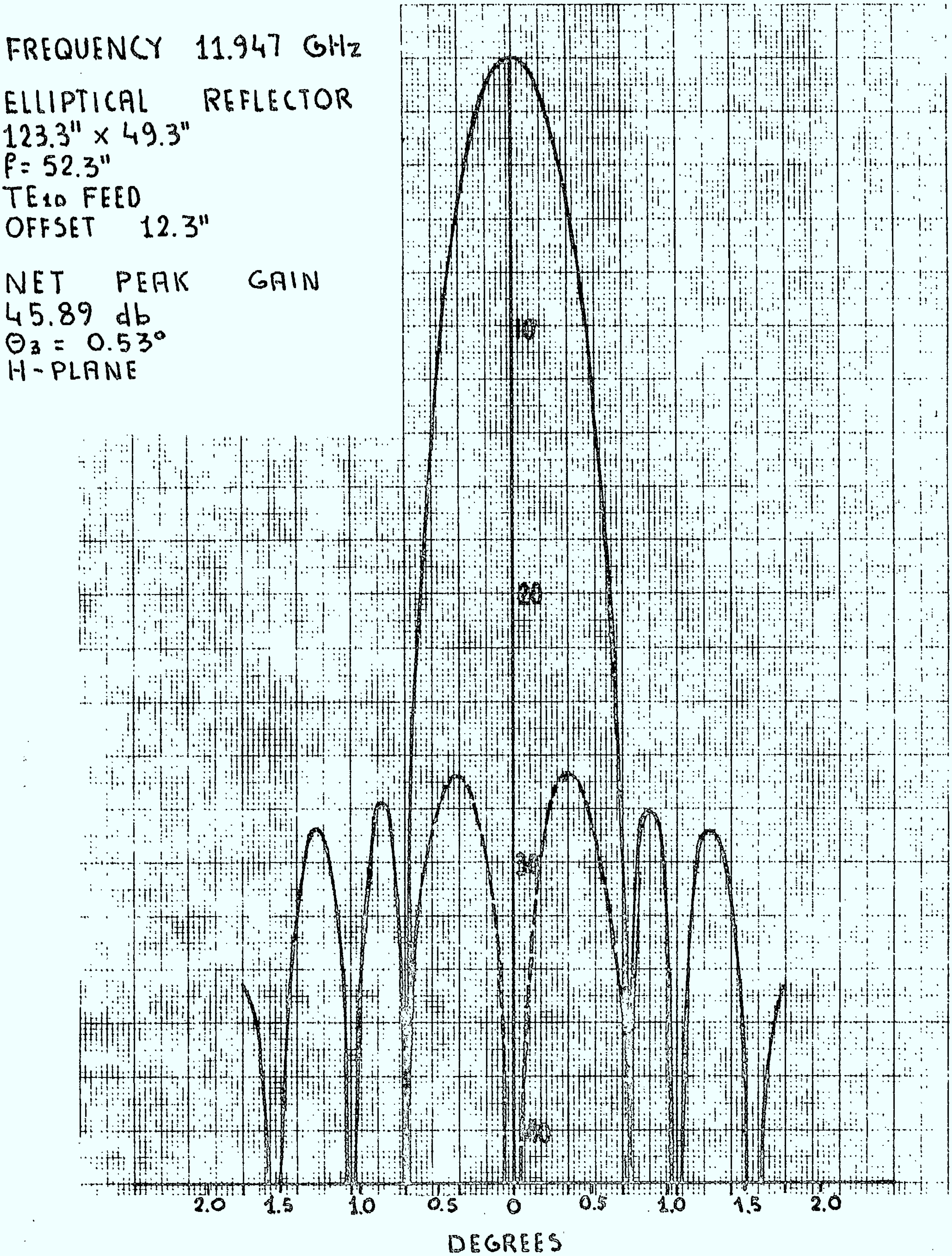

Fig. 3.8 H-plane pattern of a 2.5 aspect ratio elliptical aperture paraboloidal reflector fed by a rectangular horn

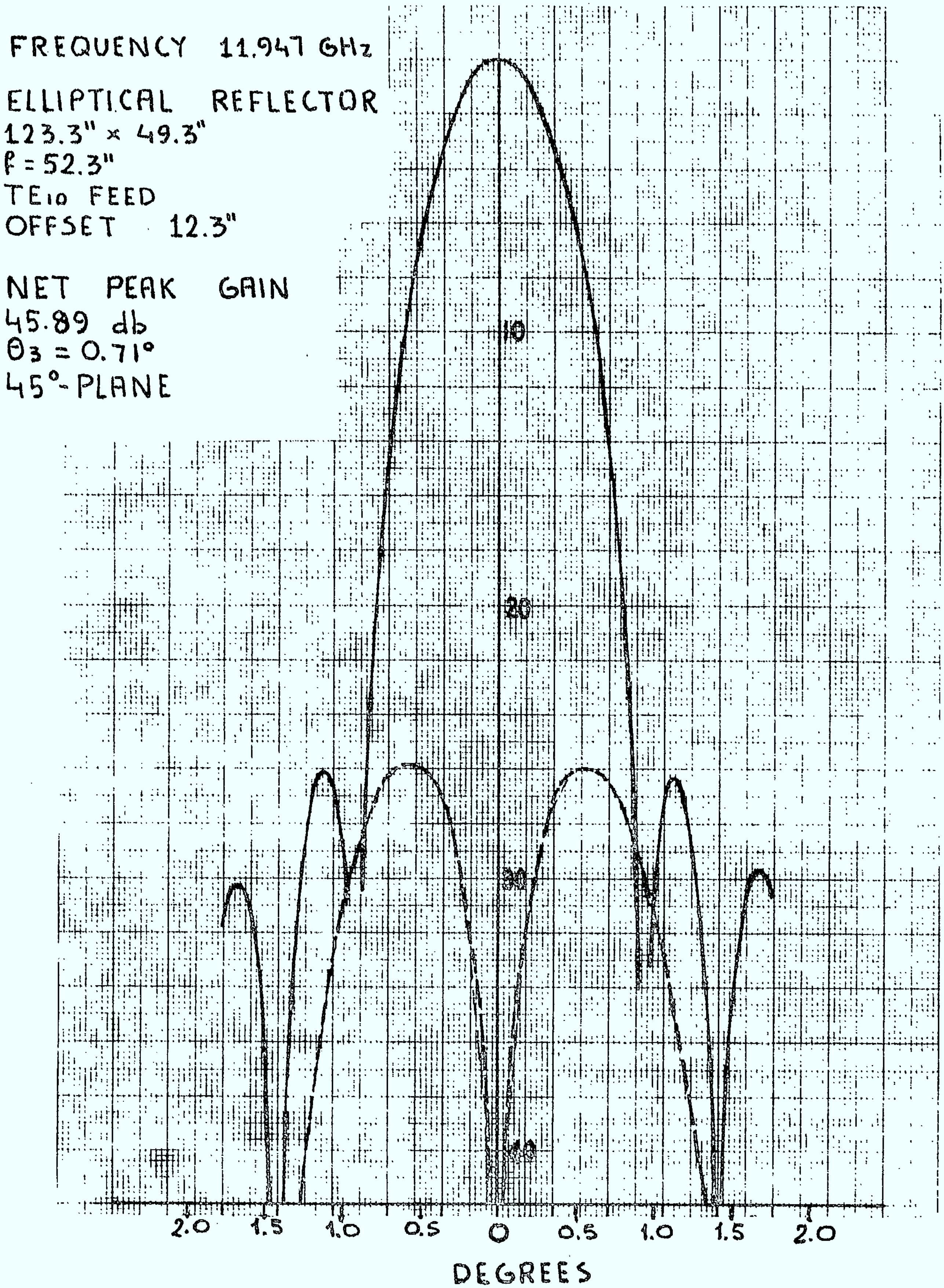

Fig. 3.9 45° plane pattern of a 2.5 aspect ratio elliptical aperture paraboloidal reflector fed by a rectangular horn

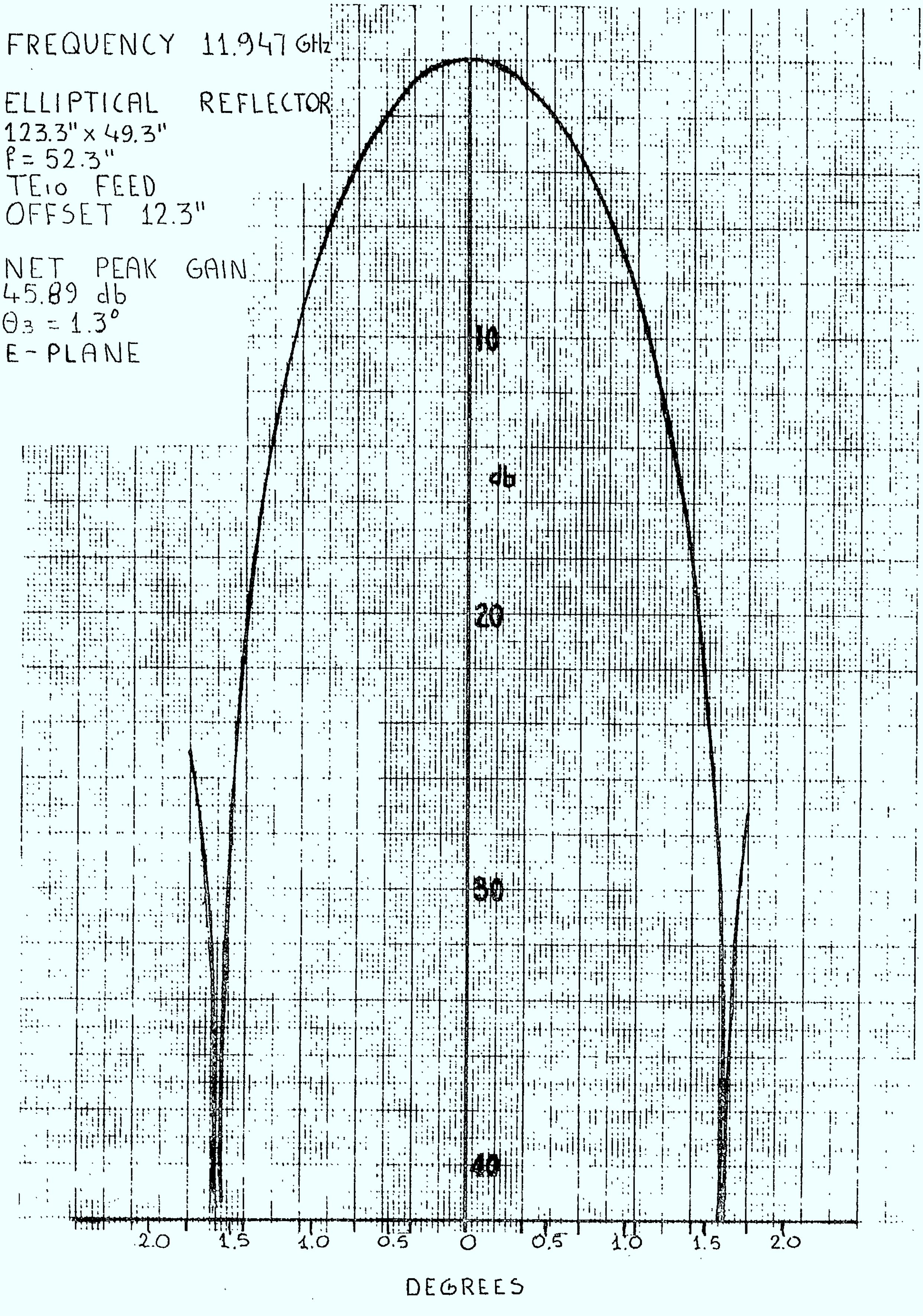

Fig. 3.10 E-plane pattern of a 2.5 aspect ratio elliptical aperture paraboloidal reflector fed by a rectangular horn

TABLE 3.2

Pattern Characteristics of an Offset Fed Elliptically Contoured Paraboloid Reflector With Aspect Ratio 2.5

Offset (in)	3 db Beamwidth deg.			Highest Sidelobe Level (db)		Beamwidth Factor		Beam Aspect Ratio	Overall Cross-Pol. Level (db below Peak)			Gain (db)
	E Θ_{3E}	45° deg.	H Θ_{3H}	E κ_E	H κ_H	k_E	k_H	Ω_b	E	45 plane	H	
12.3	1.3	.71	.53		27.5	1.154	1.139	2.53	40	26	26.5	45.89

A = 49.3 in., B = 123.3 in., F = 52.3 in., λ = .9886 in.

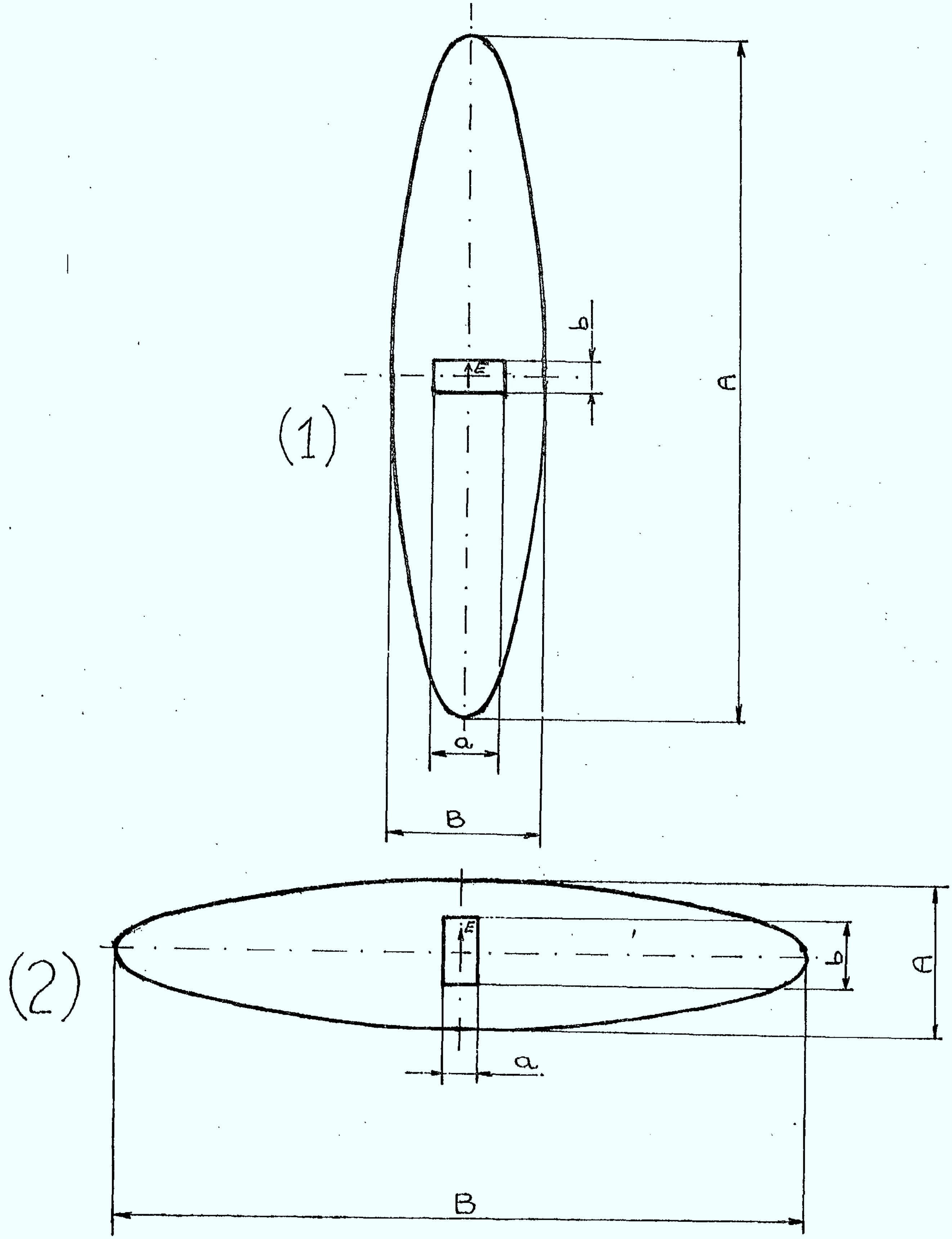

Fig. 3.11 Geometry of the 4.78 aspect ratio elliptical aperture paraboloidal reflector (1) polarized along major axis, (2) along minor axis

The feed aperture dimensions for the polarization along the major axis M are:

$$\frac{a}{\lambda} = 2.09\,\frac{F}{B} = 2.09\,(1.5) = 3.14$$

$$\frac{b}{\lambda} = 1.5\,\frac{F}{A} = 1.5\,(0.3135) = 0.47$$

For the polarization along the minor axis (m) they become $a/\lambda = .66$ and $b/\lambda = 2.25$. Here a and b are the H-and E- plane dimensions of the feed aperture. Patterns for both polarizations wered calculated with a blockage area shown in Figure 3.12. This is somewhat larger than the combined area of the two feed apertures considered above in order to allow for the possible placement of an orthocoupler directly behind the feed. The area blocked by the waveguide feed is determined by the wide dimension of the waveguide providing the m-polarized field.

The principle plane patterns of the M-polarized case are shown in Figure 3.13 while results of the m-polarized case are depicted in Figure 3.14. For the purpose of comparison the M-polarized principle plane patterns were also calculated without blockage (Figure 3.15). In each of these figures the cross-polarized components in the 45° - plane are also included. The basic electrical parameters of these cases are shown in Table 3.3

The gain of the uniformly illuminated aperture is $G_0 = \pi^2 \frac{A}{\lambda} \frac{B}{\lambda} = 46.43$ db. The gain values calculated from the 3 db beamwidths correspond to efficiencies of $\eta \simeq$ 62.5%. The actually achievable efficiency is expected to be lower. One of the so far neglected contributing factors in reducing the maximum gain is phase error contributed by the feed horn. Even an optimistic estimate produces about 0.8 db loss on that account resulting in an efficiency of about 52%.

The computer calculated gain figure for the blocked M polarized case is about .5 db lower than that calculated from the 3 db beamwidths. The spillover loss in the latter case is higher which can account for part of the extra loss. The nature of the numerical integration routine used in computing the gain could also account for part of the differences.

The presented gain figures are still considered accurate enough specially in view of the fact that the major problem is expected in obtaining a feed yielding a reasonable low phase error and corresponding gain loss. This can best be a determined accurately by an experimental evaluation of possible teed configurations.

The cross-polarized level resulting from the reflector is better than 38 db in the 45° plane. The sidelobes in the E-plane changed due to blockage by about 5.5 db to 23 db for the M-polarized case which has an H-plane sidelobe of 18 db.

3.5.2 Rectangularly Contoured Aperture

To examine the effect of aperture contour for this high aspect ratio aperture the patterns of a rectangularly contoured aperture were also calculated. This shape whose proportions are shown in Figure 2.16 (#5) is close to that obtained by cutting a circular paraboloidal reflector by two straight cuts. It thus represents a

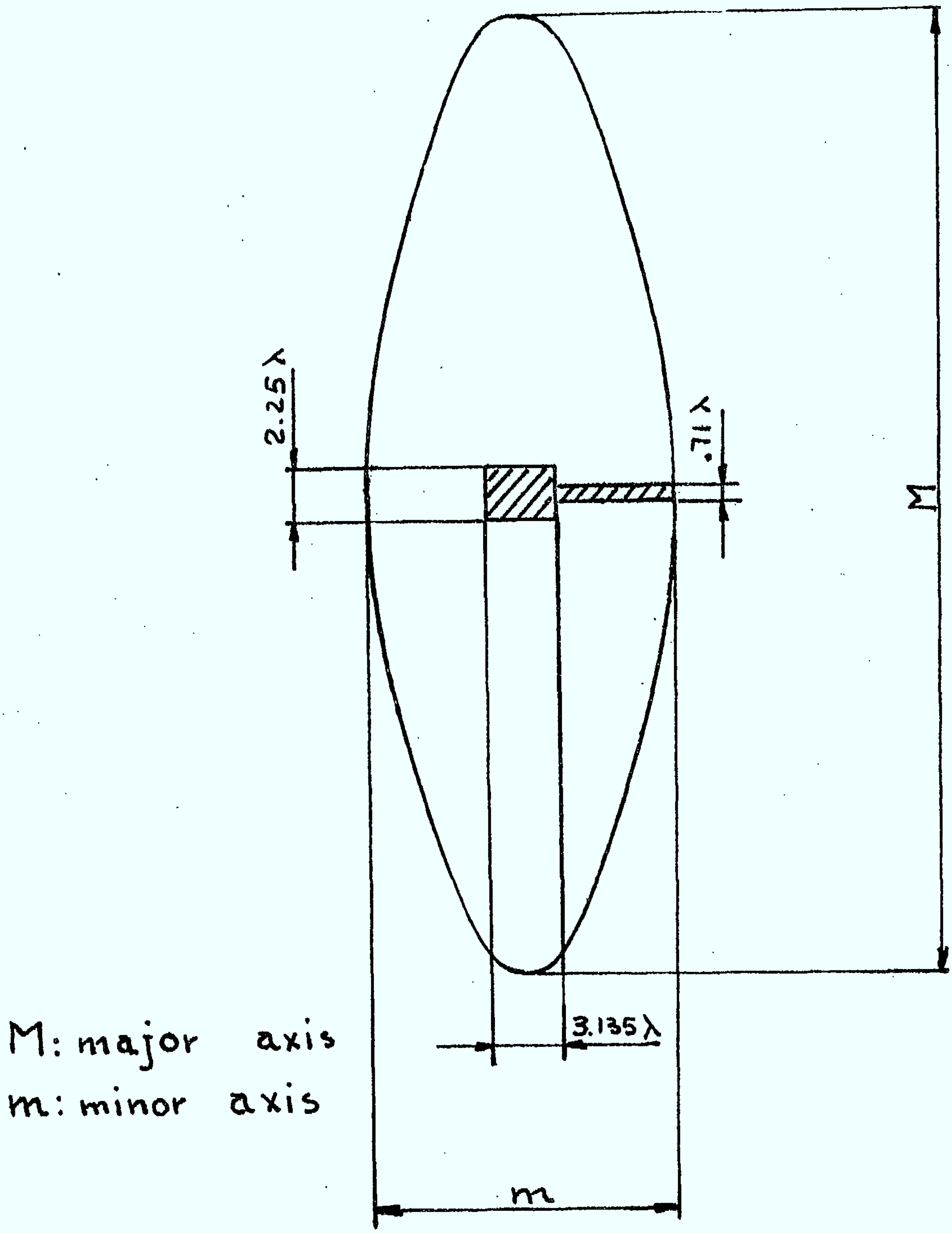

Fig. 3.12 Geometry of aperture blockage

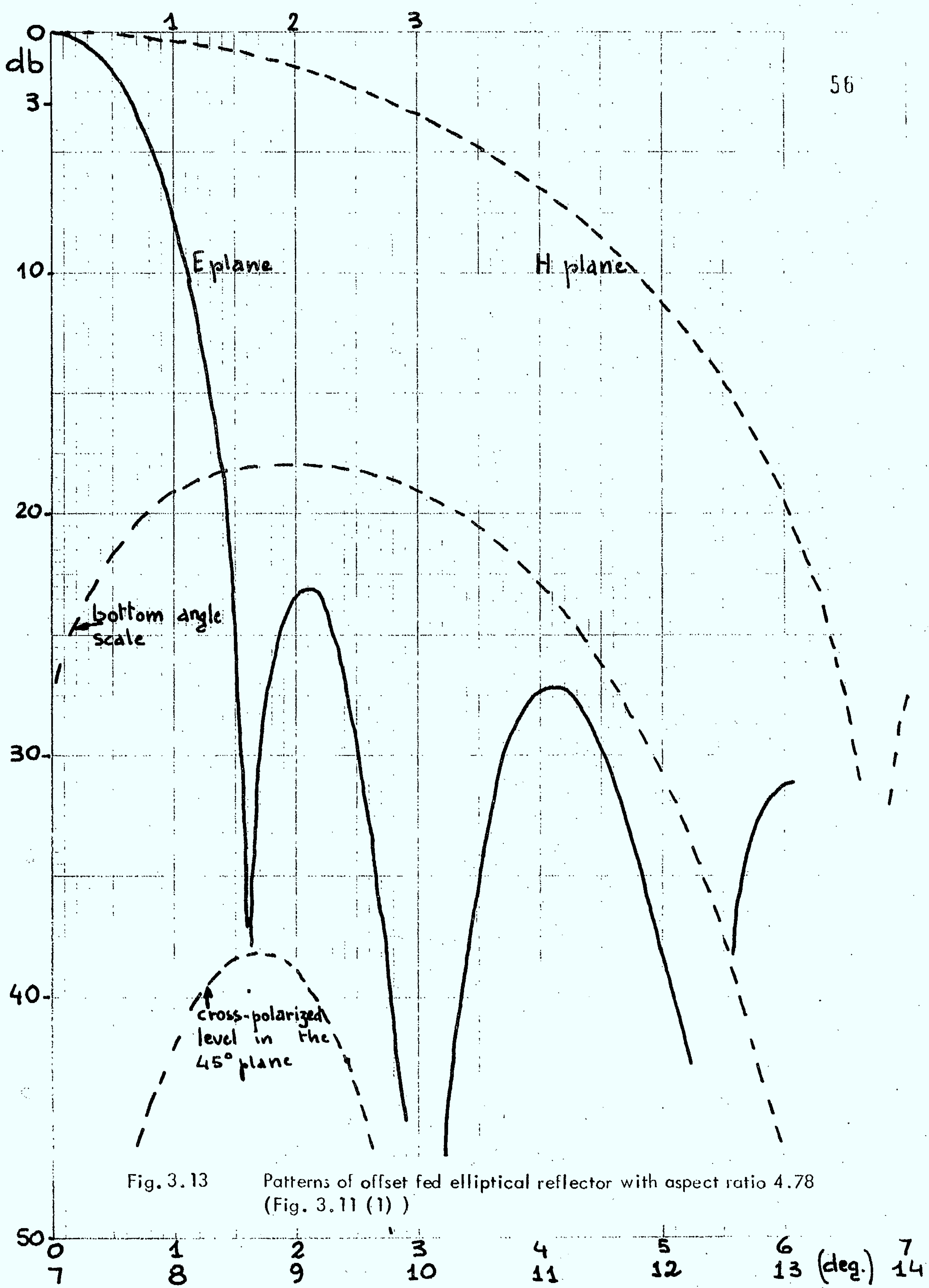

Fig. 3.13 Patterns of offset fed elliptical reflector with aspect ratio 4.78 (Fig. 3.11 (1))

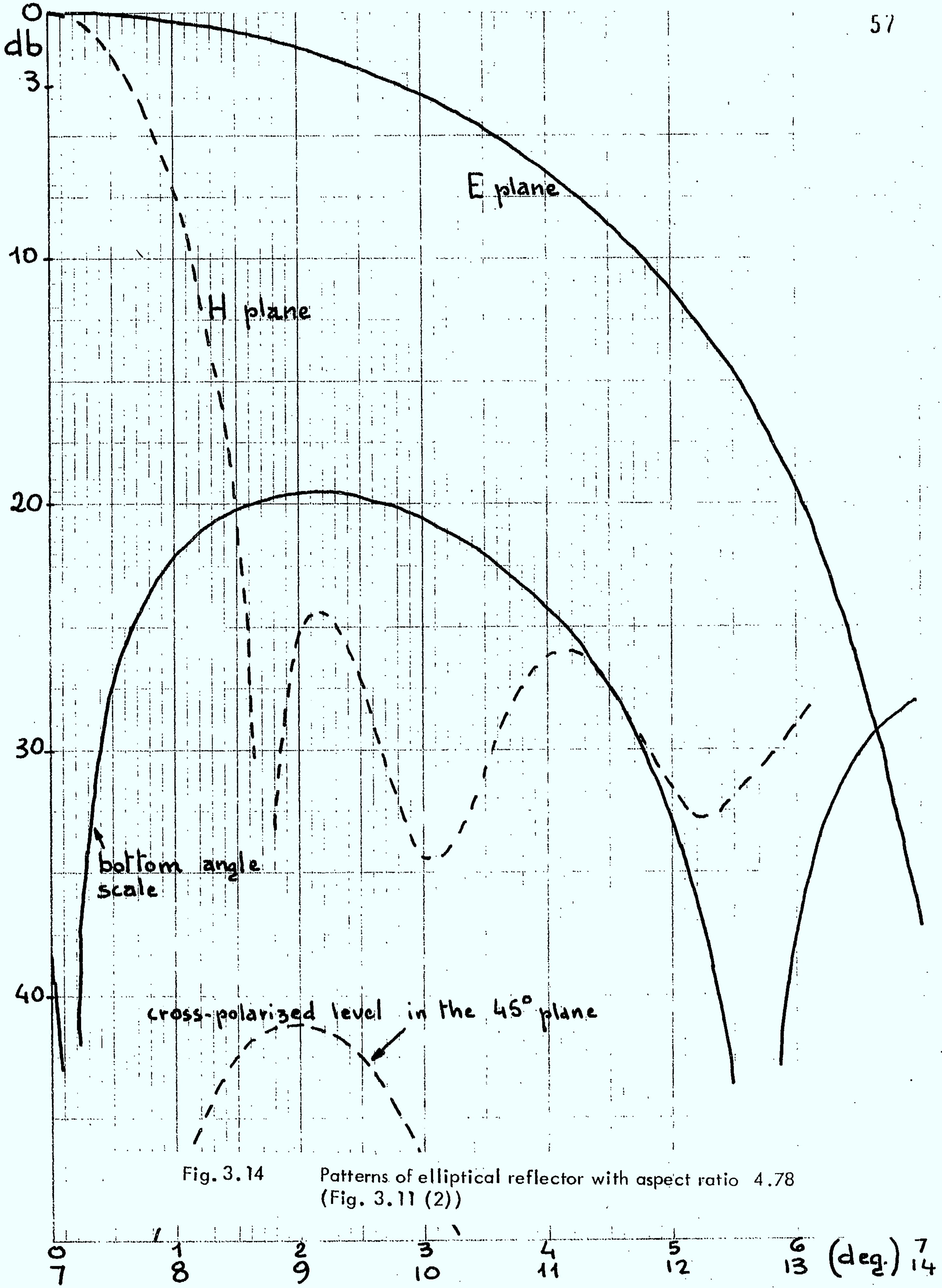

Fig. 3.14 Patterns of elliptical reflector with aspect ratio 4.78 (Fig. 3.11 (2))

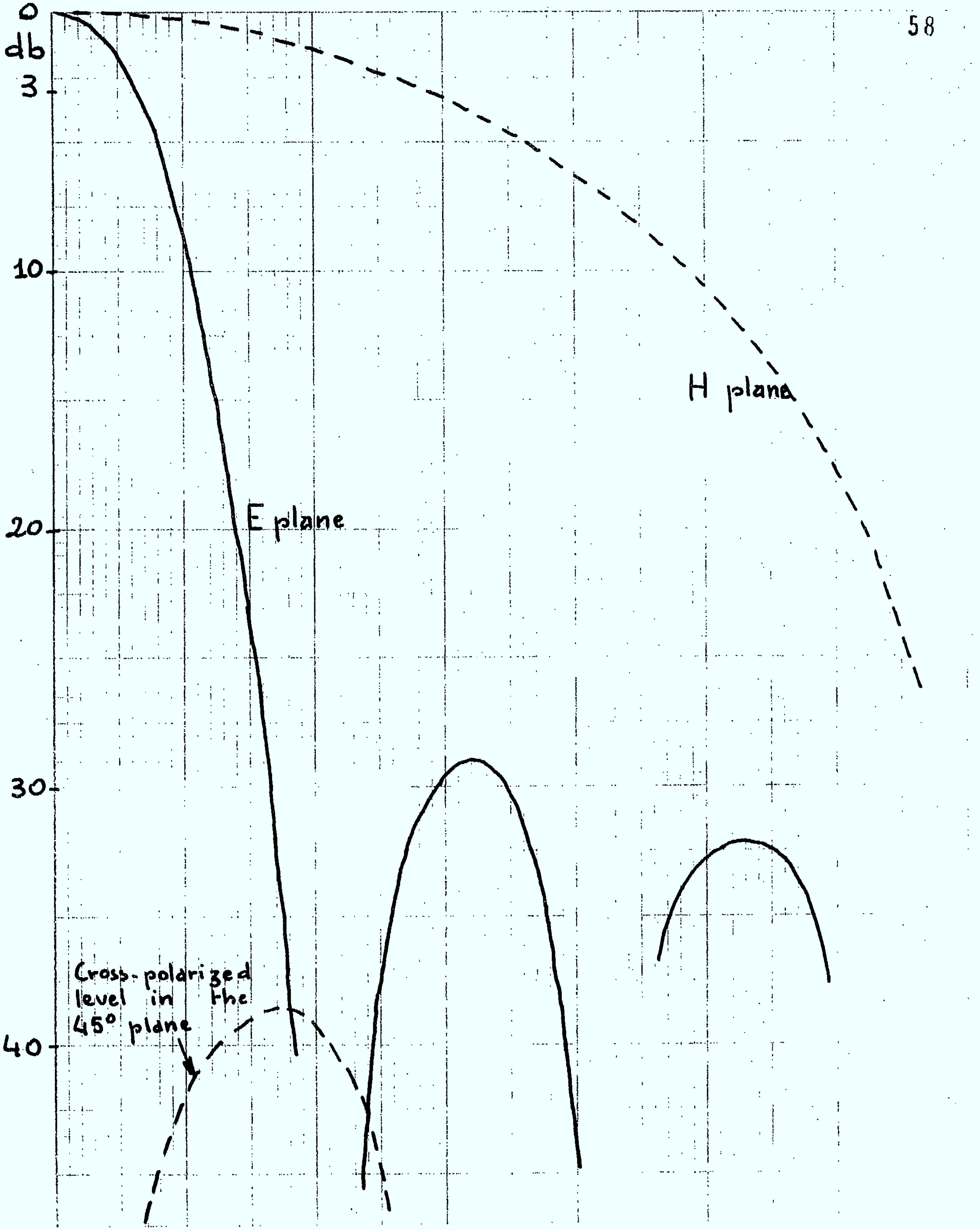

Fig. 3.15 Patterns of centre fed elliptical reflector with aspect ratio 4.78 (calculated without blockage)

TABLE 3.3

Calculated Pattern Characteristics of the Centre Fed Elliptical Aperture With Aspect Ratio 4.8

Direction of Polarization	Blockage	3 db Beamwidth Θ_{3E} deg.		Highest Sidelobe Level K (db)		Beamwidth Factor		Beam Cross-Section Aspect Ratio	Highest Cross-Pol. Level in 45° Plane	$G = \frac{27000}{\Theta_{3E}\Theta_{3H}}$	G Un-Blocked	G Blocked	Obs. Scatter Loss	Spill-Over Loss	Net Gain
		E plane Θ_{3E}	H plane Θ_{3H}	E plane	H plane	E plane k_E	H plane k_H	Ω_b	db	db	db	db	db	db	db
M	yes	.47	2.04	23	18	1.204	1.088	4.32	38	44.47	45.53	45.47	.16	.41	44.9
m	yes	2.04	.48	24	19.5	1.084	1.223	4.24	41	44.42	45.28	45.2	.21	1.07	43.91
M	no	.47	2.07	28.5		1.204	1.103	4.38	38.5	44.43	45.53		0	.41	45.12

NOTE: M: along major axis
m: along minor axis

shape of some fabrication simplicity. The dimensions of the rectangle are 144.37 in. and 30.17 in. The reflector was again centre fed using the same feed aperture dimensions as for the elliptical case. Blockage was also taken into account as in Section 3.5.1. The calculated principal plane patterns of the main-polarized component and the cross-polarized component in the 45° plane for the M-polarized case are shown in Figure 3.16 and those for the m-polarized case in Figure 3.17. The basic characteristics of these patterns are summarized in Table 3.4. The area of this rectangular aperture and the corresponding maximum gain is higher compared to the elliptical aperture of the same major and minor axes by a factor of $4/\pi$ = 1.272 or 1.05 db. The maximum gain of this aperture is 47.48 db.

The gain calculated from the 3 db beamwidths differs from the maximum by 2.01 db for the M polarized case resulting in an efficiency of 62.5%. These figures for the A polarized case are 2.41 db and 57.7%.

In these comparisons, the gain calculated from the 3 db beamwidths is used because its validity is quite well established in practice (Ref. 2), and because the accuracy of the calculated field is high near the axis on the main lobe.

When another 0.8 db is added to the losses to account for quadratic phase error in the feed aperture, the efficiency drops to about 52% and 48%.

The predicted increase in the gain of the rectangular reflector due to the increased area was 1.05 db. The increase in gain calculated from the 3 db beamwidths were for M-polarization 1.0 db, for M-polarization 0.65 db.

The beam cross-section aspect ratio at the 3 db down points ranged for the discussed cases between 4.24 and 4.42, while the major to minor diameter ratio of the reflector was 4.785.

3.5.3 Dual Polarization

For simultaneous transmit and receive operation of two orthogonally polarized waves of different frequencies through a single feed aperture an ortho-mode transducer is necessary. Such component has already been developed for use on the CTS spacecraft. (Fig. 3.18). This orthocoupler has the following characteristics:

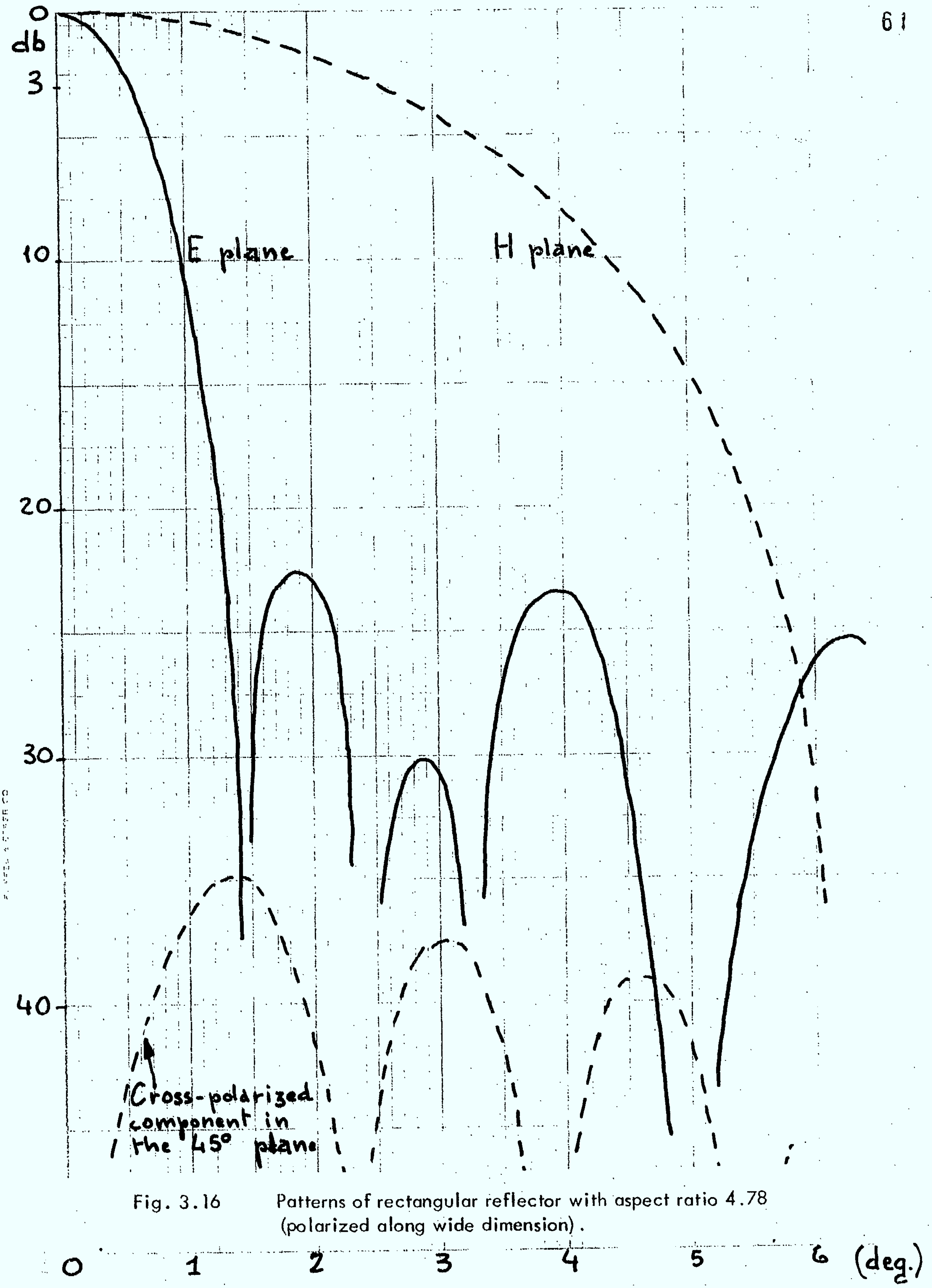

Fig. 3.16 Patterns of rectangular reflector with aspect ratio 4.78 (polarized along wide dimension).

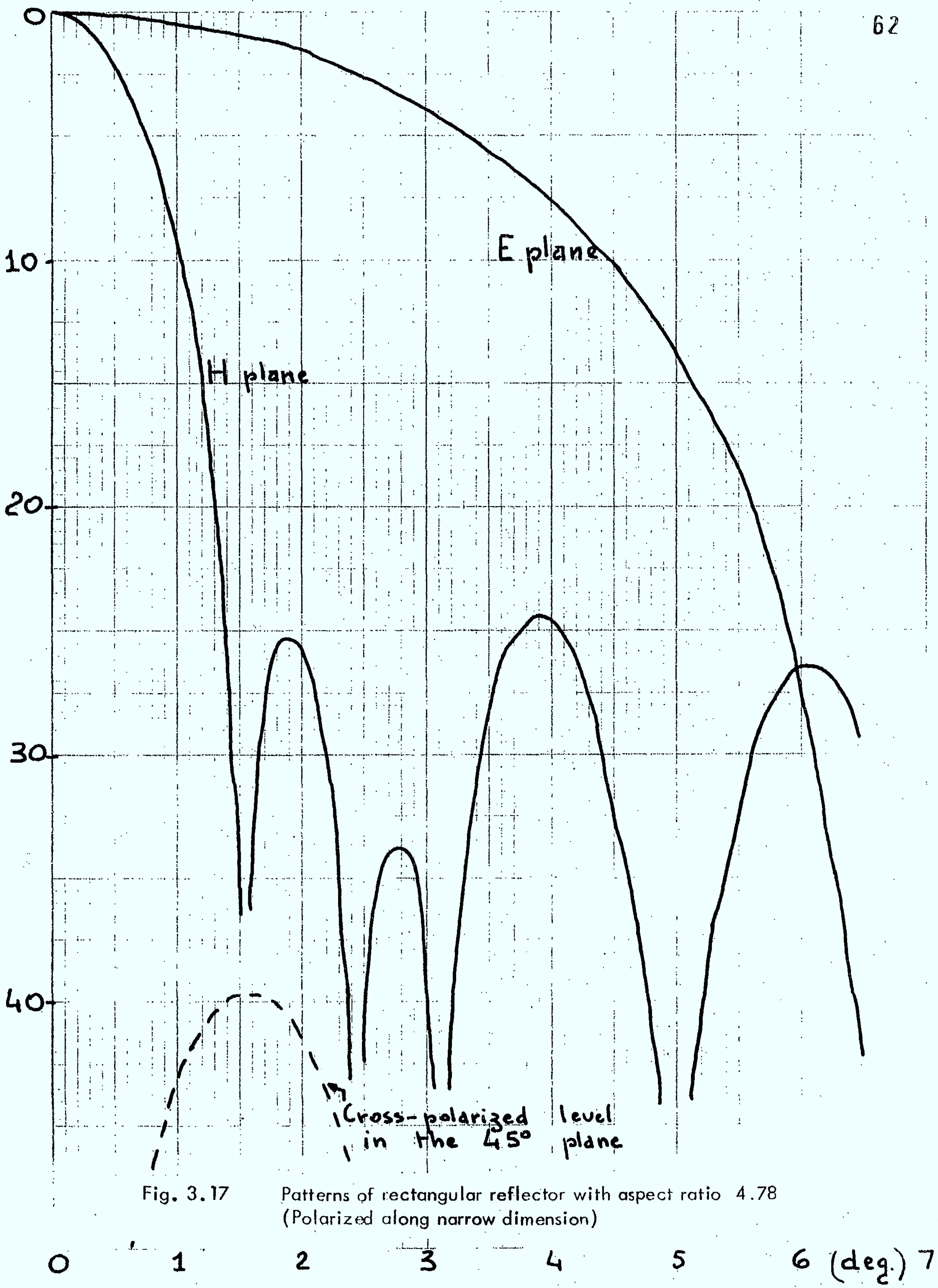

Fig. 3.17 Patterns of rectangular reflector with aspect ratio 4.78 (Polarized along narrow dimension)

TABLE 3.4

Calculated Pattern Characteristics of the Centre Fed Rectangular Aperture With Aspect Ratio 4.8

Direction of Polarization	Blockage	3 db Beamwidth Θ_{3E} deg.		Highest Sidelobe Level $\mathcal{K}$ (db)		Beamwidth Factor		Beam Cross-Section Aspect Ratio	Highest Cross-Pol. Level in 45° Plane	$G = \frac{27000}{\Theta_{3E}\Theta_{3H}}$	G Un-Blocked	G Blocked	Obs. Scatter Loss	Spill-Over Loss	Net Gain
		E plane Θ_{3E}	H plane Θ_{3H}	E plane	H plane	E plane k_E	H plane k_H	Ω_b	db	db	db	db	db	db	db
M	yes	.42	1.82	22.5		1.074	.968	4.31	35	45.47	46.27	46.23	.15	.19	45.88
m	yes	1.93	.44		24.0	1.026	1.112	4.42	39.5	45.10	40.0	45.91	.20	.99	44.72

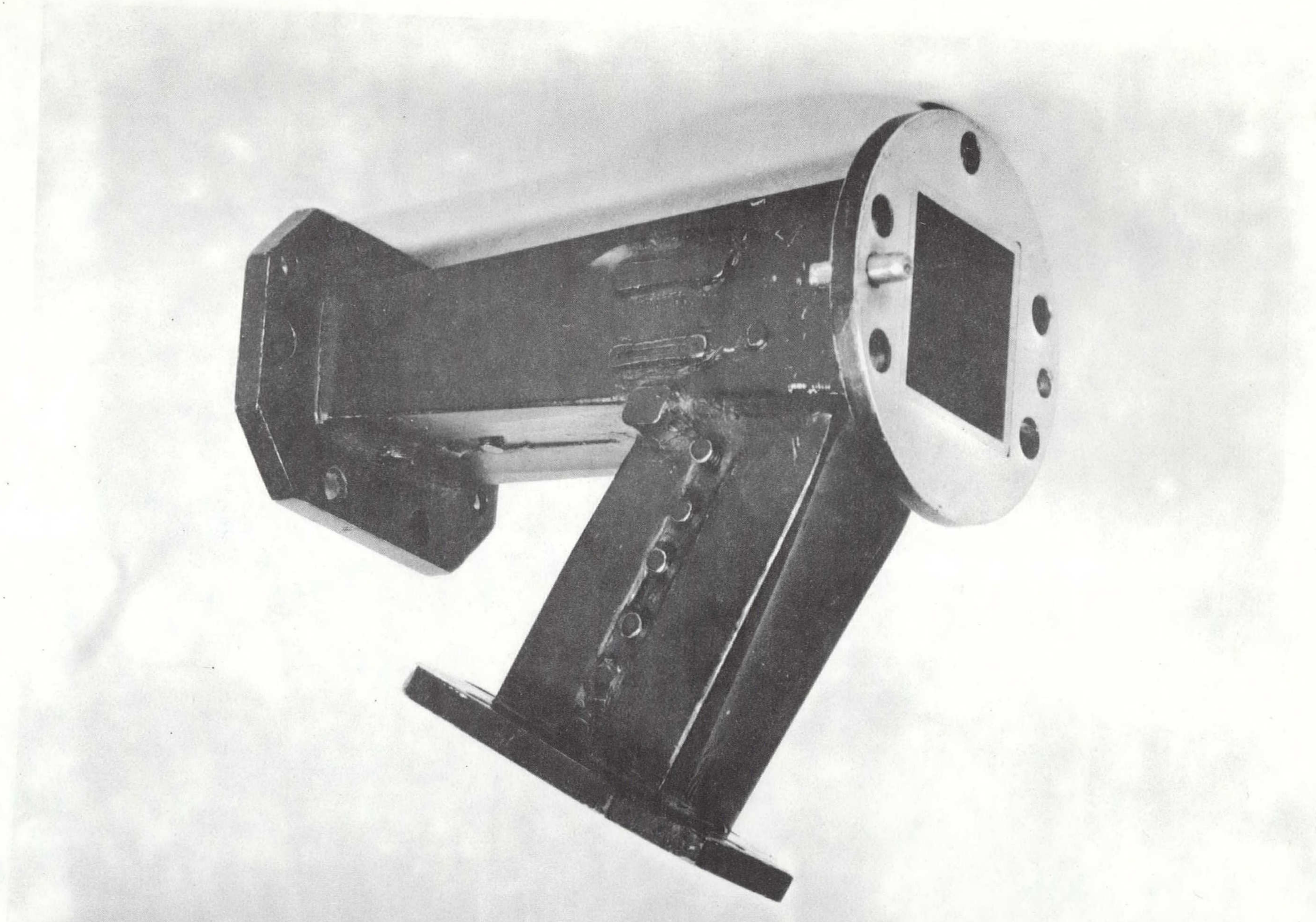

Fig. 3.18 Orthomode transducer

1. Frequency Range:

Straight Port:	11.7 GHz to 12.2 GHz
Side Port:	14.0 GHz to 14.5 GHz

2. Input Reflection Coefficient:

Straight Port:	28 db
Side Port:	23 db

3. Isolation from Straight Port to Side Port:

11.7 GHz to 12.2 GHz	35 db
14.0 GHz to 14.5 GHz	30 db

4. Loss: (either branch) 0.02 db approx.

5. Dimensions:

a) Axial length of coupler	2.38 in.
b) Side dimensions of coupler	2.00 in. approx.
c) Length of square wave-guide to 0.681 in. diameter output circular waveguide port	1.00 in. approx.

The coupler has very low cross-polarized component in its output. This allows the realization of the high isolation between the 12 and 14 GHz terminals. It also helps to achieve low cross-polarized sidelobes in the pattern of a horn following the coupler. The axis of the radiation pattern at the output closely and frequency independently coincides with the mechanical axis of the output port.

3.5.4 Feed Horn Considerations

The feed illuminating the cut paraboloidal reflector commonly is a TE_{10} mode aperture horn. In this study two basic types are to be considered:

(1) Receive only in the extended 11.7 to 12.2 GHz or minimum 11.983 $\pm$ .15 GHz frequency band.

(2) Receive in the above frequency band and transmit in the extended 14.0 to 14.5 GHz or minimum 14.15 $\pm$ .15 GHz frequency band.

The receive and transmit waves are both linearly polarized and orthogonal. This dual polarized case (2) is the technically more difficult one to solve satisfactorily. The first problem is to compensate the beamwidths of the horn for the two orthogonal polarizations. This may be done by fin-loading as shown schematically in Figure 3.19. In this figure the dimensions of the aperture are also shown, expressed in terms of wavelength, for the three major reflector aspect ratios considered.

The second problem is to reduce the effects of phase centre separation between the E and H-plane patterns, and between the two orthogonal polarizations. Several factors effect this problem and a satisfactory solution may require the manipulation of more than one of them. Some of these factors are:

1. A double curvature phase correcting lens over the horn aperture could be used to reduce the first order beam squint between the transmit and receive band. The structure is small and the weight penalty is negligible.

2. The reflector surface might be slightly distorted in the two orthogonal planes. The distortion would amount to a small change in curvature. For large aspect ratio reflectors this can be achieved easier. (Less structural coupling between the orthogonal curvatures).

3. The application of a relatively long focal length reflector also tends to reduce the beam squint for a given phase centre separation. It also has lower cross-polarized levels. The directivity of the primary radiator however has to be increased resulting in longer horn dimensions. The resulting increased blockage is counteracted by offsetting the feed.

4. Beam squint in the plane of the short dimension of the MB has less effect on the edge gain because we have sufficient reserve in that plane and the gain shape at the edge is low .

5. If the feed is not offset the phase centre separation will still cause phase error and corresponding reduction of gain, etc. but the beam squint problem would be reduced. A centre fed system however has blockage problem resulting in higher sidelobe levels, although cross-polarization is less of a problem in this case.

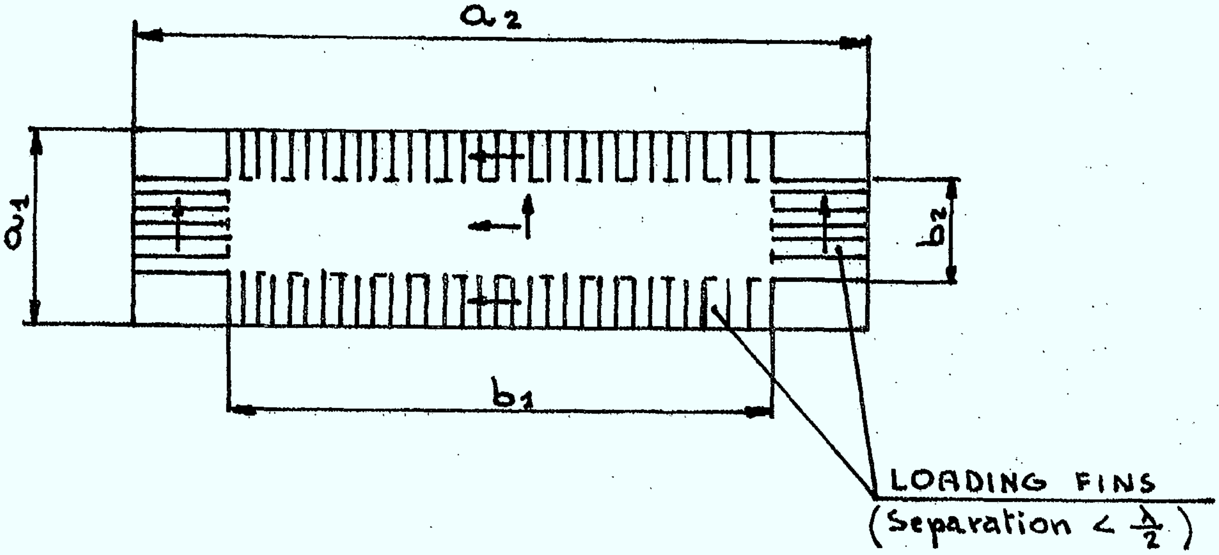

		a_1	b_1	a_2	b_2
$\Omega a = 1.8$	F = 35.7" m = 20.66" M = 37.17"	2.0	2.6	3.6 (3.26)	1.44
$\Omega a = 2.5$	F = 52.3" m = 49.3" M = 123.3"	0.886 (0.87)	1.59 (1.57)	2.21	.64
$\Omega a = 4.79$	F = 45.26" m = 30.17" M = 144.37"	.655	2.4	3.135	.47

Note: a_1, b_1, a_2 and b_2 are in wavelength

Fig. 3.19 Basic geometry of dual polarized fin-loaded rectangular horn aperture

4.0 PARABOLIC CYLINDERS

4.1 Introduction

A common technique for producing fan beams, widely applied in radar antennas is the use of a cylindrical reflector fed by a line source placed at the line focus of the cylinder. The reflector may be parabolic or shaped to yield a desired secondary pattern. This part of the study will examine simple distribution along the longitudinal sources and the tapered illumination in the transverse plane.

Line sources may typically be narrow lens compensated horn, narrow hog-horns, pillboxed paraboloids, or linear arrays of radiating elements. Arrays can be fed by a transmission line either in travelling wave fashion or by means of a branching network. Unless special precautions are taken, the former usually exhibits a frequency-dependent squint which is transformed by the cylindrical reflector directly into the secondary pattern. A slotted waveguide array is a typical linear array. The latter arrays can be designed to be relatively free from squint, but, for a large number of elements, have excessive ohmic loss. This is particularly true at SHF.

The secondary patterns of the parabolic cylinder reflector with a centrally placed (that is, maximum blockage) line source have been studied and computations made of secondary patterns for various aspect ratios, longitudinal to transverse dimension, of the reflector. Most practical applications use line sources completely offset out of the paths of reflected rays. In order therefore, to assess the offset-fed reflector, a fully offset geometry with the line focus opposite the one edge of the reflector has been assumed and further computations made.

Secondary patterns due to different source polarizations source patterns, aspect ratios, and ratios of focal length to transverse dimension, F/D, have been computed and compared.

The patterns of cheese type antennas have also been computed. In this case a flared horn was assumed as the feed.

The computation is extended to the gain and gain variation in the coverage area arising from reflectors with equivalent - area circular apertures of 2 ft. to 7 ft. in diameter.

4.2 The Parabolic Cylinder Fed by a Line Source

4.2.1. General Equations

The coordinate system used in Figure 4.1 will be used throughout this section.

The feed is a line source located along the x-axis which is the focal line of the parabolic cylinder reflector. The E-field polarization may be either in the x direction (longitudinal) or in the ψ direction (transverse). Without loss of generality the line source is located symmetrically with respect to the origin 0.

The parabolic cylinder is defined by $\rho = F \sec^2(\psi/2)$ where F is the focal length, l is the length and D is the height of the cylinder. The angle subtended by the reflector is from Ψ_1 to Ψ_2 where Ψ_1 can be either negative or zero. For a symmetrical reflector it is $2\Psi = 2\Psi_2 = -2\Psi_1$ where $\Psi = 2\tan^{-1}(D/4F)$. The principal planes in which the patterns are calculated are the xz plane (longitudinal, $\Theta = 0$) and the yz plane (Transversal, $\emptyset = 0$). The length of the line source is identical to that of the reflector. The power distribution along x is F(x) and with respect to ψ it is $G(\psi)$. The following relations are satisfied:

$$\int_{-\pi}^{\pi} G(\psi)\, d\psi = 2\pi$$

$$\int_{-\ell/2}^{\ell/2} F(x)\, dx = \ell$$

Applying the current distribution method (Ref. 5) the scattered fields, after dropping some constants are shown to be as follows.

In the transverse plane ($\emptyset = 0$):

$$E_\phi(\theta) = \int_{\Psi_1}^{\Psi_2} [G(\psi)]^{1/2} \sec\frac{\psi}{2}\, e^{-jkF\sec^2\frac{\psi}{2}[1+\cos(\theta+\psi)]}\, d\psi$$

for longitudinally polarized source and

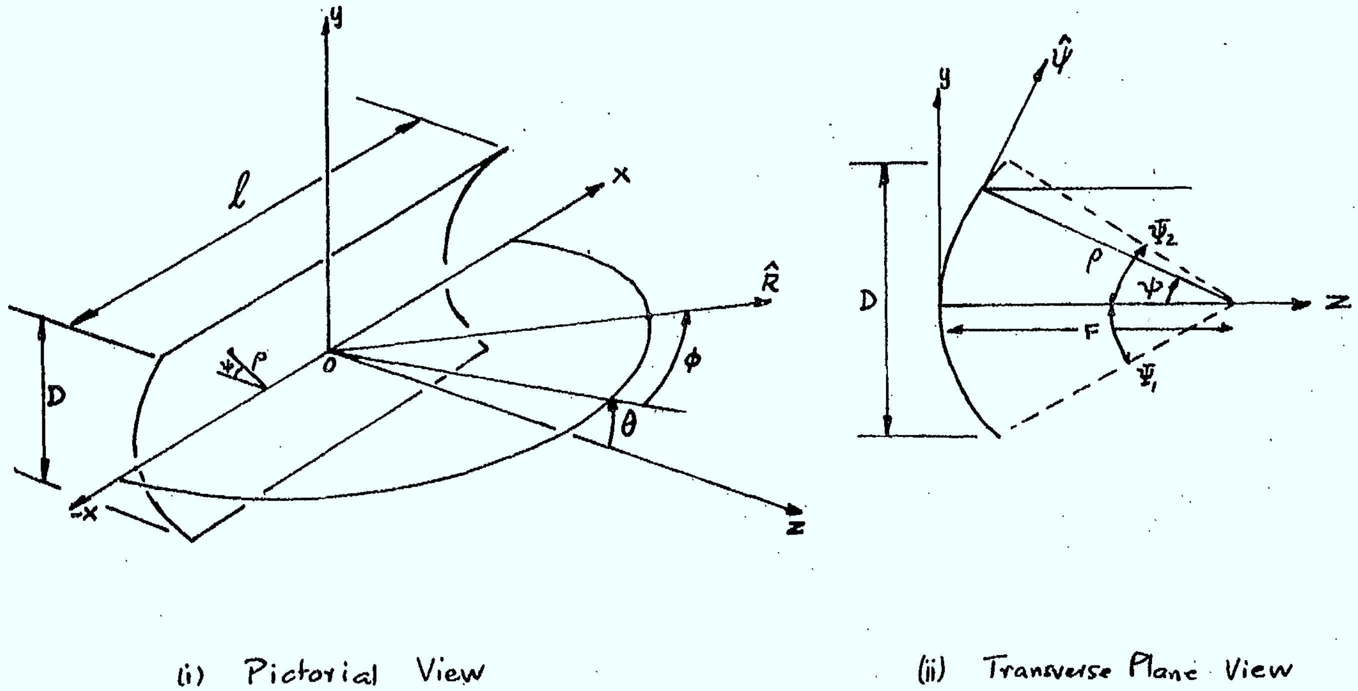

Fig. 4.1 Coordinate system for a parabolic reflector line source

$$E_\theta(\theta) = \int_{\Psi_1}^{\Psi_2} [G(\Psi)]^{1/2} \sec^2\frac{\Psi}{2} \cos\left(\theta + \frac{\Psi}{2}\right) e^{-jkF\sec^2\frac{\Psi}{2}[1+\cos(\theta+\Psi)]} d\Psi$$

for transversally polarized source

In the longitudinal plane ($\Theta = 0$):

$$E_\phi(\phi) = \cos\phi \int_{-\ell/2}^{\ell/2} [F(x)]^{1/2} e^{jkx\sin\phi} dx \int_{\Psi_1}^{\Psi_2} [G(\Psi)]^{1/2} \sec\frac{\Psi}{2} e^{-jkF\sec^2\frac{\Psi}{2}(1+\cos\phi\cos\Psi)} d\Psi$$

for longitudinally polarized source

$$E_\theta(\phi) = \int_{-\ell/2}^{\ell/2} [F(x)]^{1/2} e^{jkx\sin\phi} dx \int_{\Psi_1}^{\Psi_2} [G(\Psi)]^{1/2} \sec\frac{\Psi}{2} e^{-jkF\sec^2\frac{\Psi}{2}(1+\cos\phi\cos\Psi)} d\Psi$$

for transverse polarized source

The above equations are derived under the assumptions that

$$\ell \gg \lambda \qquad \rho_{max} < \ell^2/\lambda$$

i.e. the field incident on the reflector is essentially a cylindrical wave and the effect of finite length of source and reflector can be neglected.

These limitations may be removed by placing two parallel plates at the ends of the cylinder. The equations can thus be applied to cheese and pillbox antennas as well.

The gain and gain factor for a source of either polarization are

$$G = \frac{\ell D}{2\lambda^2} \cot\frac{\Psi_2 - \Psi_1}{2} \left[\frac{1}{\ell}\int_{-\ell/2}^{\ell/2} [F(x)]^{1/2} dx\right]^2 \left[\int_{\Psi_1}^{\Psi_2} [G(\Psi)]^{1/2} \sec\frac{\Psi}{2} d\Psi\right]^2$$

$$g = \frac{G}{4\pi A/\lambda^2}$$

From the above equations some conclusions may be derived:

1. The field pattern in the transverse plane is independent of the source pattern in the longitudinal plane while the pattern in the longitudinal plane is dependent on the source pattern in the transverse plane but the dependency is of second order importance only.

2. The effect of different polarizations on the field pattern can be observed only at large angles from the axis.

3. If the source patterns and the F/D ratio of the reflector are kept constant the gain is proportional to the aperture area and the gain factor is constant.

For the numerical evaluation of the various field components, gain, and gain factor for any desired reflector geometry and source distribution computer programs have been developed. Their listing is shown in Appendix .

4.2.2. Source Equations

For the calculations of field patterns and gain in this chapter simple but practical source patterns are assumed. Measured source patterns may also be included in the computer program.

For most calculations the source patterns were assumed to have about 10 db tapering towards the edge of the reflector.

The assumed power distribution along x is

$$F(x) = a + b\cos^n\left(\frac{\pi x}{\ell}\right)$$

Here n, a and b are constants selected to produce a required pattern. To satisfy $\int_{-\ell/2}^{\ell/2} F(x)\,dx = \ell$, the following relation must hold:

$$a + \frac{b}{\sqrt{\pi}}\,\frac{\Gamma\left(\frac{n+1}{2}\right)}{\Gamma\left(\frac{n}{2}+1\right)} = 1$$

where $\Gamma\left(\frac{1}{2}\right) = \sqrt{\pi}$ is useful in using this equation.

The tapering in dB is related to a and b by

$$DB = 10\log_{10}\left(1 + \frac{b}{a}\right)$$

The angular distribution selected is of the form

$$G(\psi) = C\cos^m\left(\frac{\psi}{2}\right)$$

Assuming a front to back ratio of infinity the far-field pattern is contributed by the scattered field only. To satisfy the condition

$$\int_{-\pi}^{\pi} G(\Psi)\, d\Psi = 2\pi$$

we must have

$$C = \sqrt{\pi}\; \frac{\Gamma\left(\frac{m}{2}+1\right)}{\Gamma\left(\frac{m+1}{2}\right)}$$

Here m is related to the tapering through the equation

$$DB = m \times 10 \log_{10} \cos \frac{\Psi}{2}$$

An alternate expression for F(x), which makes it similar to G(Ψ) in form, is

$$F(x) = a \cos^n \left(\frac{\pi x}{b\ell}\right)$$

Here n and b can be determined from the distribution curve and the normalization constant "a" from the relation $\int F(x)dx = 1$

4.2.3. Fully Offset Fed Parabolic Cylinder

The centre fed case (See Section 4.2.4) obviously suffers from blockage by the feed. A partial offset of the feed may notbe a practical solution if for example a pillbox is used for the feed. Such a feed would block completely a good part of the aperture. Partial offset might be used to advantage with a linear array type feed. However, in the present case full offset has been assumed.

As a consequence the amplitude distribution across the aperture in the transverse plane becomes asymmetric. By changing the beam direction of the primary source this distribution and the resulting secondary pattern may be effected. To evaluate the importance of this effect the aperture distribution, the far-field pattern and gain factor have been calculated for the following cases: (1) the beam centre coincident with the aperture centre, (2) the maximum field being at the aperture centre, (3) the tapering being equal at the two edges, and for comparison (4) centre fed case. For all cases the source distribution in the transverse plane was kept unchanged: $G(\psi) = 4.06 \cos^{10}(\psi/2)$ (10 db down at 75^{o}). The aperture aspect ratio was $\ell/D = 1$ and $F/D = 0.326$ and the area of the aperture was equal to that of a 2 ft. diameter dish. The aperture distributions are shown in Figure 4.2 and the far-field patterns in Figure 4.3 . Based on these results the case having equal taper at the edges has been used for most comparative calculations because it provided the highest gain factor at the expense of a slightly higher sidelobe. The main beam has been found insensitive to these changes.

The effect of F/D on the gain and gain factor was evaluated for an $\ell/D = 5$ aperture equivalent to a 2 ft. diameter dish. The source distributions have been selected for 10 db taper at $\psi = 75^{o}$ a quite practical figure. The results are shown in Figure 4.4 . The selected F/D = .326 results in a gain factor close to the maximum (78.5%). The field patterns in the transverse plane are plotted in Figures 4.5 and 4.6 . . For low values of F/D the first null is filled in and the near in sidelobe becomes a shoulder. The level of this shoulder 17 db down is almost optimally lowest for F/D = 0.326. The patterns also show some asymmetry due to the feed offset. The longitudinal pattern shown in Figure 4. 7 indicates some slight effects on the height of far off sidelobes only. The aperture distributions corresponding to the F/D values for which the patterns were calculated are shown in Figure 4.8 .

The far-field patterns corresponding to a 15 db tapered reflector have also been calculated and in Figures 4. 9 to 4. 11 they are compared to the 10 db tapered case. In the transverse plane the more highly tapered distribution produces a wider beam and no improvement at the shoulder. Only the second sidelobe levels drop by about 5 db. The gain factor also drops from 78.3% to 68.3%. The effect in the longitudinal plane is normal i.e. wider main lobe, lower sidelobes.

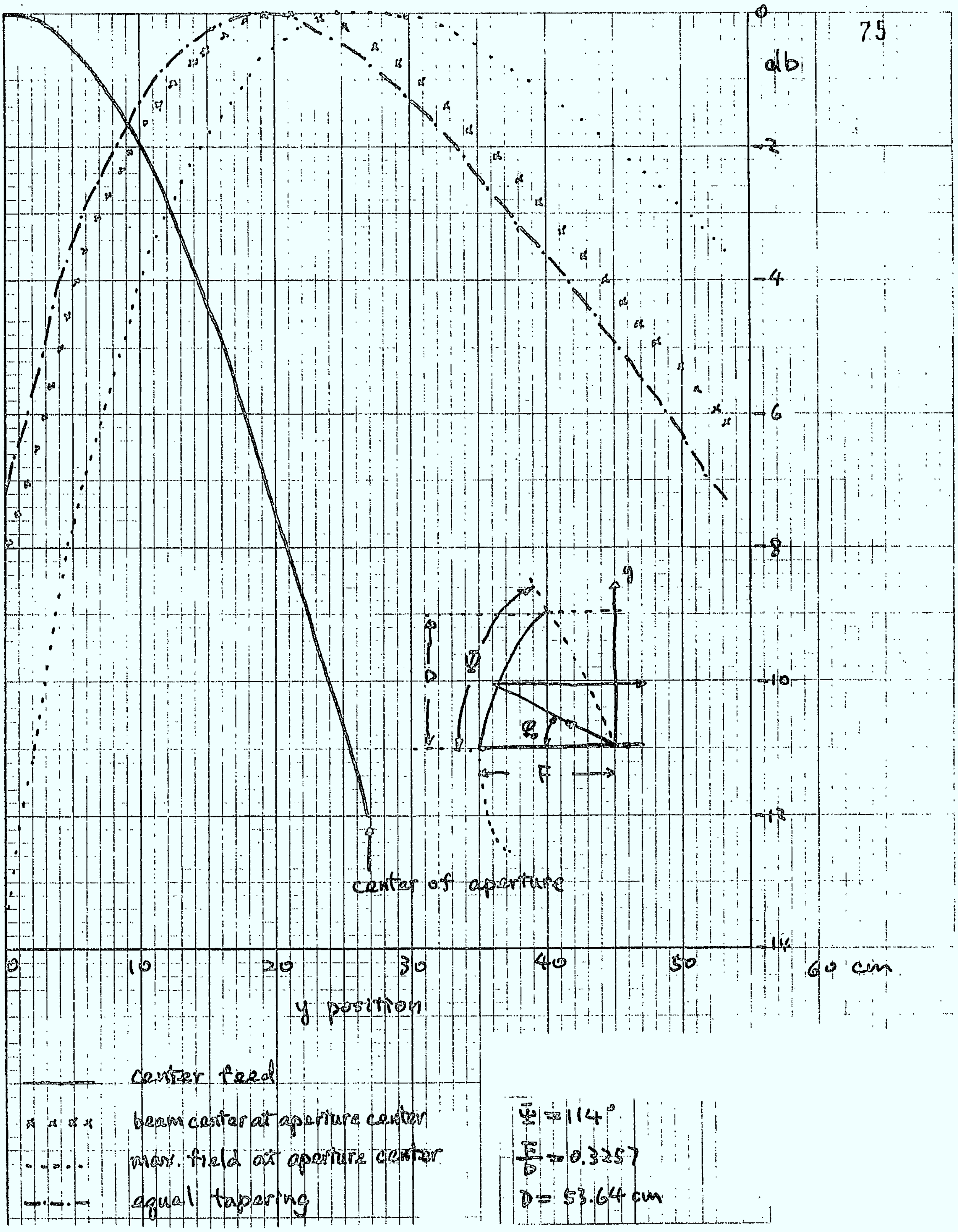

Fig. 4.2 Field distribution in the aperture plane containing the parabolic cylinder for various positions of the axis of the main beam of the source.

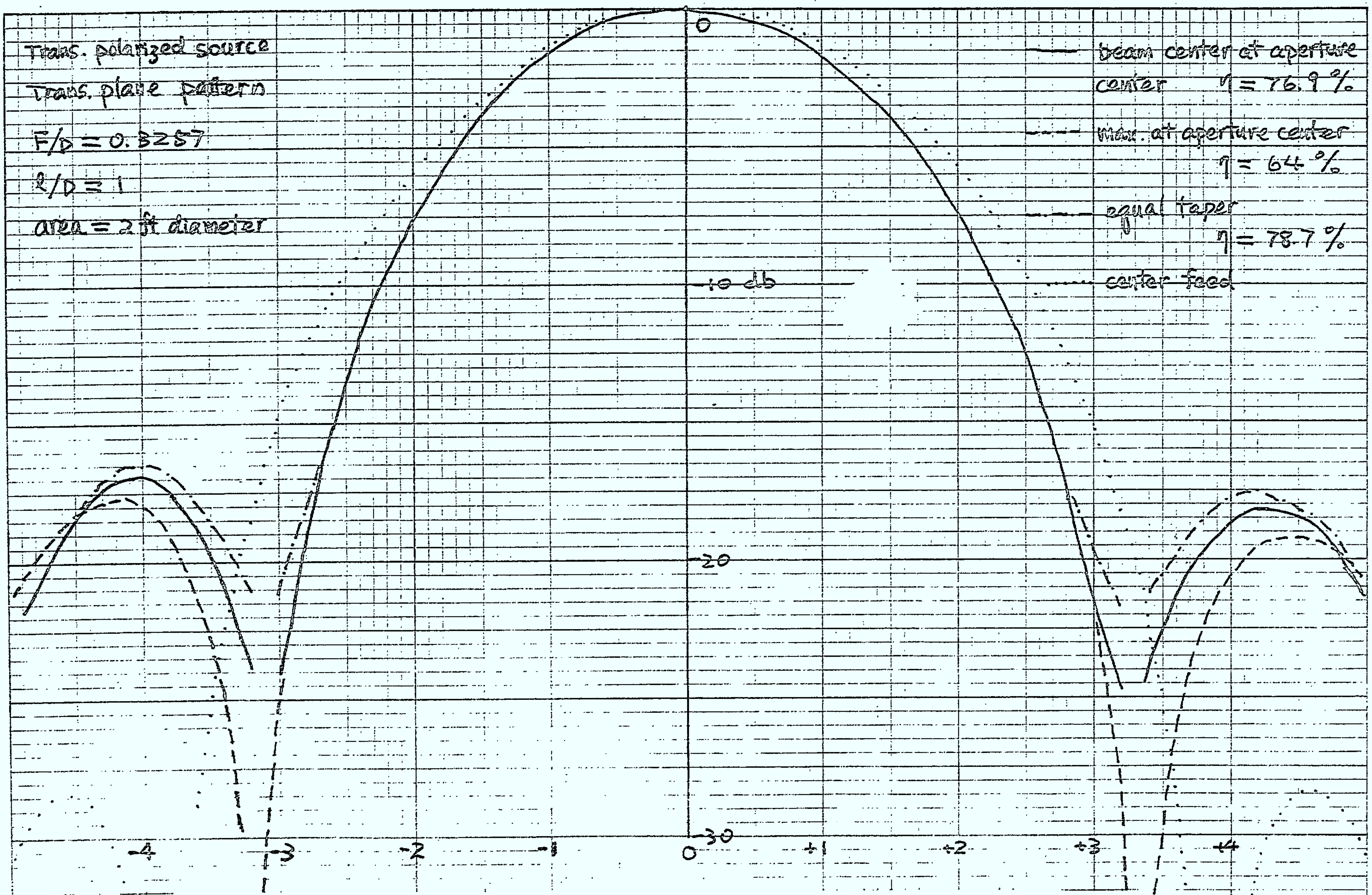

Fig. 4.3 Field distribution in the aperture plane parallel to the axis of parabolic cylinder (transverse plane) for various positions of the axis of the main beam of the source.

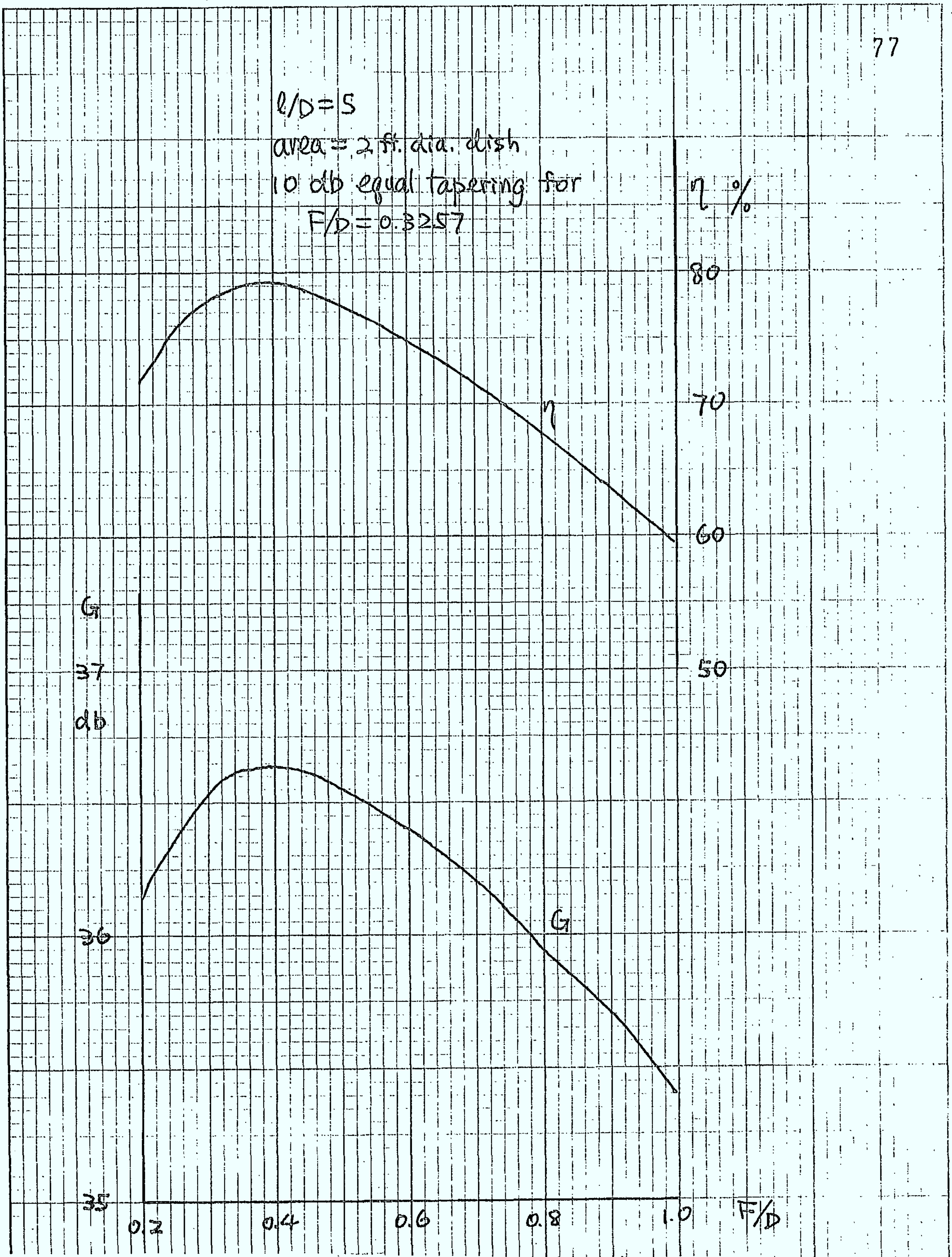

Fig. 4.4 On-axis gain and efficiency vs F/D ratio

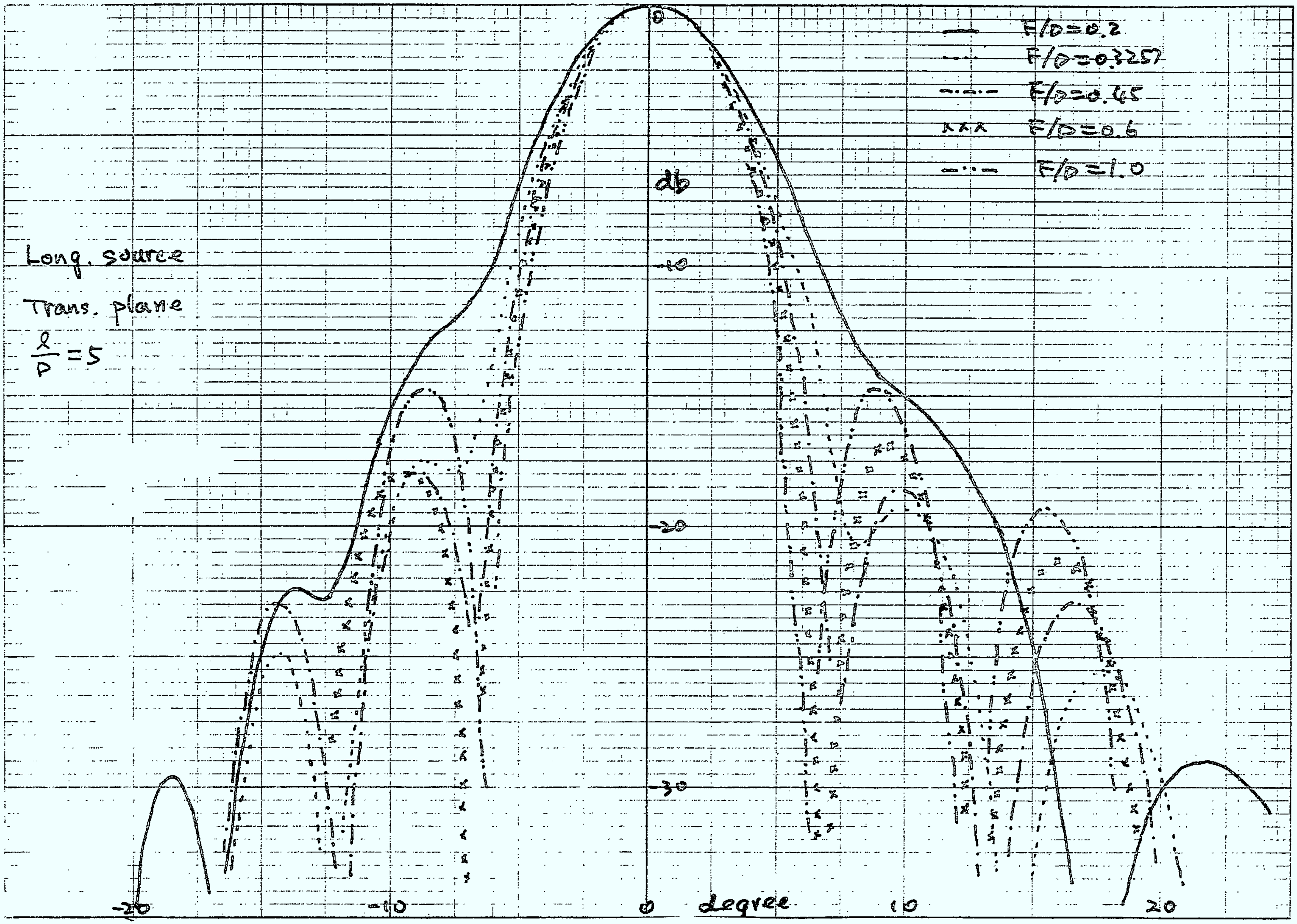

Fig. 4.5 Field patterns vs F/D ratio in the transverse plane for longitundinally polarized source

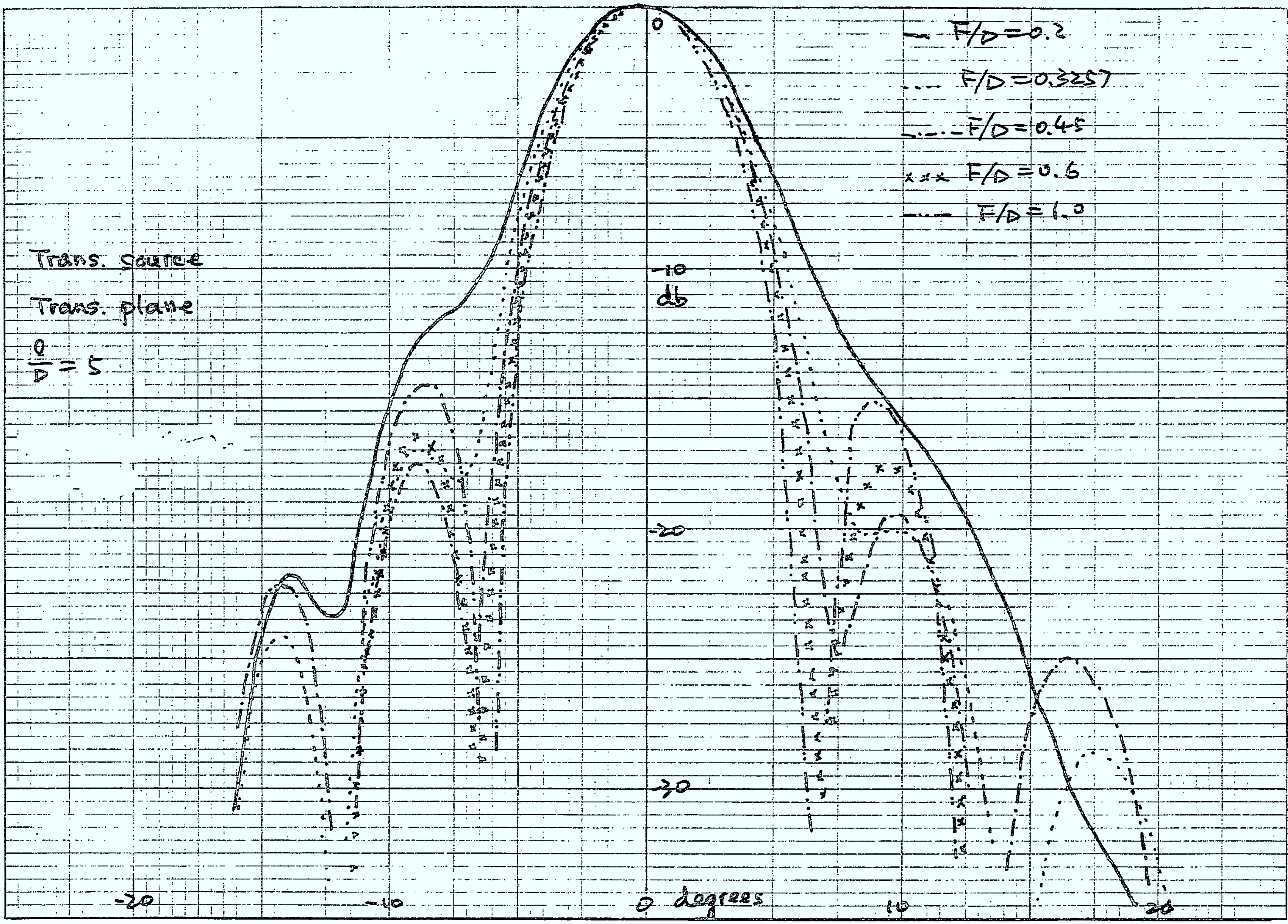

Fig. 4.6 Field patterns vs F/D ratio in the transverse plane for transversally polarized source

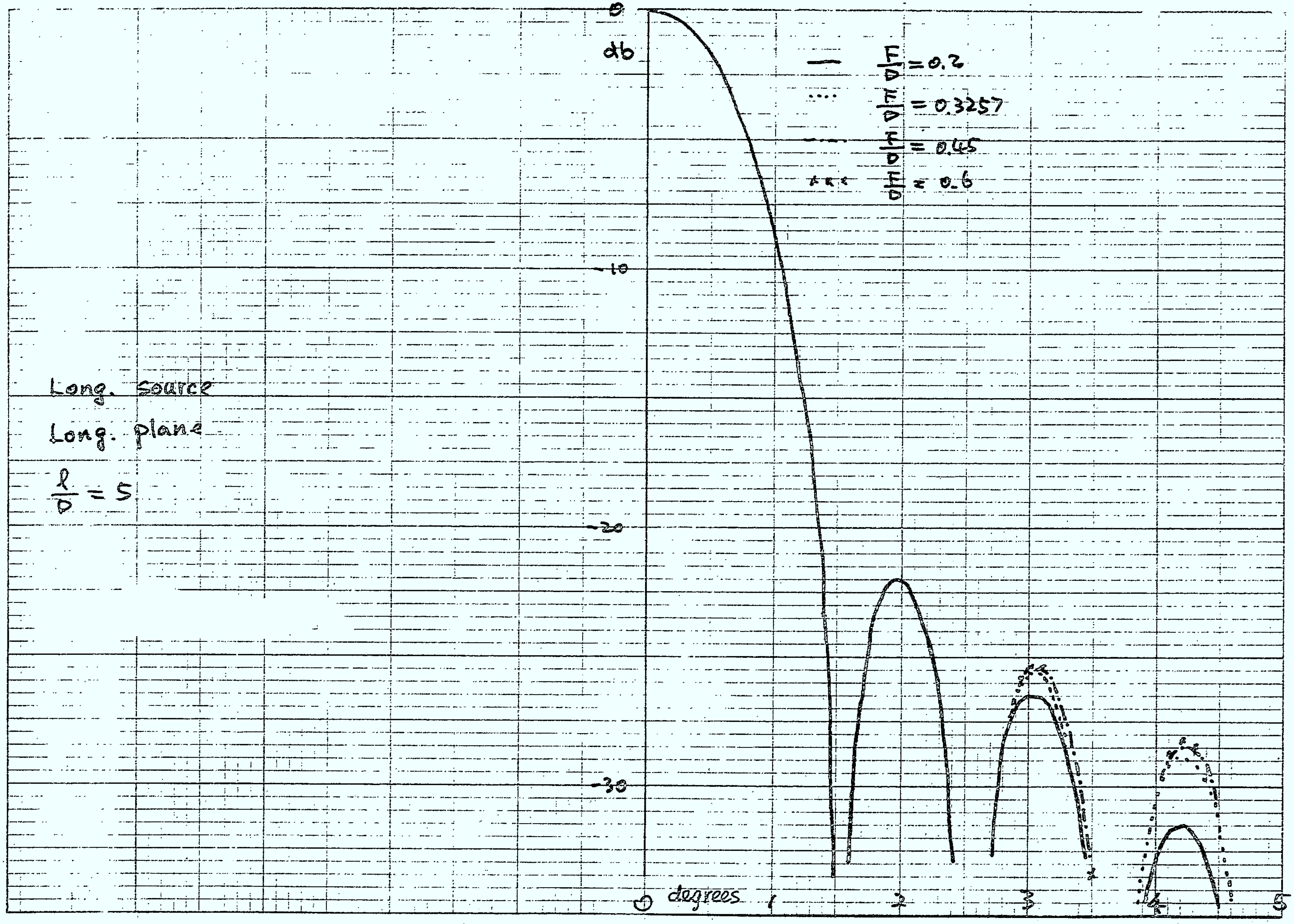

Fig. 4.7 Field patterns vs F/D ratio in the longitudinal plane for source of either polarization

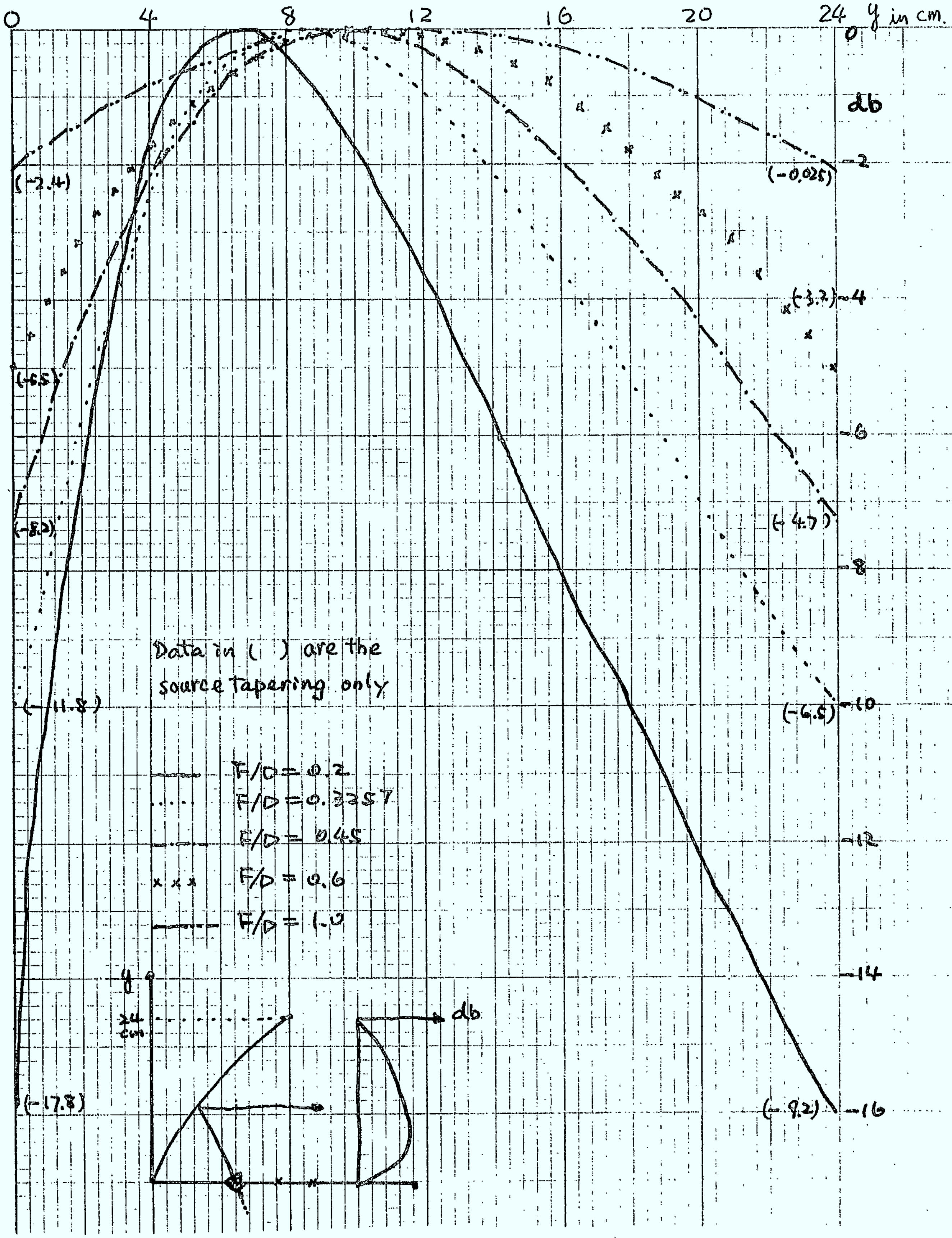

Fig. 4.8 Field distribution in the aperture plane vs. F/D ratio

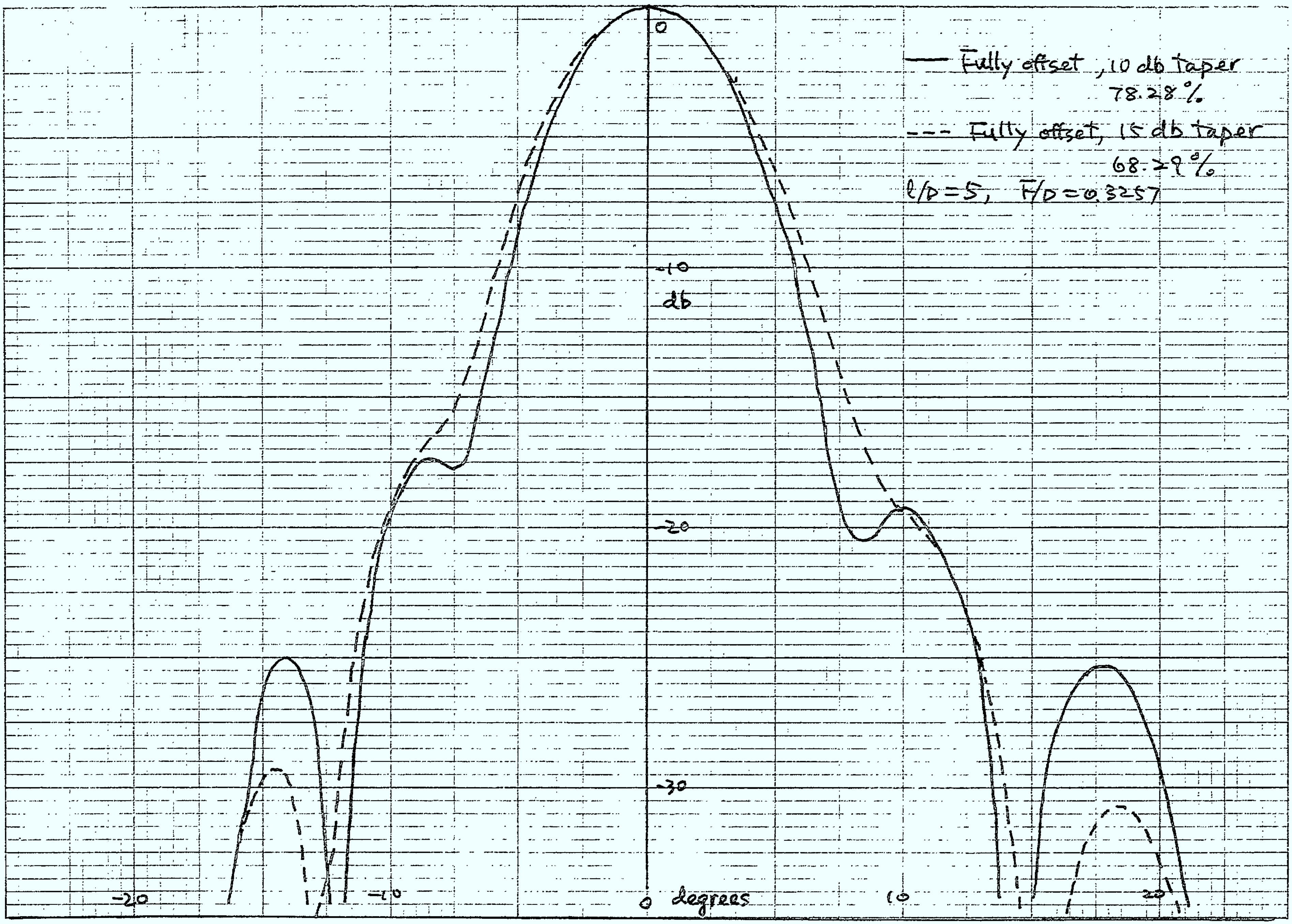

Fig. 4.9 Field patterns vs tapering in the transverse plane for longitudinally polarized source

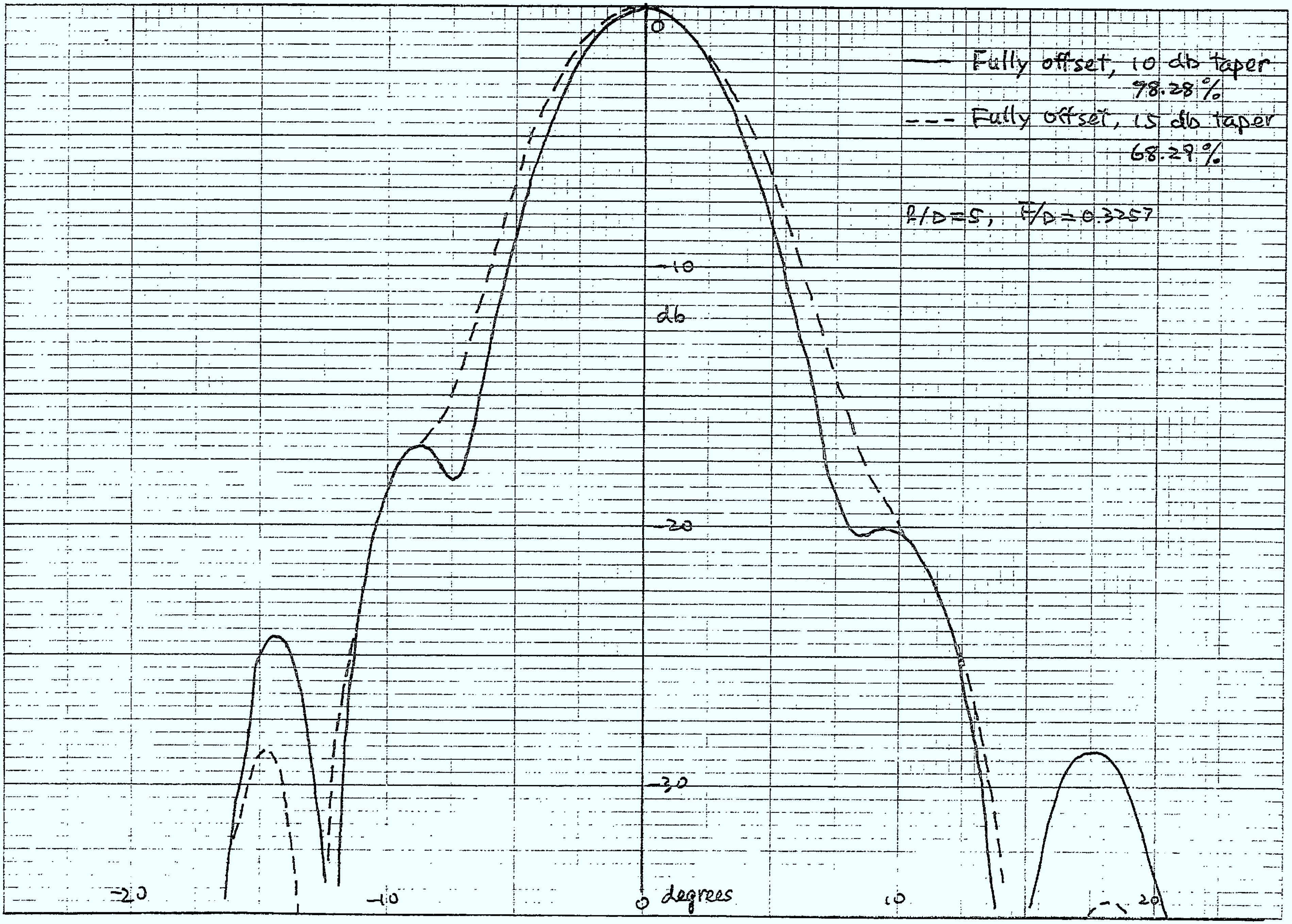

Fig. 4.10 Field patterns vs tapering in the transverse plane for transversally polarized source

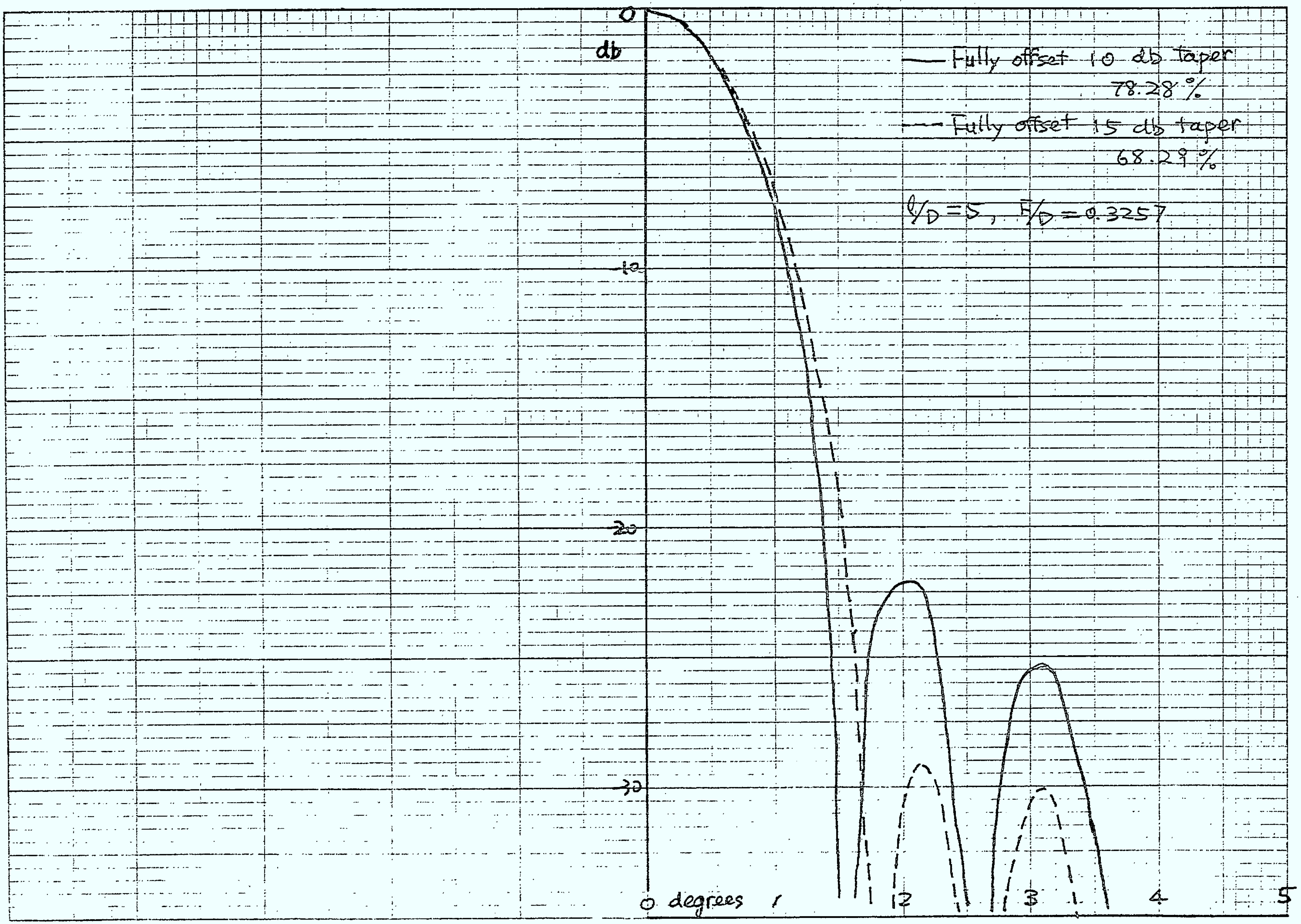

Fig. 4.11 Field patterns vs tapering in the longitudinal plane for a source of either polarization

Maintaining about 10 db taper the patterns of parabolic cylinders of aspect ratios $\ell/D = 1$ to 5 were calculated for equivalent circular dish diameters of 2 and 3 ft. The patterns of the latter case are shown in Figures 4.12-4.14. The beamwidth factor is about 1.05 ± 0.01 in the transverse plane for both polarizations and about 1.04 ± 0.01 in the longitudinal plane. The first sidelobes are better than 17.7 db at negative angles and better than 18.5 db at positive angles in the transverse plane. They are about 22 db in the longtudinal plane. The envelopes of the 3 db down and 1 db down contours are shown in relation to the $2.2^{o} \times .46^{o}$ motion box (MB2) in Figures 4.15 and 4.16 and the edge gain variation vs ℓ/D in Figure 4. 17.

For the purpose of comparison with Figure 2.6 the edge gain of parabolic cylinders of aspect ratios 3, 4 and 5 were plotted against the diameter of equivalent on-axis gain circular apertures (Figure 4.18). The letter following the aspect ratio indicates whether the edge is in the longitudinal or transverse plane of the motion box. The latter are the critical curves. The gain scale indicates gains reduced by the gain factor.

For applications where it is found convenient to place the feed in the aperture plane the F/D value of 0.5 was also investigated. Figure 4.19 shows the edge gain vs D for the $2.2^{o} \times .46^{o}$ MB2. In this case a feed was directed so that the beam centre is at the aperture centre. The gain factor is 77.35% (calculated). For this larger F/D to maintain the same edge taper the feed has to be a little larger.

4.2.4 Centre Fed Parabolic Cylinder

For parabolic cylinders whose length ℓ is less than its transverse dimension D, a line feed in its focal line presents less blockage problem. For such applications and for comparative purposes patterns of a centre fed reflector was also evaluated. The equivalent gain circular dish diameter was 2 ft., the F/D = 0.326, λ = .9886. The source functions were selected to be 10 db down at reflector edge direction: $F(x) = 0.15 + 1.34 \cos(\pi x/\ell)$ and $G(\Psi) = 4.06 \cos^{10}(\Psi/2)$. The subtended angle by the reflector is 150^{o}. Maintaining the edge tapering the following values were calculated independently of the aperture aspect ratio: Gain 36.95 db, gain factor 85.22%. In the transverse plane the beamwidth factor is 1.2 ± 0.02 and the sidelobe is 28 db. In the longitudinal plane the beamwidth factor was 1.06 ± 0.03 and the sidelobe 18.2 ± 0.1 db. With a uniform axial source distribution F(x) = 1 the beamwidth factor in the longitudinal plane was 0.904 ± 0.01 and the first sidelobe 13.3 db $\pm$ 0.1 db. The patterns for $\ell/D = 3$ shown in Figure 4. 20 may serve as a typical example.

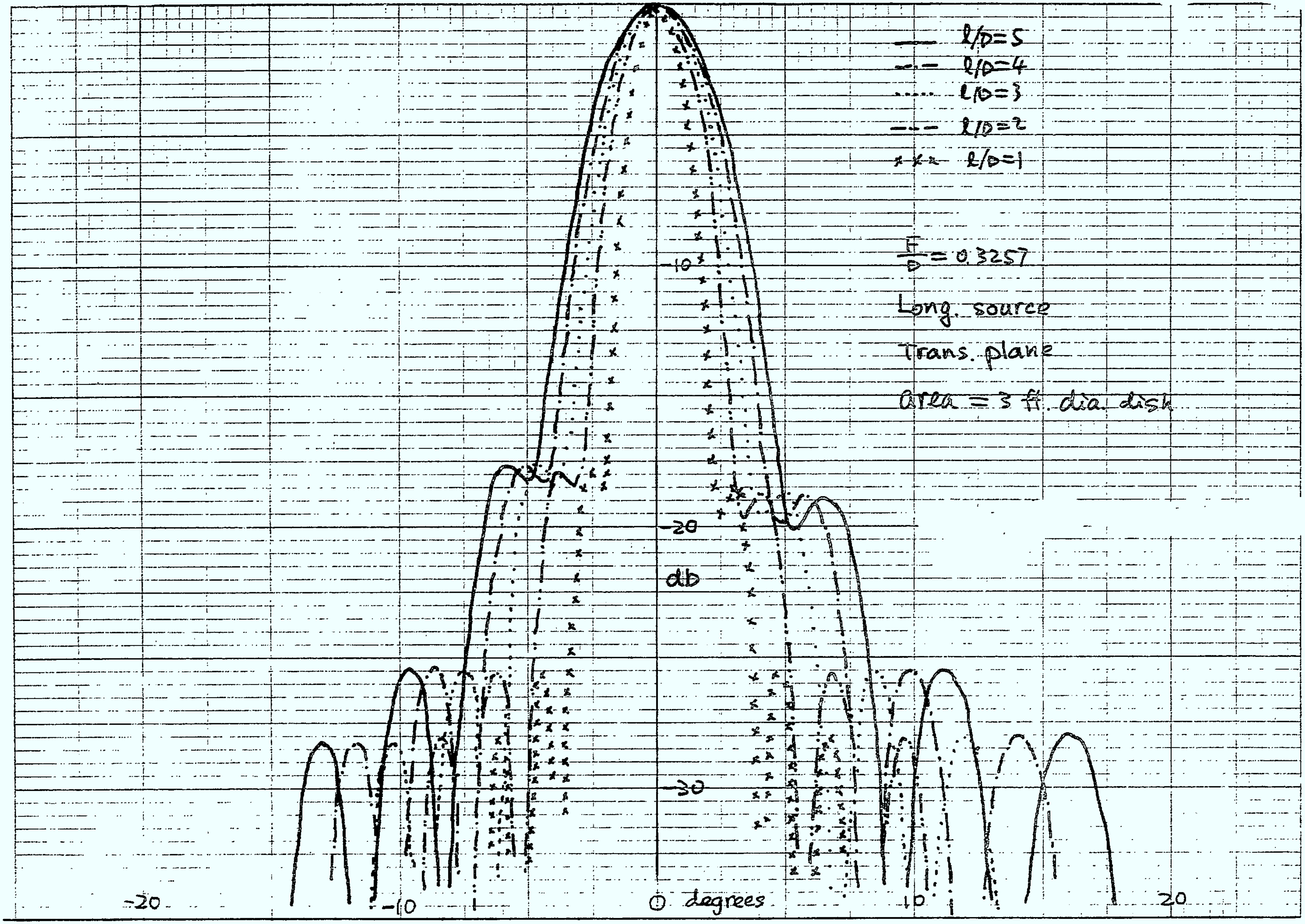

Fig. 4.12 Field patterns vs L/D ratio in the transverse plane for longitudinally polarized source

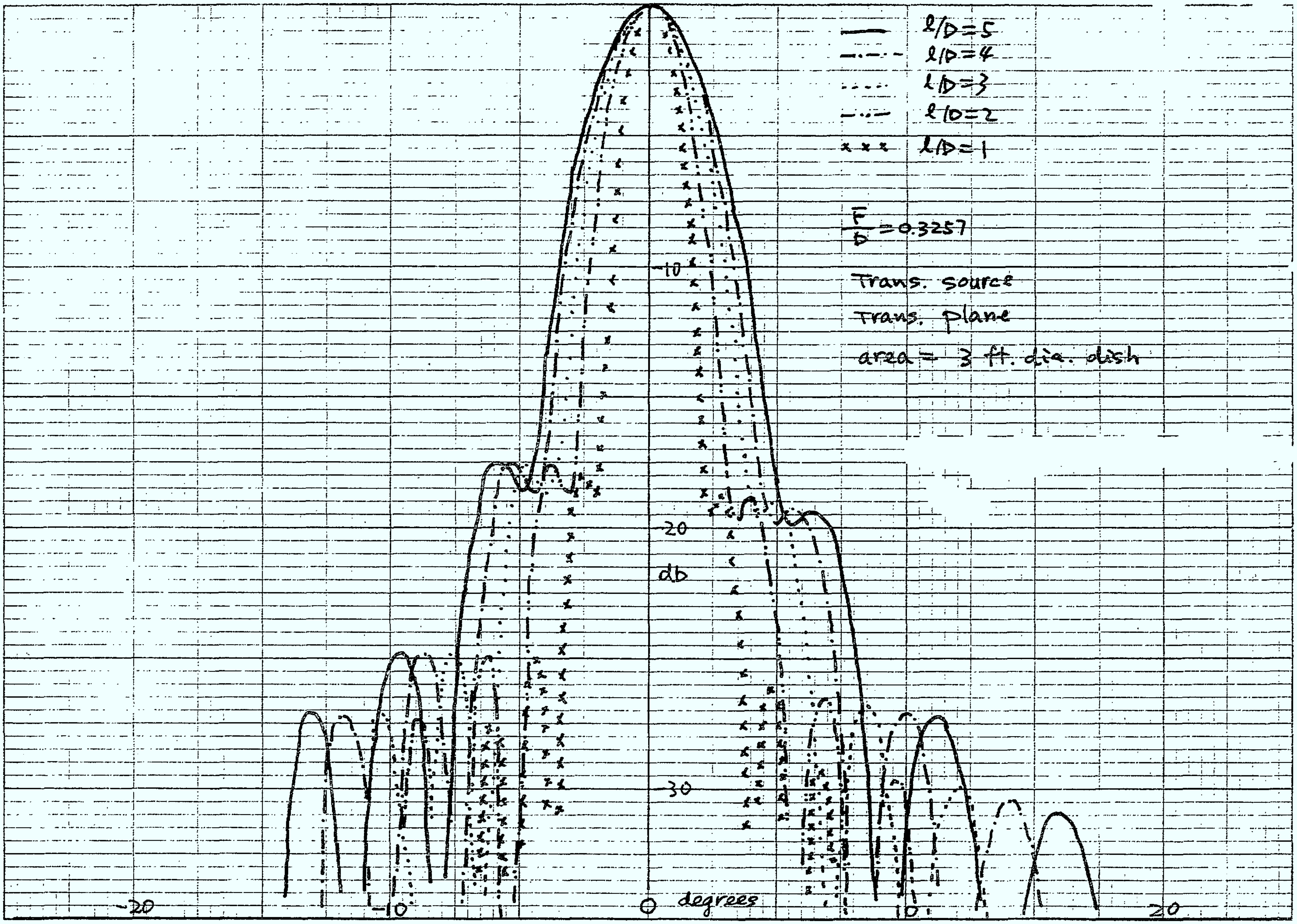

Fig. 4.13 Field patterns vs L/D ratio in the transverse plane for transversally polarized source

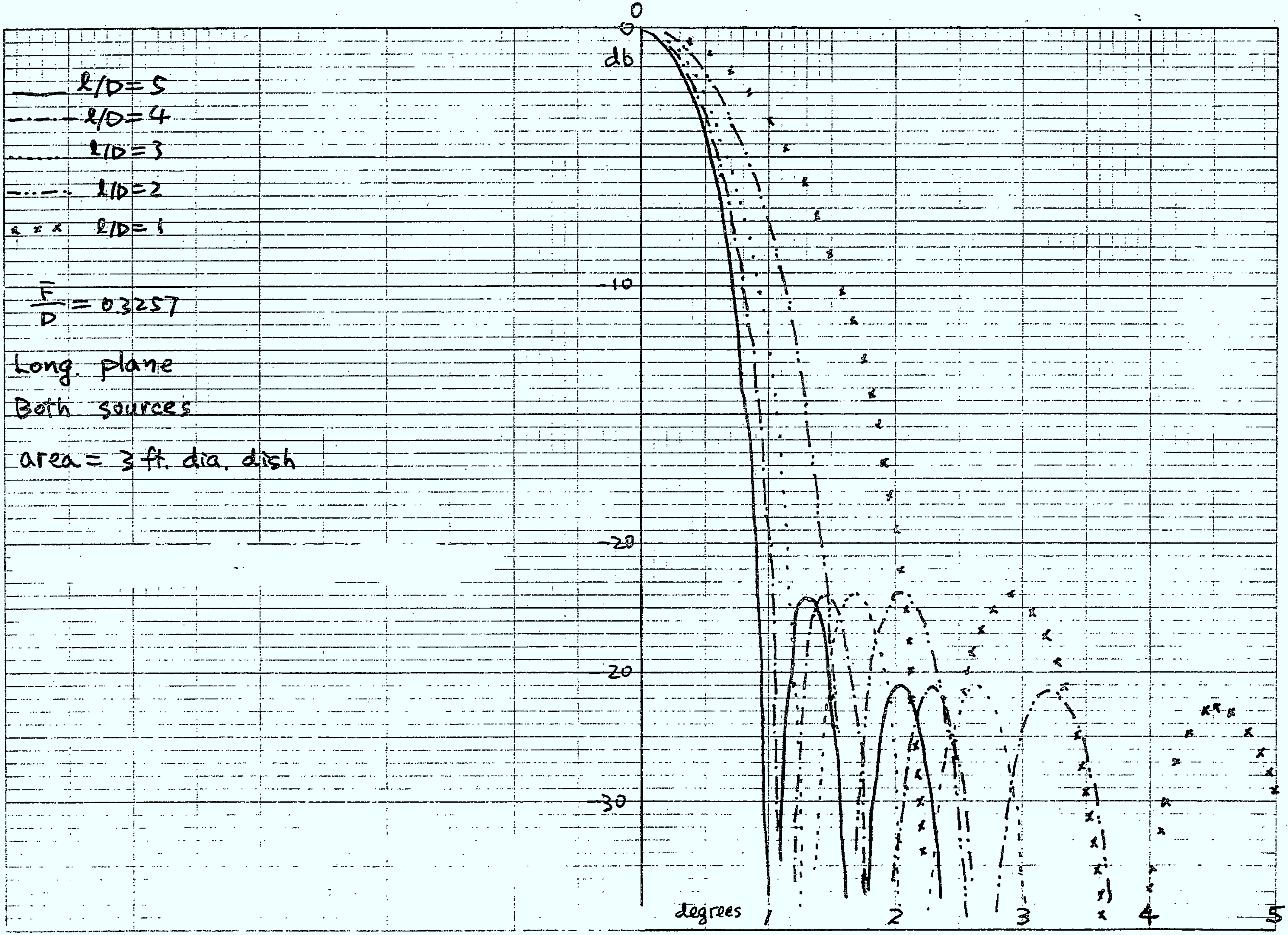

Fig. 4.14 Field patterns vs L/D ratio in the longitudinal plane for a source of either polarization.

1" = ½ degree

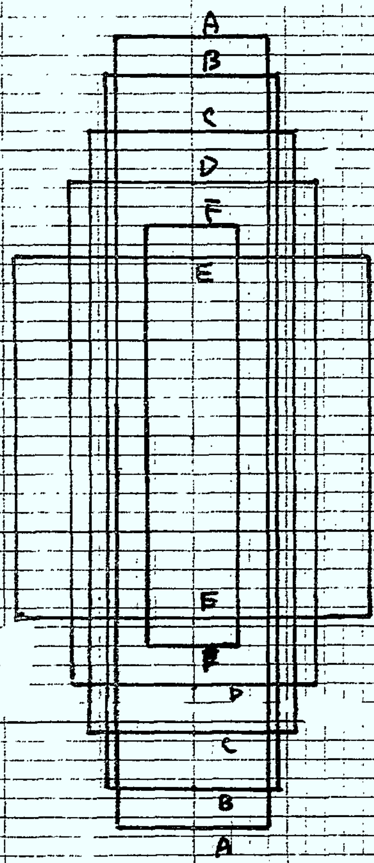

	l/D	3 db beam ratio
A	5	5.06
B	4	3.90
C	3	2.96
D	2	2.07
E	1	1.0
F	coverage area	

3 ft. dish G_{max} = 40.1 db

Fig. 4.15   The 3 db contour of the beam vs L/D ratio.

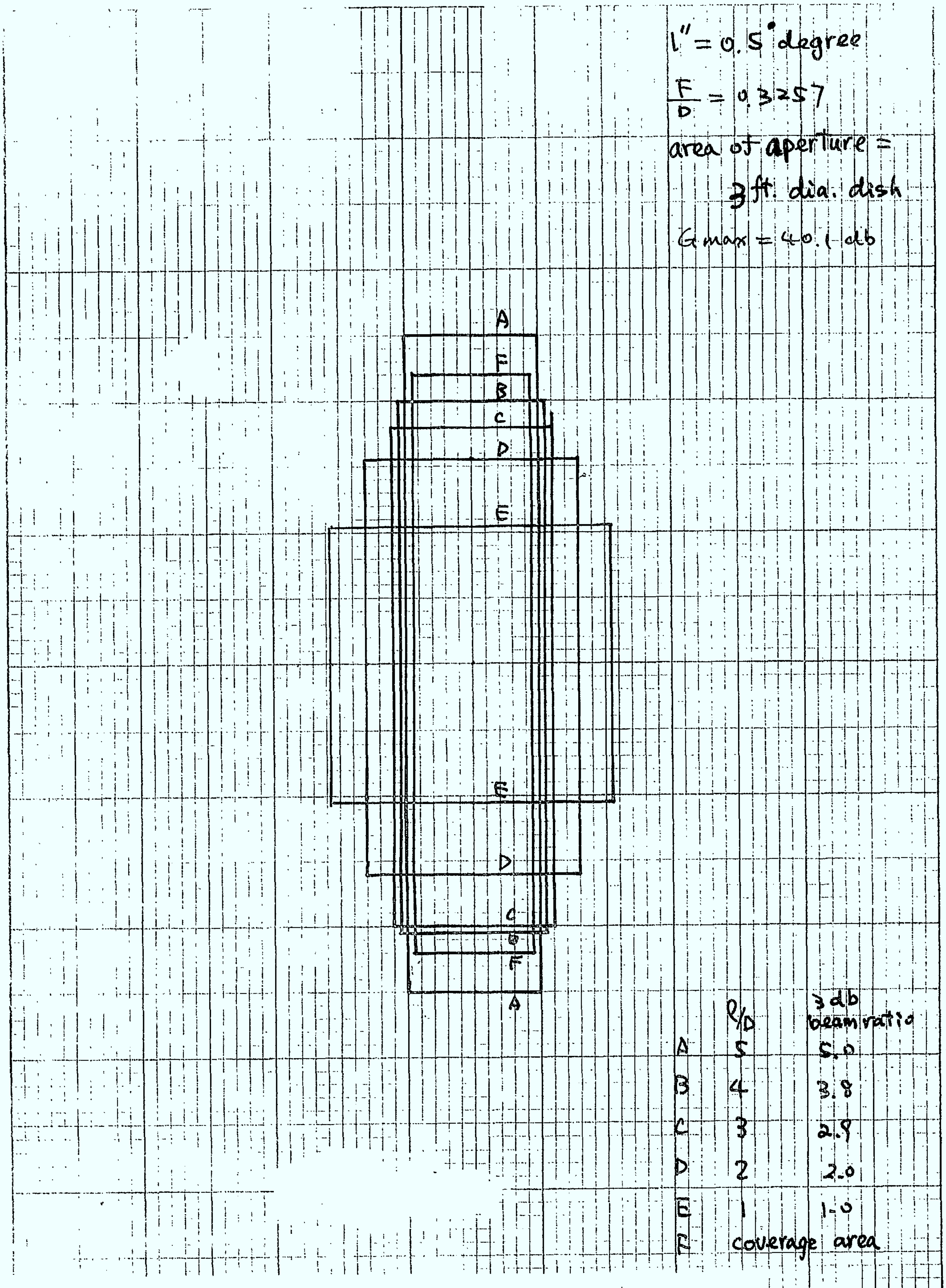

Fig. 4.16 The 1 db contour of the beam vs L/D ratio.

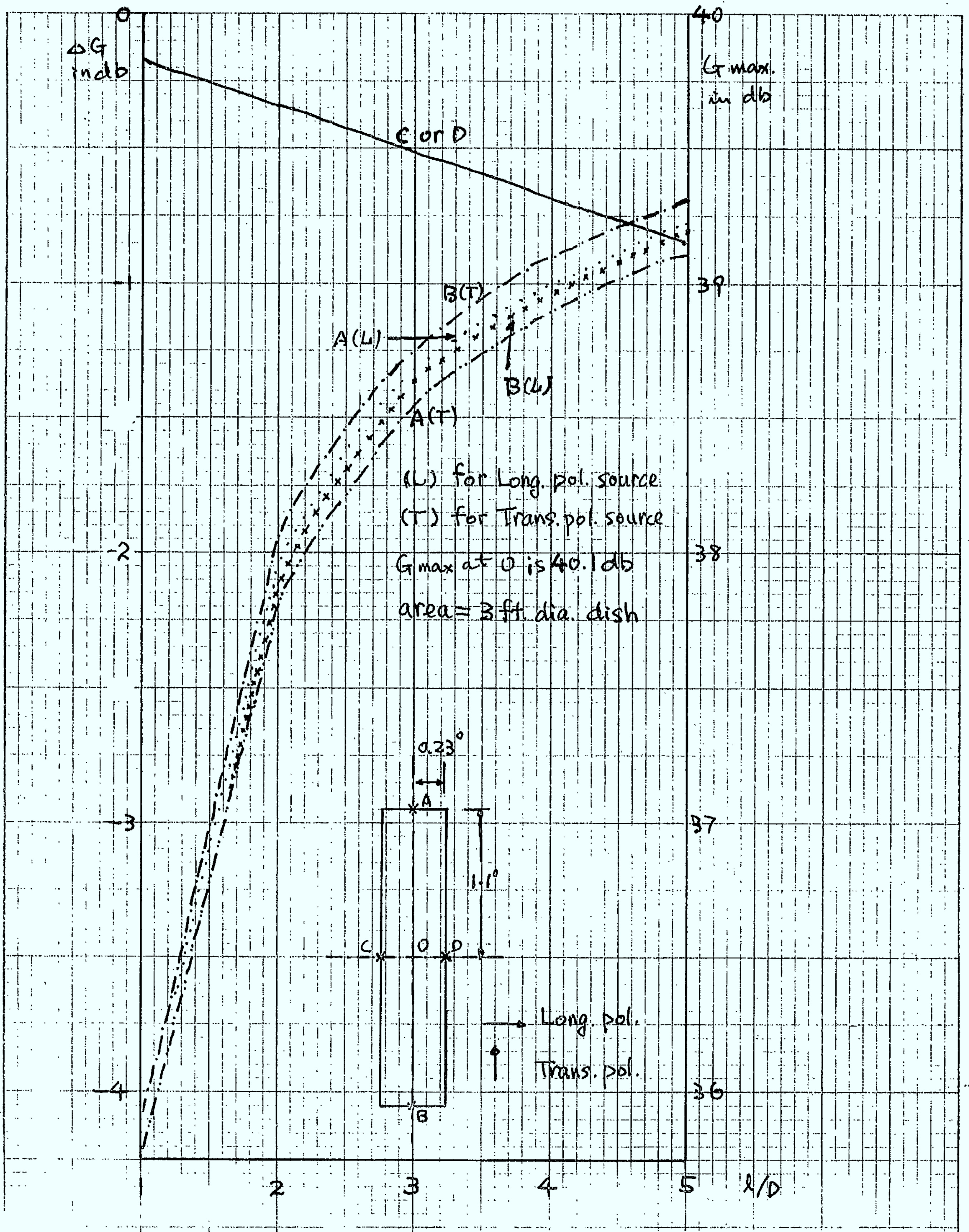

Fig. 4.17 Edge gain variation for MB2 ($\pm 0.23°$, $\pm 1.1°$) vs L/D ratio

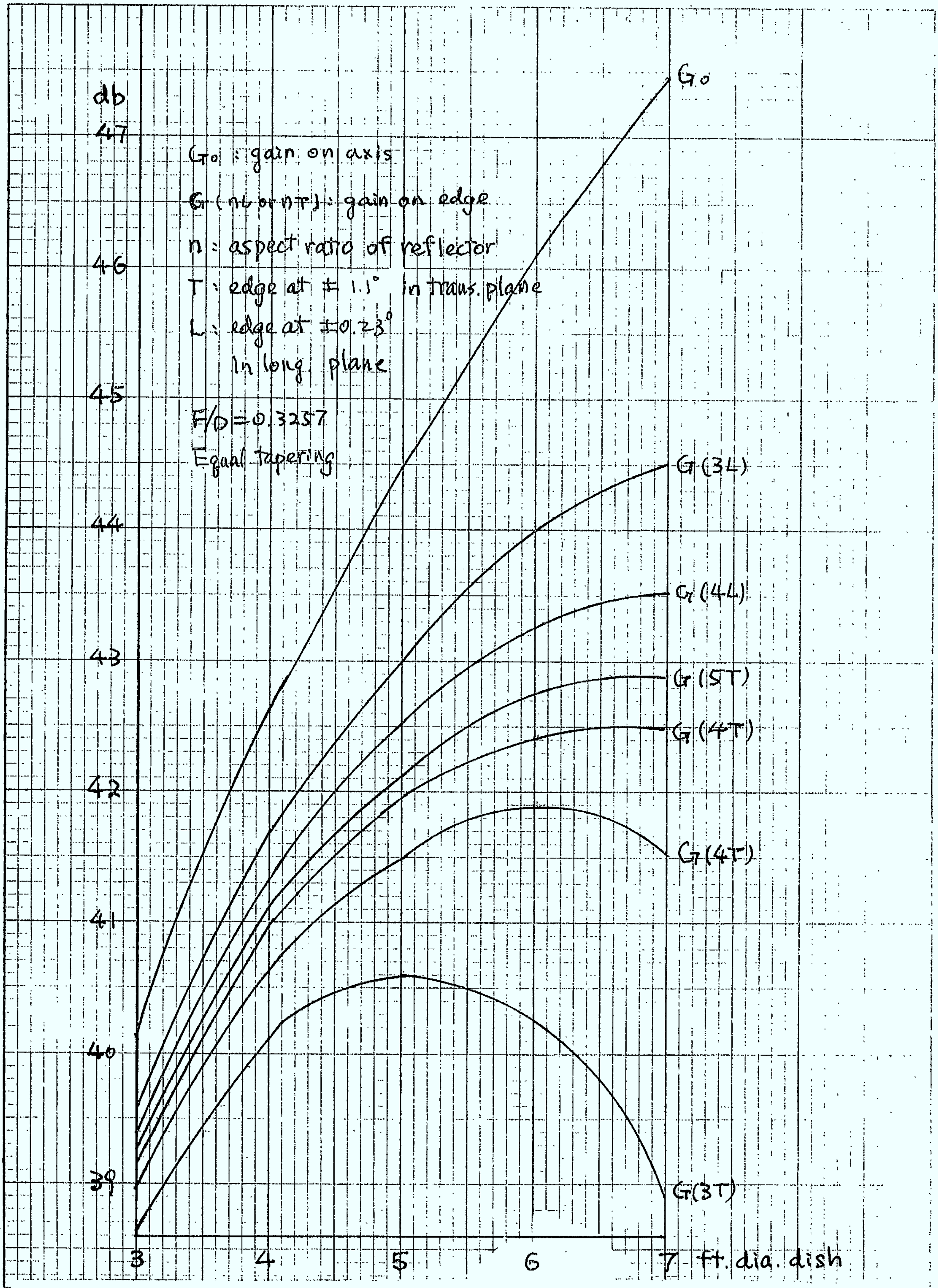

Fig. 4.18 On-axis gain and edge gain for MB2 ($\pm$ 0.23°, $\pm$ 1.1°) vs. aperture area and aspect ratio, F/D = 0.3257.

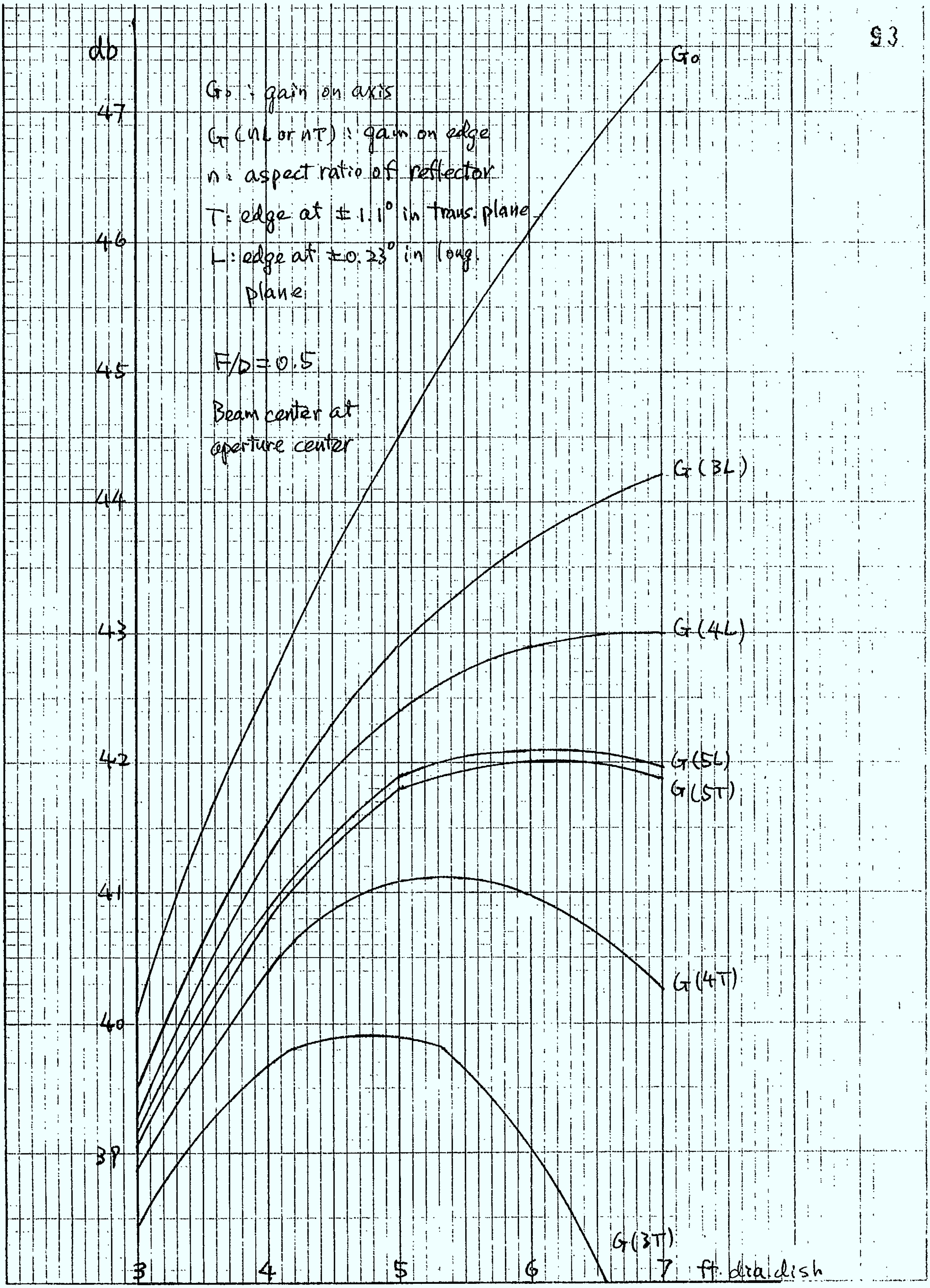

Fig. 4.19 On-axis gain and edge gain for MB2 (± 0.23°, ± 1.1°) vs. aperture area and aspect ratio, F/D = 0.5.

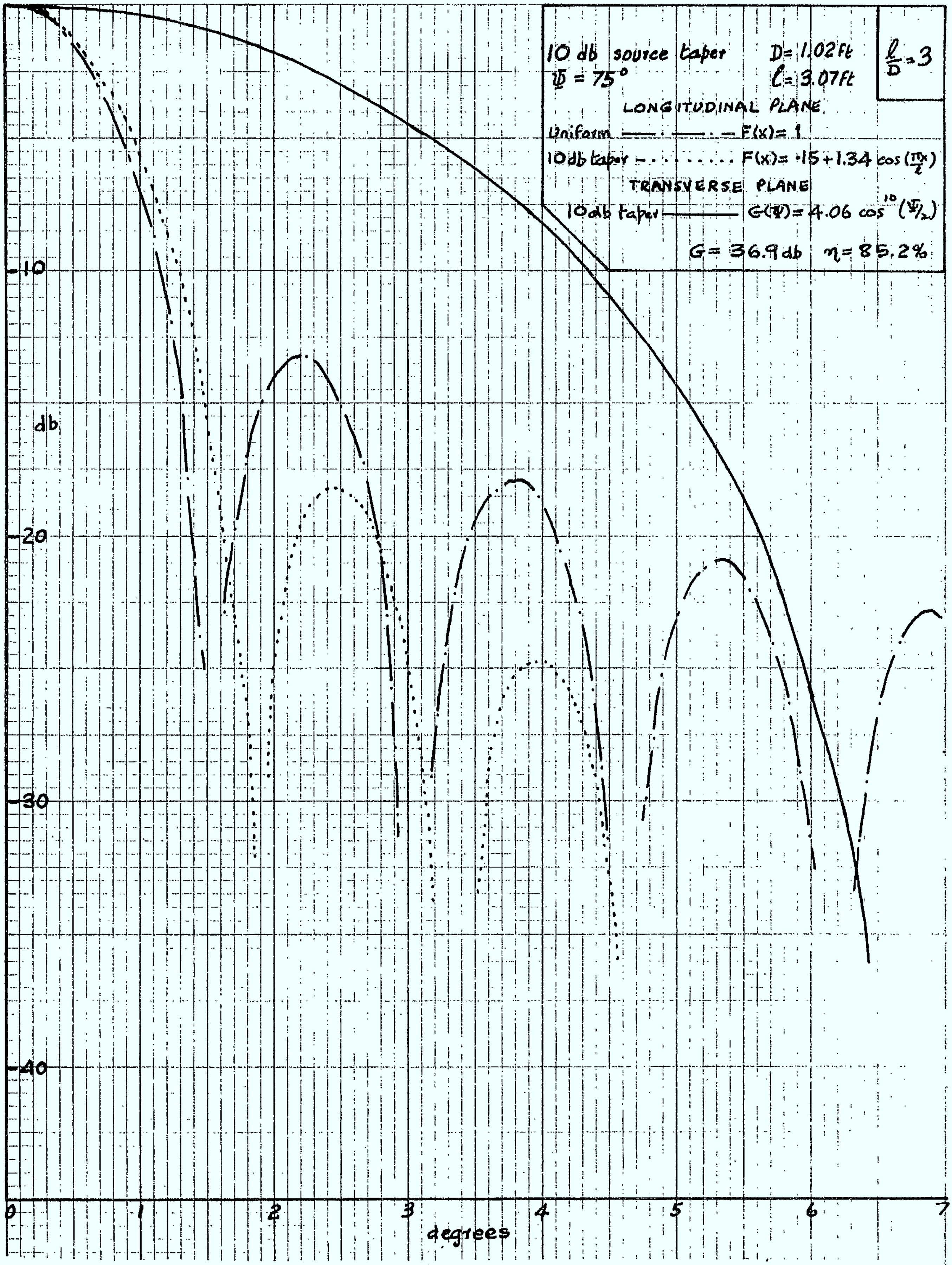

Fig. 4.20 Field patterns in transverse plane of centre fed system with L/D = 3

Considering a practical centre fed parabolic cylinder its performance will be modified by blockage effects. The gain will be lower, the main beam wider and the first sidelobe levels higher.

4.3 The Chesse Antenna

To produce an elliptical beam cross-section, a type of parabolic cylinder antenna, the cheese antenna may also be used. This is characterized by the fact that the length L of the reflector is shorter than the height D. At both ends of L a transverse plate covers the cylinder. For this configuration the blockage by the source is not excessive so that a centre fed system may be considered again.

If the length of the reflector is not too great, a rectangular horn or hoghorn can be used as a feed operating in the TE_{10} mode. If we assume that the phase centre of the feed is in the aperture plane of the cheese antenna then the F/D ratio is 0.25.

Two source distributions have been considered: 1) 15 db taper at 90° including space attenuation and 2) 10 db taper at 90° under the same condition. Two orthogonal polarizations have been investigated.

The source pattern in the transversal plane may be controlled by the flare angle or the F/D ratio. The source pattern in the longitudinal plane is determined by the field distribution in the waveguide. Using an orthogonal coupler to feed the horn dual polarized operation may be achieved in two frequency bands.

To evaluate the performance of such antenna the characteristics of a typical case were calculated. The aperture area is equivalent to a 2 ft. diameter dish and the aspect ratio of the aperture is L/D = 0.2 (L is about 10 λ).

The calculated general characteristics of this antenna are listed in Table 4. 1 . The patterns corresponding to the two source polarizations are plotted in Figures 4.21 to 4.23 . In the longitudinal plane, the patterns show differences in beamwidth and sidelobe level due to differences in tapering for the two source polarizations. Note also that the beam aspect ratio can differ considerably from the aperture aspect ratio.

An effective feed horn with closely spaced phase centres for the two polarizations is a necessity for efficient dual polarized dual band operation. The horn dimensions are also limited by the ill effects of blockage.

Table 4.1 shows an example of the main characteristics of a cheese antenna.

The geometry of the system is defined by

$D = 3.97$ ft. $L = .794$ ft. $F = .99$ ft.
(equivalent diameter = 2 ft.)
$L/D = 1/5$ $F/D = 0.25$

TABLE 4.1

Characteristics of a Cheese Antenna

Case a: Longitudinally polarized source

Source Patterns	$F(x) = 1$ $G(\psi) = 2.945 \cos^5 (\Psi/2)$, 10 db		$F(x) = 1$ $G(\psi) = 3.657 \cos^8 (\Psi/2)$, 15 db	
Pattern plane	Long.	Trans.	Long.	Trans.
$1/2\,\Theta_3^o$	2.6	0.64	2.6	0.7
1st Sidelobe Level *db*	15.3	26.6	15	27.5
1st null position *deg.*	6°	1.6°	6°	2.2°
Θ_3/ϕ_3	4.05		3.7	
Maximum gain *db*	36.94		36.7	
Efficiency	85%		80.8%	

TABLE 4.1 (cont'd)

Case b: Transversally polarized source

Source Patterns	$F(x) = 2\cos^2\left(\frac{\pi x}{\ell}\right)$ $G(\psi) = 2.945\cos^5(\psi/2)$, 10 db		$F(x) = 2\cos^2\left(\frac{\pi x}{\ell}\right)$ $G(\psi) = 3.657\cos^8(\psi/2)$, 15 db	
Pattern plane	Long.	Trans.	Long.	Trans.
$1/2\,\Theta_3^\circ$	3.5	0.64	3.5	0.7
1st Sidelobe Level db	28.1	26.6	27	27.5
1st null position deg.	9	1.6	9	2.2
Θ_3/Φ_3	5.5		5	
Maximum gain db	36		35.8	
Efficiency	68.9%		65.5%	

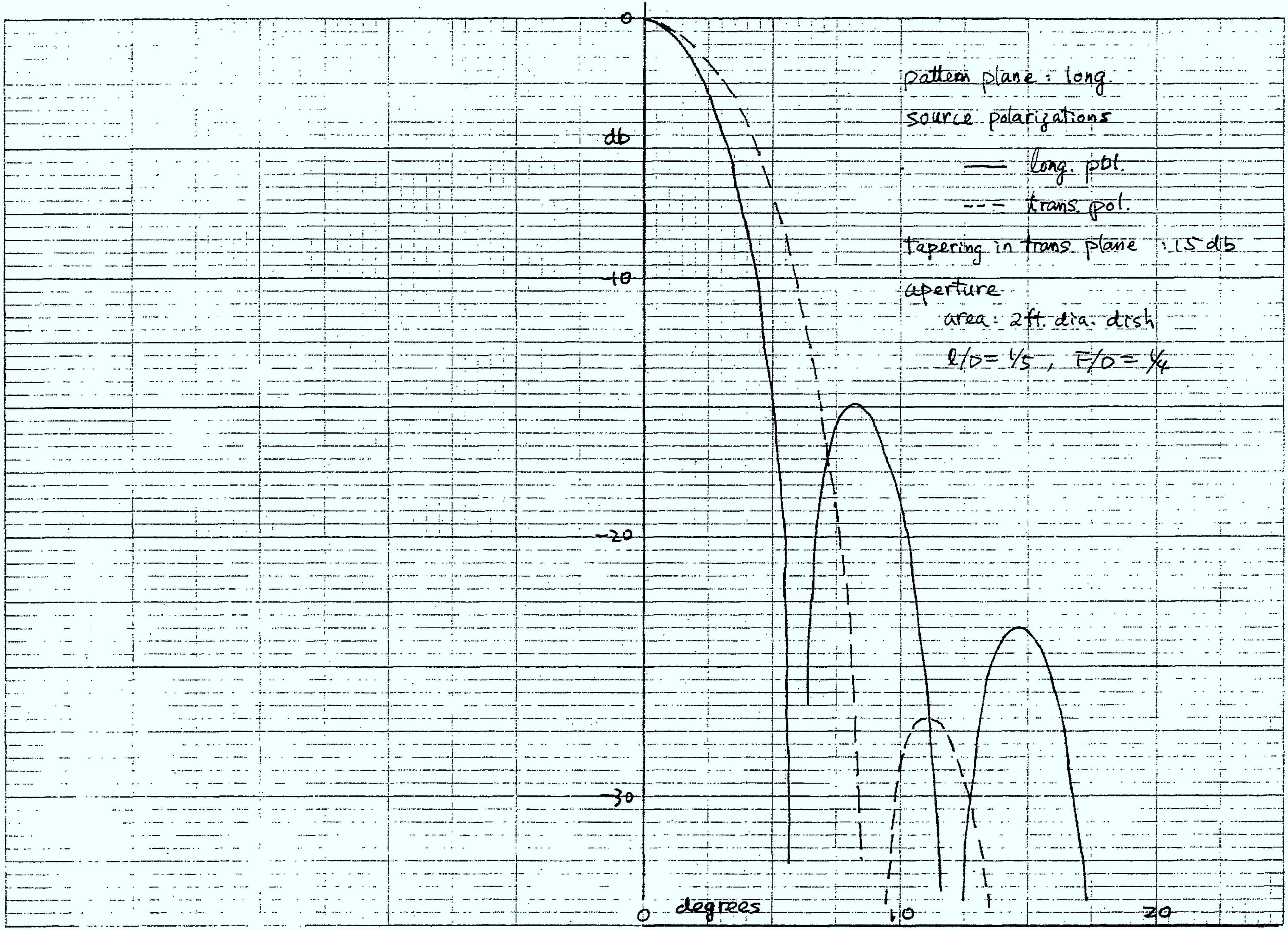

Fig. 4.21 Patterns of a cheese antenna in the longitudinal plane, 15 db edge tapering.

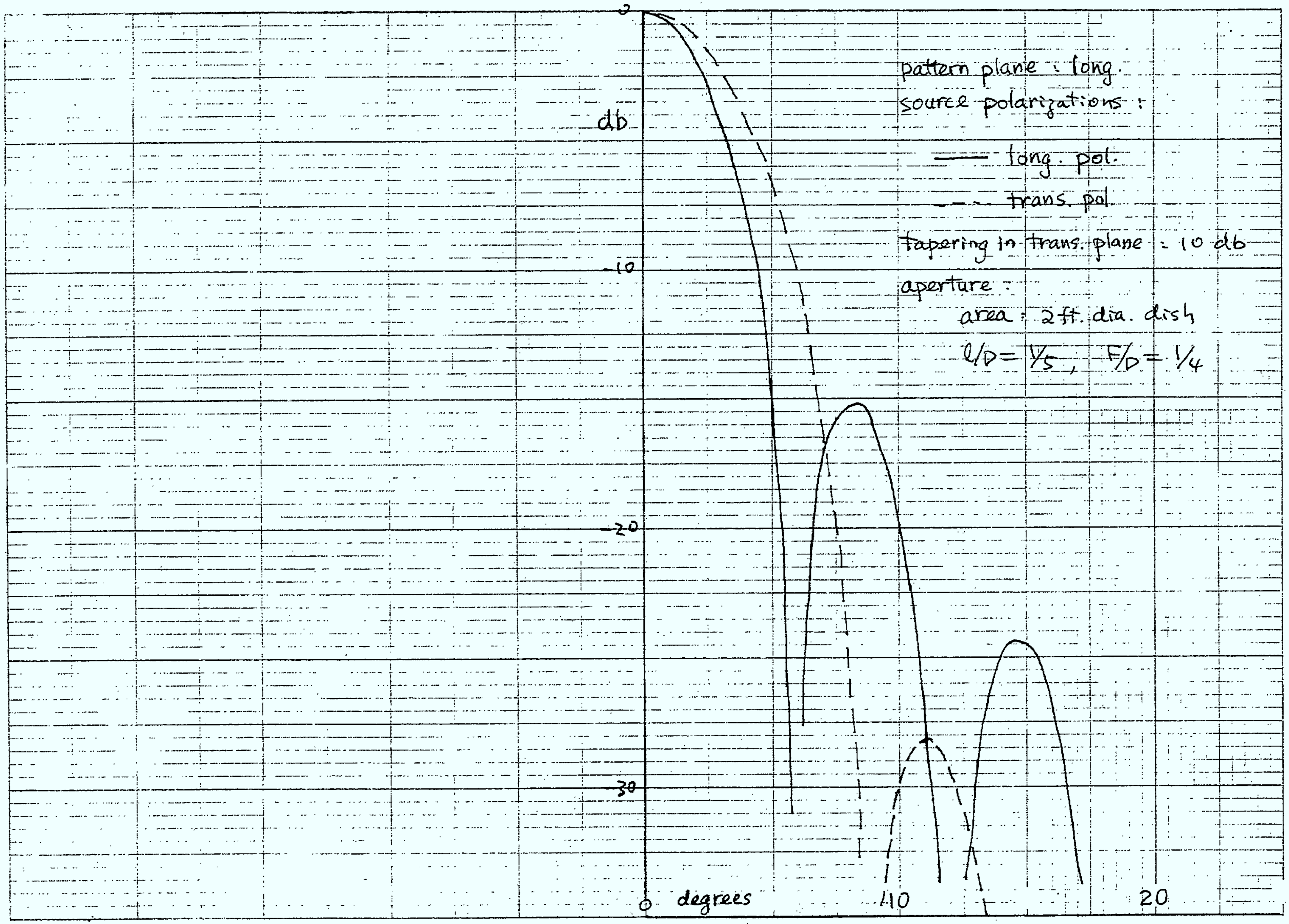

Fig. 4.22 Patterns of a cheese antenna in the longitudinal plane, 10 db edge tapering.

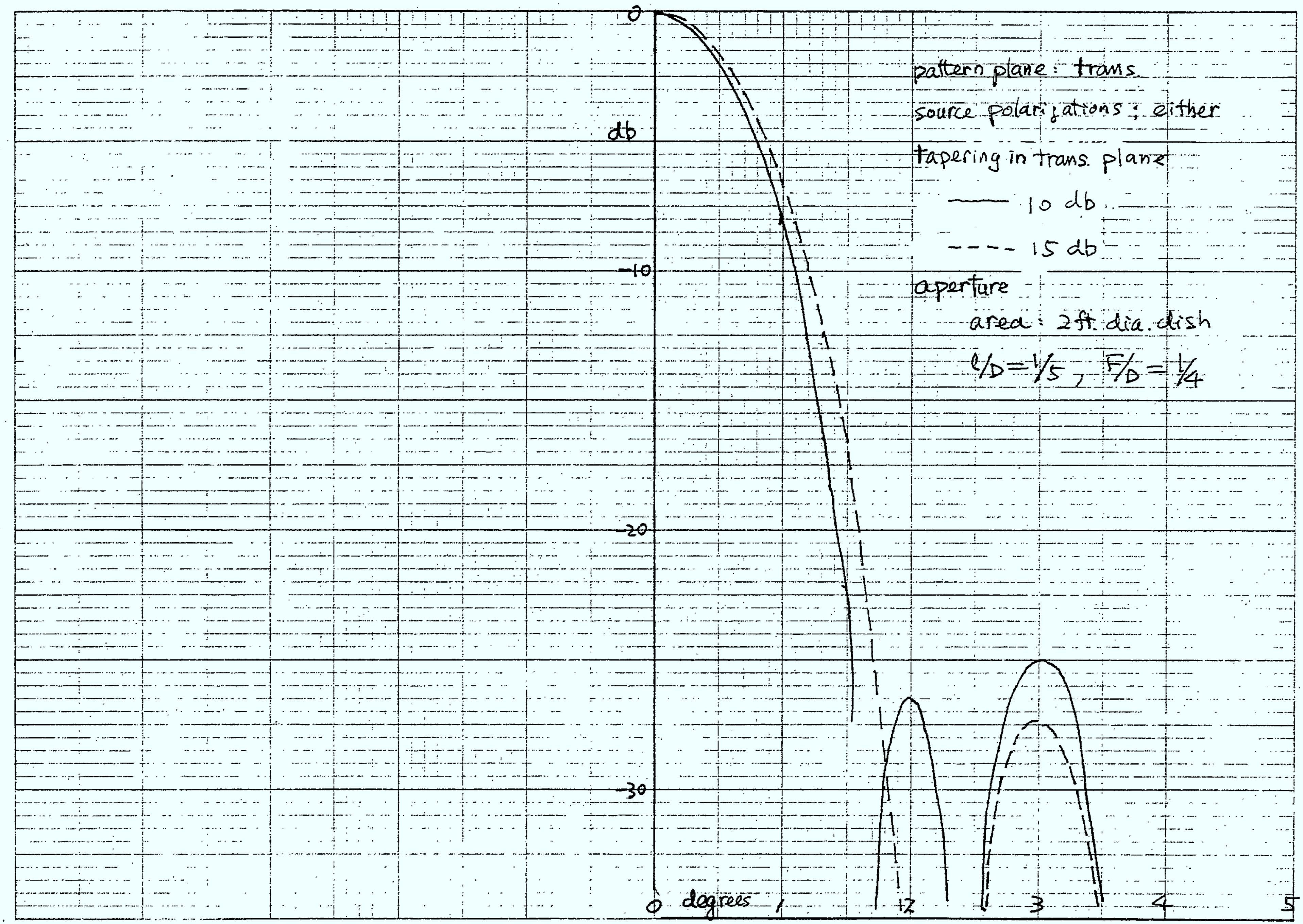

Fig. 4.23 Comparison of transverse plane patterns for a cheese antenna with 10 db and 15 db edge tapering.

4.4 Pillbox As A Line Source

A possible line source that may be used with parabolic cylinders is a pillbox. If its height is selected to be between 0.5 and 1 wavelength it can support two orthogonal modes: TEM that is polarized normal to the side plates and the TE_{10} mode polarized parallel to those plates. The pillbox could then be fed by a rectangular (square) waveguide and an orthocoupler. The phase centre of the waveguide radiator could be near the aperture. The pattern in the plane transverse to the aperture can be controlled by for example flaring the aperture into a linear horn. The field distribution along the aperture may be controlled by the dimensions of the feed waveguide and the F/D ratio of the pillbox. At λ = .9886 in. with a 0.75 λ square waveguide feed the tapering at the edge of an F/D = 0.25 pillbox is about 20 db. If F/D > 0.25 is adviseable the sidewalls might have to be extended. The parallelism of the sidewalls specially for the TE_{10} mode is quite critical and to ensure it the mechanical construction has to provide the sufficient accuracy and rigidity. To reduce the reflection coefficient of the system an offset fed arrangement may be provided using half a pillbox. In this case the pillbox antenna degenerates to a narrow aperture hoghorn.

5.0 ARRAY TYPE OF ANTENNAS

5.1 Introduction

Before the use of array type antennas for the present applications are considered, it is worthwhile to list a few of the basic characteristics of microwave arrays.

Main advantages:

1. Array antennas can generally be packaged into smaller volumes than equivalent aperture size reflector or lens based antennas. This may result in smaller overall weight.

2. The amplitude and phase distribution of the exciting field can be controlled - in principle - by an appropriately designed feed network. This may result in high aperture efficiency, low sidelobe level, shaped beam, etc., depending on which characteristics are given priority.

3. Arrays are capable of providing simultaneously or in time sequence multiple beam positions. This may result in a single or multiple target tracking by a stationary antenna.

4. Arrays are capable of providing practically arbitrary beam aspect ratios.

5. Arrays, due to their modular construction, are not very sensitive for catastrophic failures. This may result in a gracefully failing device with a high reliability.

Main disadvantages:

1. The number of building blocks is large for arrays with large gain and large coverage areas in terms of 3 db beamwidth. This may result in a large cost, even if the individual building blocks are simple.

2. The design of arrays for large element numbers is complex due to the electromagnetic complexity of the radiating elements, their interaction, complexity of the feeder line, frequency dependency of element characteristics, power division, beam squint. This may result in long development cycles, not fully understood analytical behavior.

3. The interaction among elements and transmission lines usually result in a relatively narrow bandwidth. This raises difficulties in designing wideband or dual frequency band single aperture systems.

4. The complexity of the antenna is further aggrevated if the operation has to be provided simultaneously for two orthogonal polarizations. This typically increases the complexity of the array by a factor of two, while in a high gain reflector type of antennas, the added complexity for dual polarization is negligible.

5. The power handling capability of the radiating element or the power distributing network is usually less than possible with a simple feed in a reflector type antenna.

A non-ceasing effort of array designers over the years was the attempt to utilize some of the listed advantages and somehow avoid or minimize the associated penalties. It is obvious that most of the difficulties in array building are associated with the large numbers of elements. Thus, a logical step is to reduce the number of elements, while still retaining the large gain, large aspect ratio capabilities, beam steering capability, etc.

This idea leads to the subarray concept in which either large gain elements form an array or low gain elements feed a large gain optical system. For the first choice, a good example is the array of "high" gain horns or "low" gain reflectors. For the second choice, a good example is the multiple feed horn excited paraboloid or multiple horn excited parabolic cylinder.

It must be mentioned that the one or two orders of magnitude reduction in the number of array elements reduce the resolution of the array in the same manner. Fortunately, this has no significance for the present application, which is aiming for the provision of elliptical beam cross-section with high aspect ratios rather than for a large number of simultaneous beams or widely scannable beams with low sidelobe levels.

Thus, for the present application, one specific advantage of arrays, namely the practically arbitrary aspect ratio capability can be fully utilized without the usual cost and complexity disadvantage of arrays. The resulting array antennas by nature will be hybrid designs: combination of high gain elements or low gain elements and optical systems (reflector, lenses). On the other hand, pure arrays with astronomical element numbers, necessary to build up the required high gain obviously does not have more than an academic interest. Such "pure" arrays will not be discussed further.

Among the "subarray" type antennas, several have great practical significance for the present application. The following types will be discussed later in some detail:

1. Linear array of feed horns feeding a circular aperture paraboloid.

2. Linear array of feed horns feeding an elliptical aperture paraboloid.

3. Linear array of high gain horns.

4. Linear array of circular paraboloids.

All the above listed systems utilize already existing, available antenna elements or elements which can be scaled from other frequency bands. They require one, two or four power divider hybrids (Magic Tee's) to achieve the specified beam aspect ratios. They are all capable of providing variable gain and various beam shapes, depending on how many elements are connected. However, for Nos. 1 and 2 of the above list, the antenna gain decreases and the aspect ratio increases as the number of used array elements are increased, while for Nos. 3 and 4, the antenna gain as well as the aspect ratio increases proportionally with the number of array elements. That difference means that, for the first group, the antenna efficiency decreases with increasing aspect ratio, while in the second group, the antenna efficiency remains constant.

Assuming a given high gain and increasing aspect ratio requirement, the cost of the first group type of antennas is proportional to the aspect ratio, while in the second group, it is nearly independent of the aspect ratio.

This can be demonstrated on a simple example by comparing Type 1 and 4 antennas. Assume as a starting point, a single source fed paraboloid with an aperture radius of R for each case, resulting in an aspect ratio of 1 and a gain of G.

If the aspect ratio has to be increased to 2, while G = constant, then for Type 1, a second feed horn has to be provided and the aperture diameter increased to $\sqrt{2}$ R. Assuming that the cost of feed and power divider hybrid is negligible compared to the reflector and the cost of reflector is proportional to its area (in practice, the cost is more likely proportional to the 2.7th power of R), the cost of the new system is doubled. (See Figure 5.1).

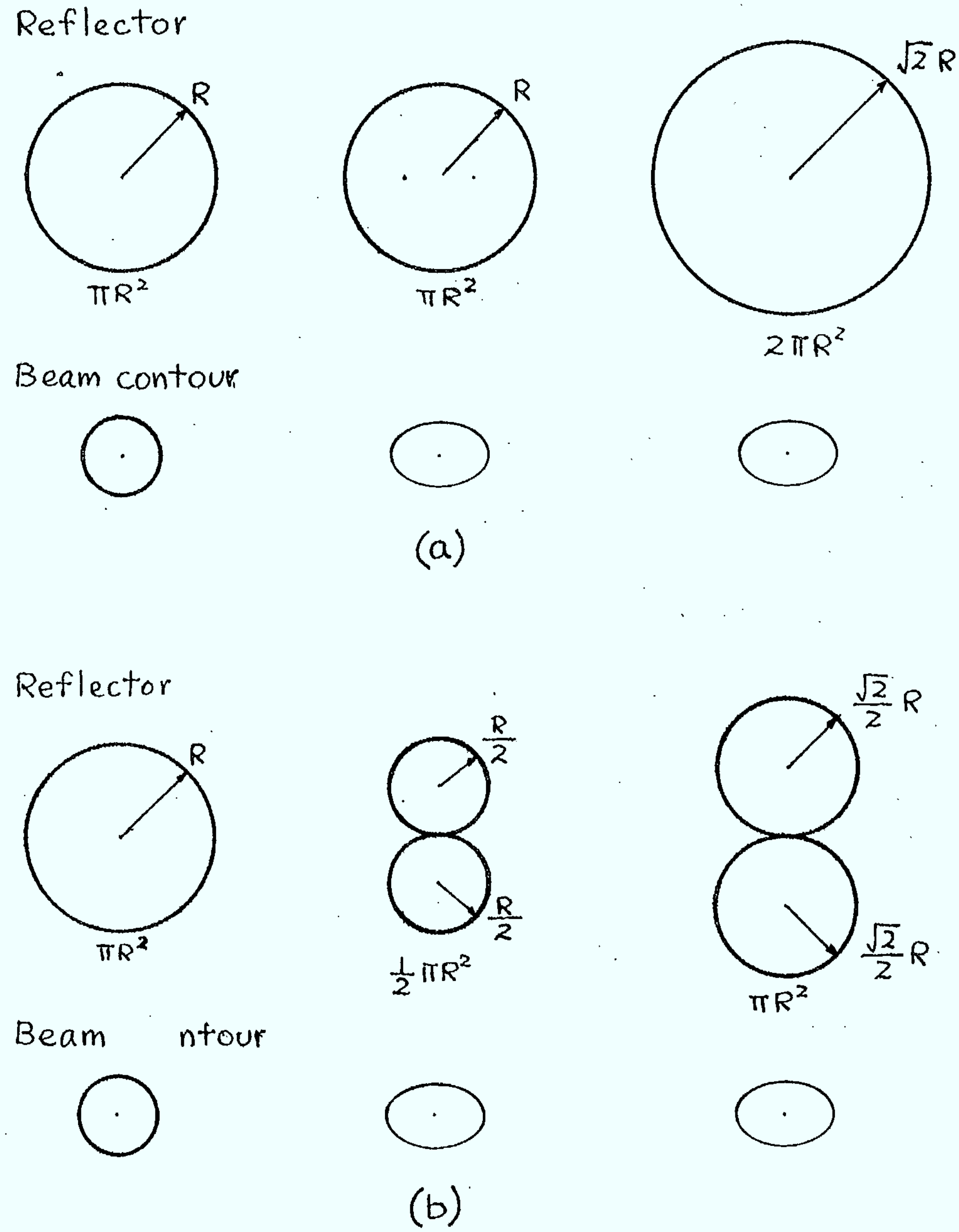

5.1 Variation of aperture radius for constant gain as a function of beam cross-section for a) arrayed feeds and for b) arrayed antennas.

For the Type 4 system, the same change in beam cross-section can be achieved by using two paraboloids with an R/2 radius in a linear array form. The aperture area of this system did not change relative to the initial, thus the cost also remains unchanged, if the same assumptions are made as before.

In actual practice, the above assumptions are not quite correct. In the case of Type 1, the required feed horn size decreases, thus the cost of the feed decreases, while the cost of connecting lines between them tend to remain small. In the case of Type 2, the required feed horn size increases, the cost and loss of connecting waveguide between them may not be negligle and a separate support and alignment technique is required for the two dishes. These tend to reduce the cost gap between the two approaches but does not alter the basic conclusion that Type 4 has a higher aperture efficiency, thus it yields a more effective gain approach. From this, it follows that the Type 4 design is more cost effective for transmit operations.

For receive operations, the antenna is characterized by its G/T instead of G. For high gain, the length and loss of the connecting lines in Type 4 are not negligible and yield a large antenna noise temperature, if a single receive terminal is desirable. Thus, for receive or combined receive and transmit operations, for large gain and aspect ratio, the Type 1 design may become more cost effective.

The above example demonstrates that one or the other of the listed types of arrays may be more advantageous, depending on the gain requirements and other system parameters, such as beam aspect ratio or receiver noise temperature.

The actual selection requires a more detailed analysis depending on the individual circumstances.

5.2 Linear Array of Feed Horns Feeding a Circular Aperture Paraboloid

The components of such a system are fairly conventional. They require, for dual band, dual polarized operation, the following elements:

square or circular feed horn
orthogonal coupler
hybrid
connecting waveguide

The optical system can either be focal point fed or subreflector fed main reflector. For the first case, the main reflector has to be a paraboloid, while in the second case, the main and subreflector can form a shaped reflector set resulting in about .6 – .8 db higher aperture efficiency and even larger increase in G/T.

The obtainable aspect ratio follows from the scanning characteristics of focal point and subreflector fed optical systems. Within the latter category, the scanning characteristics are nearly independent whether the system is a paraboloid – hyperboloid or dual shaped reflector combination.

The obtainable aspect ratio can be best demonstrated by measured results, some of them directly on the 28 inch paraboloid developed for the CTS satellite in the 12 – 15 GHz frequency band. Figure 5.2 shows a series of the measured scanning patterns. This antenna has a 2.5° beamwidth and it can scan within $\pm 8^{\circ}$. However, note that this scanning is achieved by rotating the reflector relative to the feed, thus by simply feed scanning only half this range or a peak to peak scanning of 8° can be achieved without a serious loss of gain. This is equivalent to an aspect ratio of 3.2. In actual practice, such a beam can be synthesized by 3 horns which are fed from a ring hybrid power divider, providing 120° phase between horns. The resultant pattern will have a gain of 3.2 less than the spacecraft antenna. An increase of antenna diameter by a factor of 4 to 108 in. would result in an $.62^{\circ} \times 2^{\circ}$ beam with $16/3.2 = 7$ db higher gain than for the satellite antenna, or 43.2 db.

The aspect ratio can be improved by increasing the F/D ratio of the paraboloid. Figure 5.3 exhibits measured patterns for F/D $\approx$ 1 and for a partially offset fed paraboloid. ($\approx 2^{\circ}$ beamwidth with 5 Ft. reflector at 6 GHz). These patterns indicate that for a beam scan of $\pm$ 4 beamwidth, practically no beamwidth and sidelobe level deterioration can be achieved. The use of an 8 horn array in such a paraboloid can produce an aspect ratio of 8 or a $.5^{\circ} \times 4^{\circ}$ beam at 12 GHz and 10 Ft. diameter reflector. The feed network requires a total of 7 hybrids and 8 horns for single polarization or 14 hybrids, 8 orthocouplers and 8 horns for dual polarizations. Although the complexity of such a feed network is not prohibitive, the above example indicates the rapidly increasing complexity in the feed network with this method of increasing the aspect ratio. The increasing complexity of the feed network increases not only the cost, but also the size of the integrated feed assembly. The size of feed on the other hand, will increase blockage, unless the reflector is offset fed – as in the above example – or Cassegrain fed if the gain of the system is large enough.

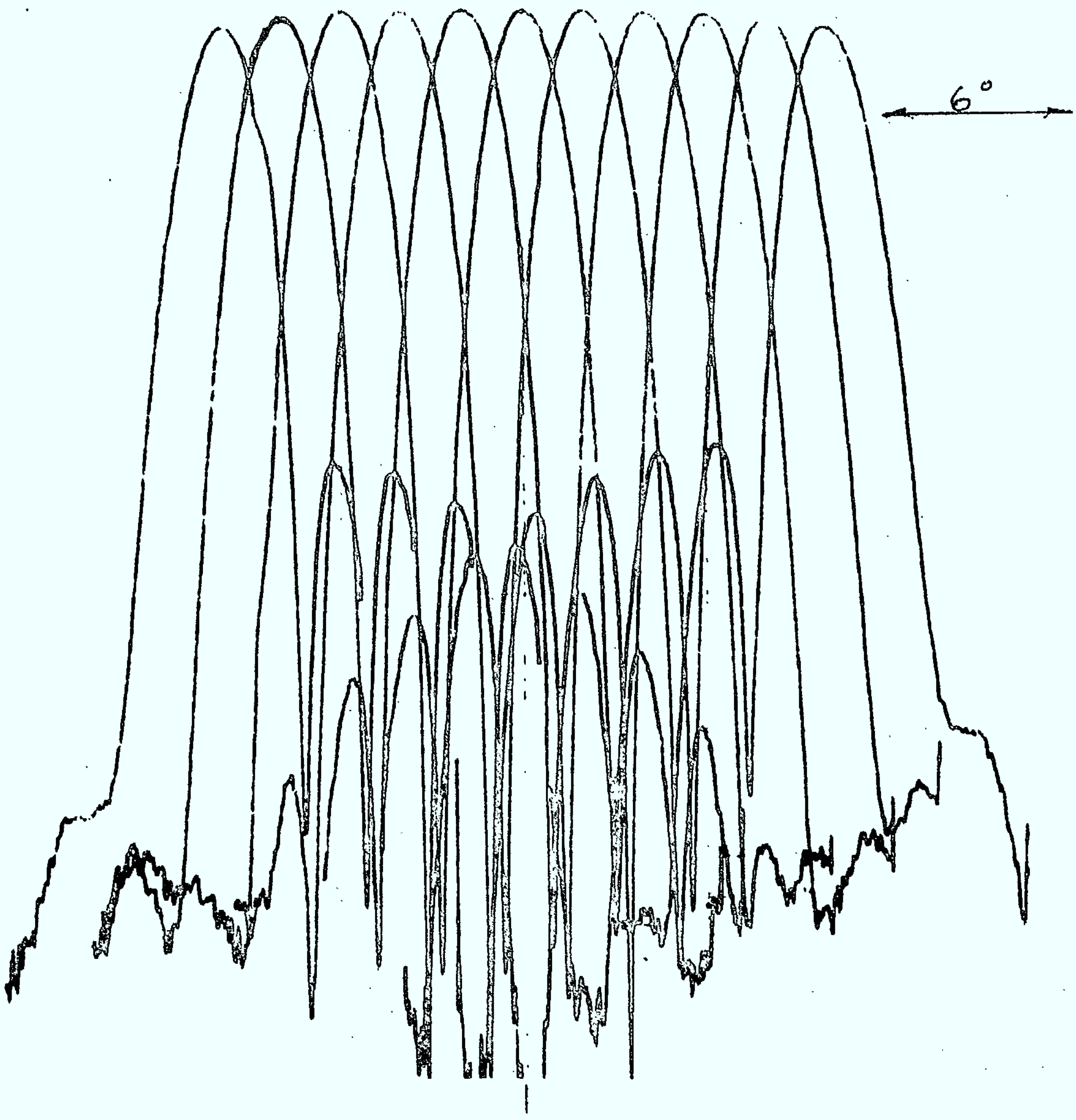

5.2 Measured scanning characteristics of a typical focal point fed paraboloid (28 in. diameter CTS spacecraft antenna) in the 12 GHz frequency band. Actual scanning without rotation of reflector corresponds to $\pm 4^{\circ}$, $\Theta_3 = 2.5^{\circ}$.

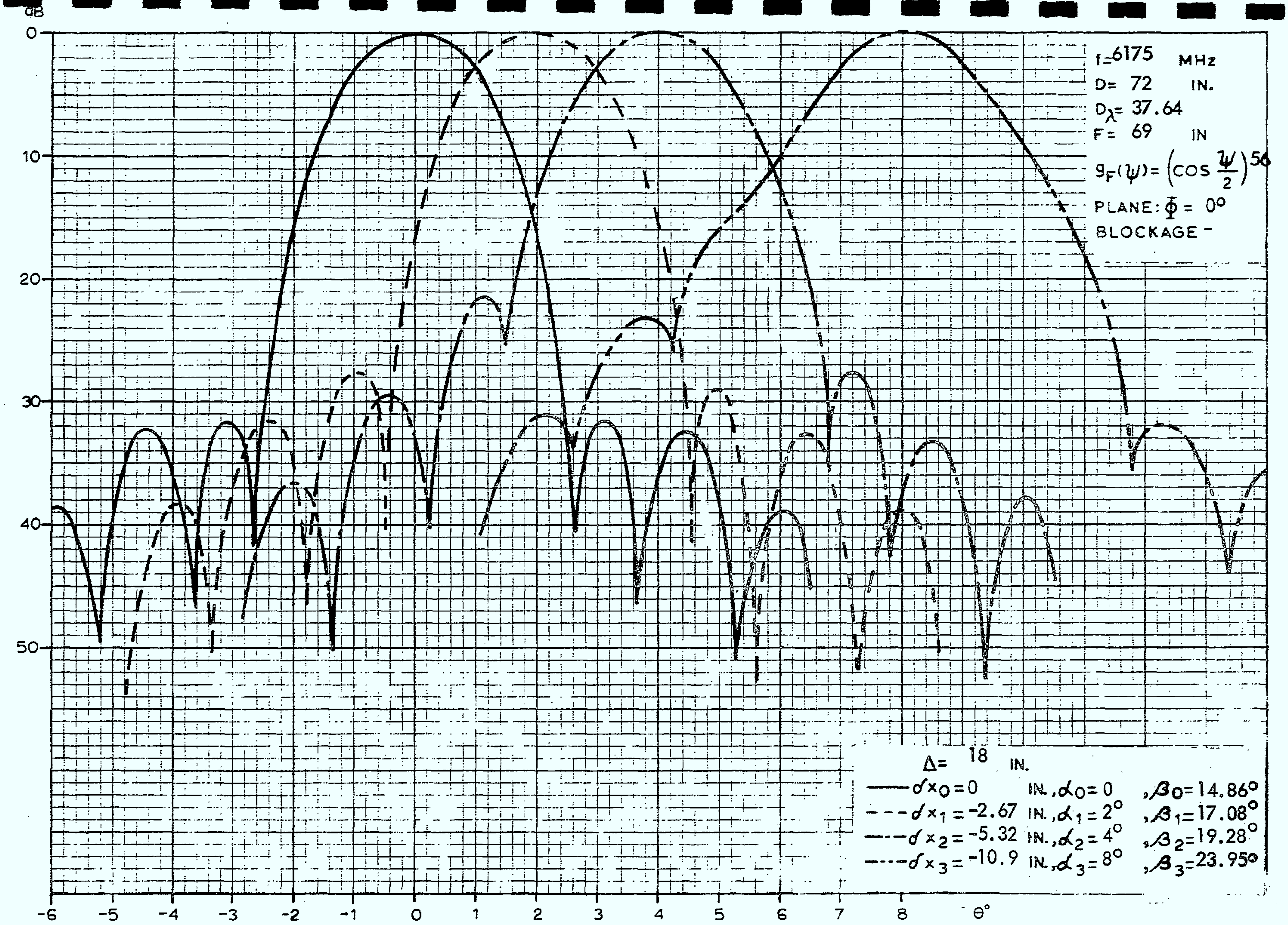

Fig. 5.3a Theoretical scanning characteristics of a long focal length offset fed paraboloid. at 6175 MHz.

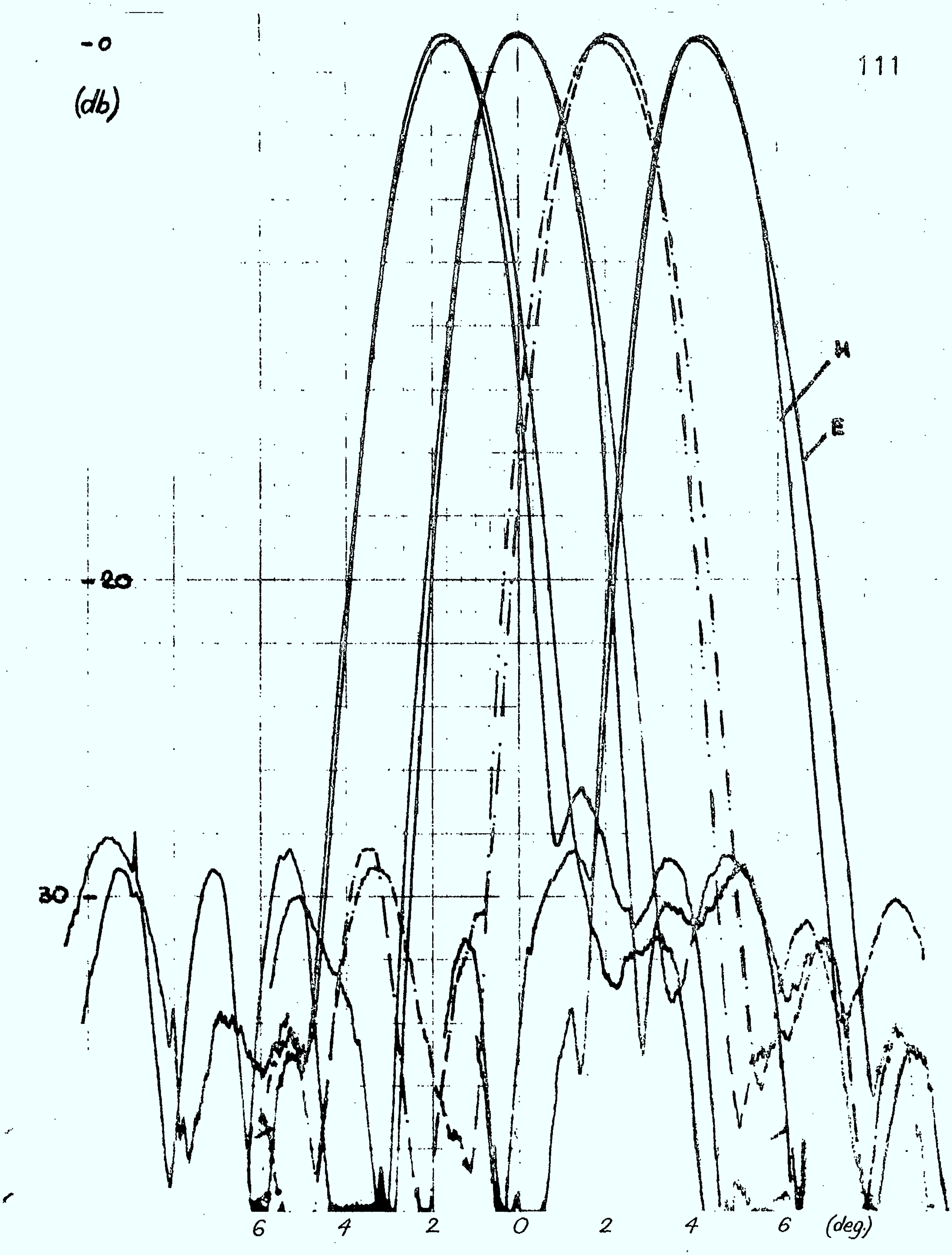

Fig. 5.3b Measured scanning characteristics of a long focal length offset fed paraboloid.

Typically, it is not practical to use a feed array for a Cassegrain antenna, unless the overall gain of the antenna for a single radiating source does not exceed 42 - 45 db. The reason for this is that the size of the required subreflector and/or feed horn is prohibitively large, which in turn limits the number of usable radiating elements.

Figure 5.4 shows the measured pattern of a scanned Cassegrain system using paraboloid - hyperboloid reflector combination. These measurements were done by using an 8 Ft. reflector at 10.45 GHz. The measured beamwidth is $\approx .94^\circ$ for a single feed. It can be seen that a $\pm$ 1.86 beamwidth scan can be achieved with this system before appreciable gain degradation occurs. Thus, this system can provide an aspect ratio of 3.72 or a $.94^\circ \times 3.5^\circ$ beam at 10.45 GHz, yielding a $.65^\circ \times 2.41^\circ$ beamwidth at 12 GHz with a 10 Ft. diameter reflector.

The required feed network for such a system can be built up from 1 Magic Tee and 2 Ring hybrids yielding

$$0^\circ,\ 120^\circ,\ 240^\circ,\ 180^\circ,\ 300^\circ,\ 60^\circ$$

for the consecutive, adjacent horns. The maximum phase difference at the approximately 3 db crossover points of the individual beams will be maximum 120°, yielding a reasonable smooth pattern cut across the center of the individual beams. The 3 db contour of the resultant beam will be approximately a rectangle, quite close to the specified "box" for the satellite movement. The pattern in the long dimension of the box approximates a sector beam.

For dual polarizations, 3 orthocouplers and 3 additional hybrid have to be added to the feed circuit. Since the system is Cassegrain fed, no blockage problem other than the one associated with the subreflector occur, the feed package can be kept behind the reflector and the low noise receiver can be integrated with this package.

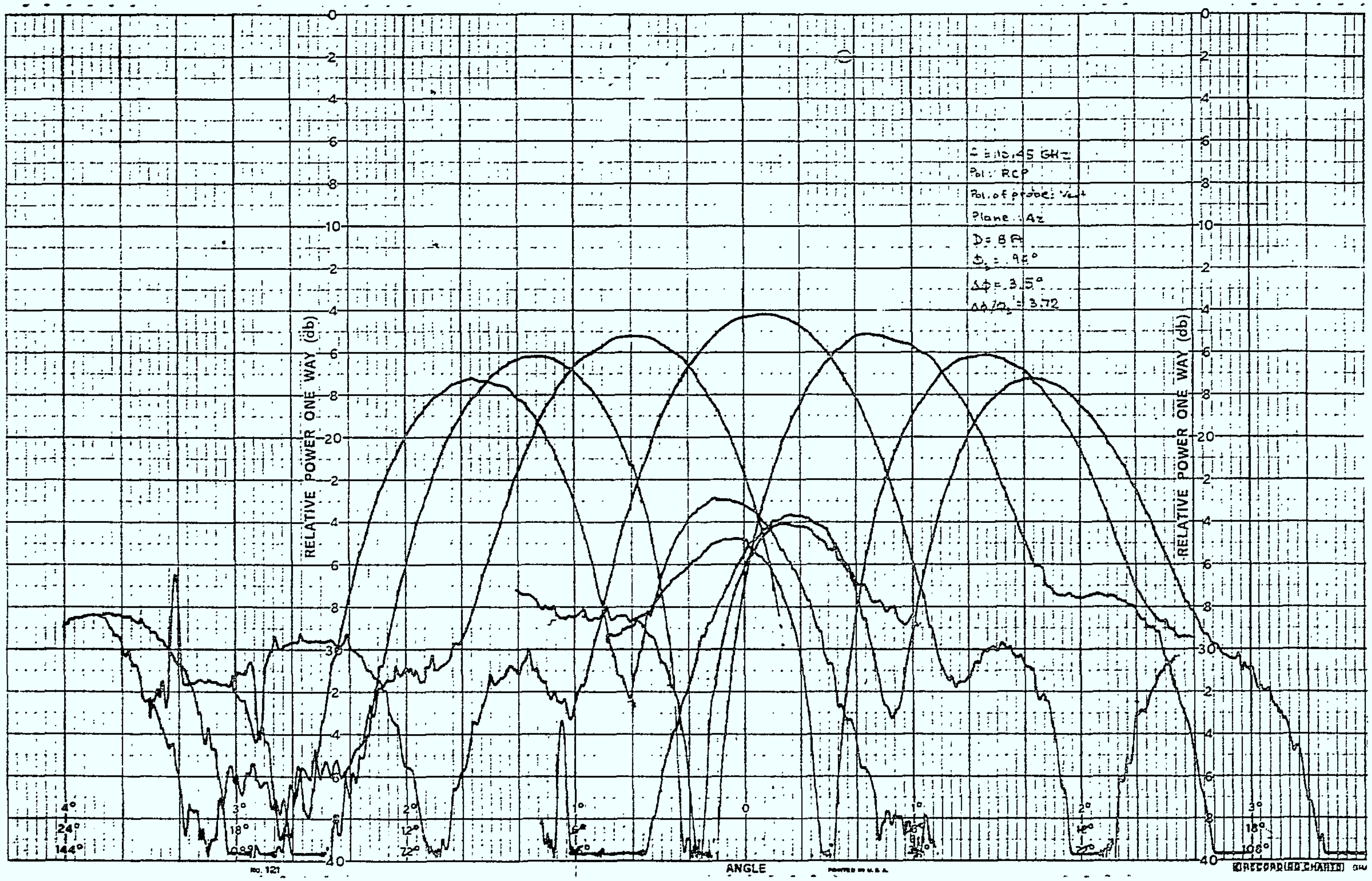

Fig. 5.4 Measured scanning characteristics of a typical 8 Ft. diameter Cassegrain type paraboloid at 10.45 GHz. Achievable aspect ratio with 6 horns $\Omega_b = 3.72$.

5.3 Linear Array of Feed Horns Feeding An Elliptical Aperture Paraboloid

This type of configuration is aimed to reduce the aperture deficiency associated with the configurations discussed in Section 5.2 and at the same time further reduce the number of necessary feed elements.

The concept is very similar to the antennas described in the previous section except that the basic antenna (and feed array element) now utilizes the previously analyzed configurations with moderate aspects ratios.

It was previously shown that it is relatively easy to design a single antenna with a beam aspect ratio of 2.5. Such beams require a horn with an aspect ratio of approximately 1:2.5 and a paraboloid aperture shape of 2.5:1. If, in such an antenna, a 2 element feed array is placed as shown on Figure 5.5, then the aspect ratio of the resulting beam can be increased by a factor of 2.

Figure 5.6 shows the measured scanning characteristics of a 26" x 65" elliptical contoured aperture with a 30 in. focal distance paraboloid at 4 GHz. The resulting beamwidth is $3.2^{\circ} \times 8^{\circ}$. With a pair of such horns, side by side with their narrow dimensions, the beam cross-section can be increased to 3.2° 16° with some deterioration of spillover efficiency. Increasing the frequency to 12 GHz and the antenna size to 52" x 1.30", a factor of 6 reduction of beam cross-section is achieved, yielding $.53^{\circ} \times 2.7^{\circ}$ beam cross-section and an aspect ratio of 5. Such a system requires only 1 power divider hybrid and 2 horns for single polarization and an additional hybrid and 2 orthocouplers for dual polarizations.

It is interesting to compare this system with 6 element array fed Cassegrain, yielding about the same beam cross-section characteristics than with a circular 10 ft. reflector. Note the saving in circuit components and in the reduction of aperture area to about half.

The comparison indicates the superiority of the Type 2 systems relative to Type 1 in terms of complexity and cost. However, it must be pointed out, that the Type 2 system has limitations relative to Type 1 systems, namely:

a) it has larger spillover radiation, thus lower gain and higher noise temperature for a given beam cross-section.

b) it can not be optimized for both polarizations as well as the Type 1 system, thus it will have a poorer transmit gain if the receive gain of the two types are designed to be equal.

c) it will have a poorer cross-polarized component for the mode when the main polarization is parallel to the wide dimension of the horn. (However, better then 20 db within the 3 db contour of the main beam.

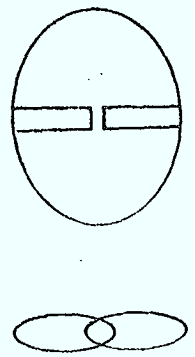

5.5 Concept of an elliptical aperture contour paraboloid with a feed array.

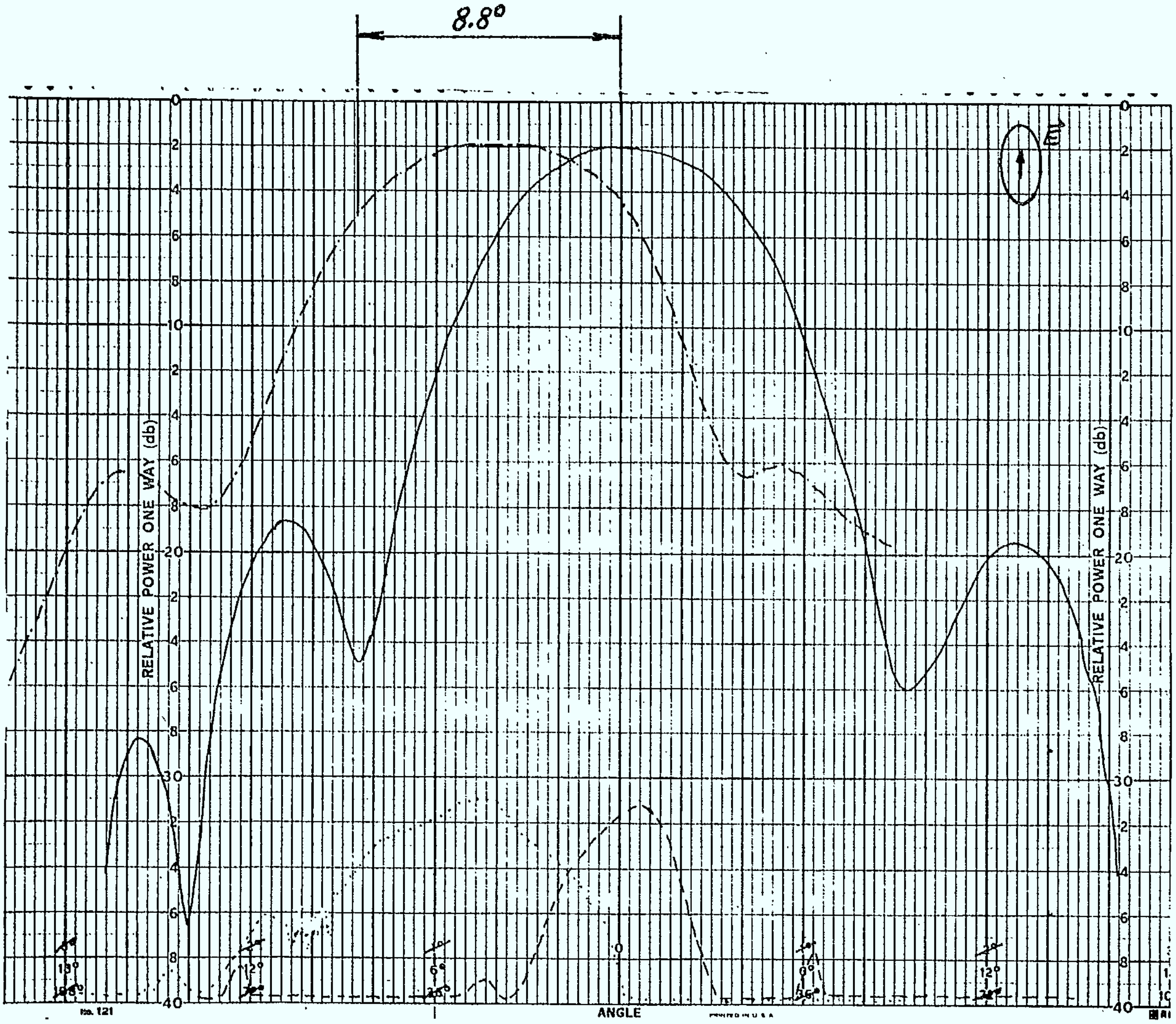

5.6a Measured scanning characteristics of a typical focal point fed, elliptical aperture, contour paraboloid (26 in. x 65 in. aperture dimensions) in the 4 GHz frequency band. (H-plane scan, H-plane patterns. Shown amount of scanning corresponds to $\Omega_b = 8.8/2.3 = 3.83$).

5.6 b Measured scanning characteristics of a typical focal point fed, elliptical aperture, contour paraboloid (26 in. x 65 in. aperture dimensions) in the 4 GHz frequency band. (E-plane scan, E-plane patterns)

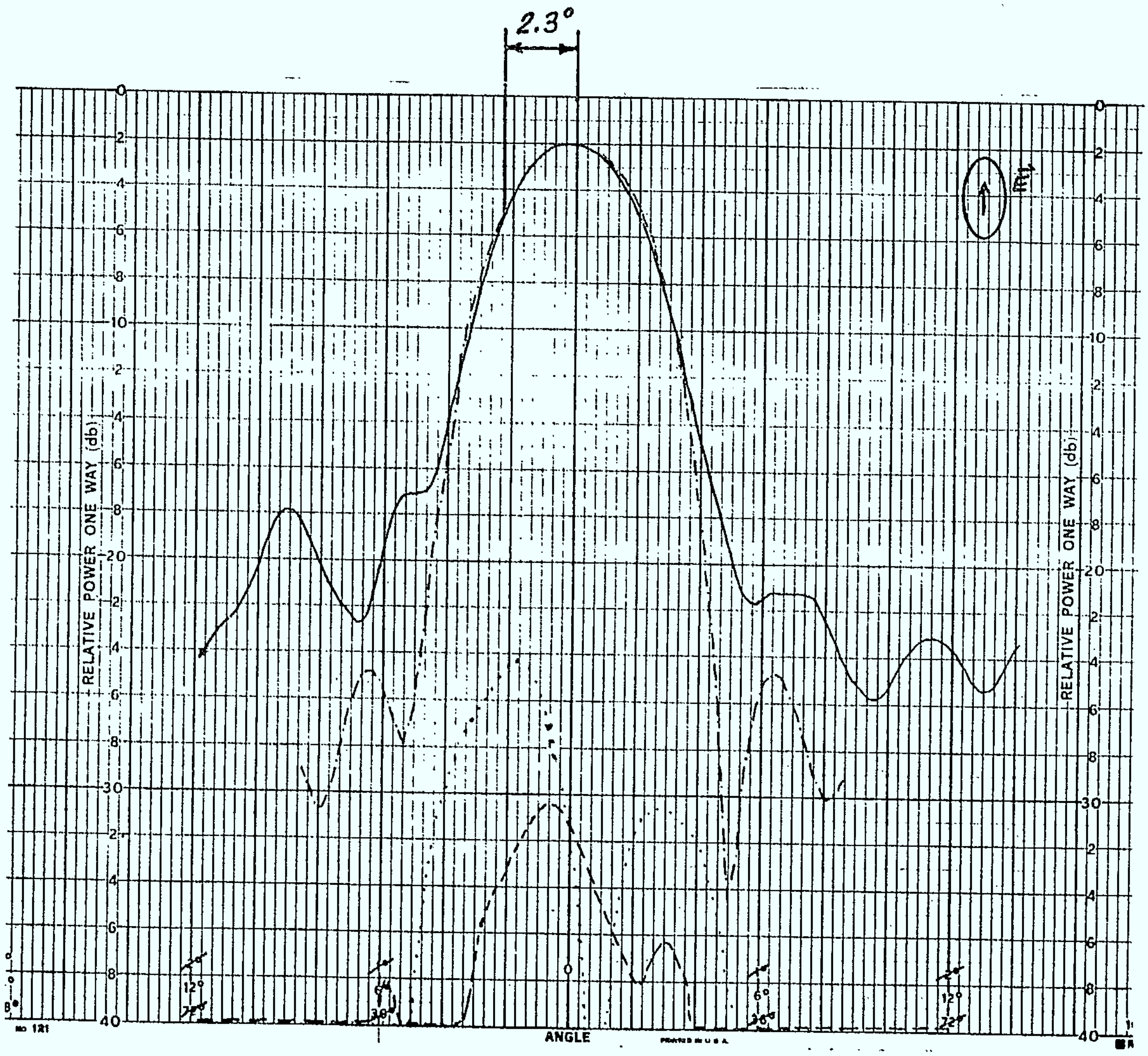

5.6 c Measured scanning characteristics of a typical focal point fed, elliptical aperture, contour paraboloid (26 in. x 65 in. aperture dimensions) in the 4 GHz frequency band. (H-plane scan, E-plane patterns)

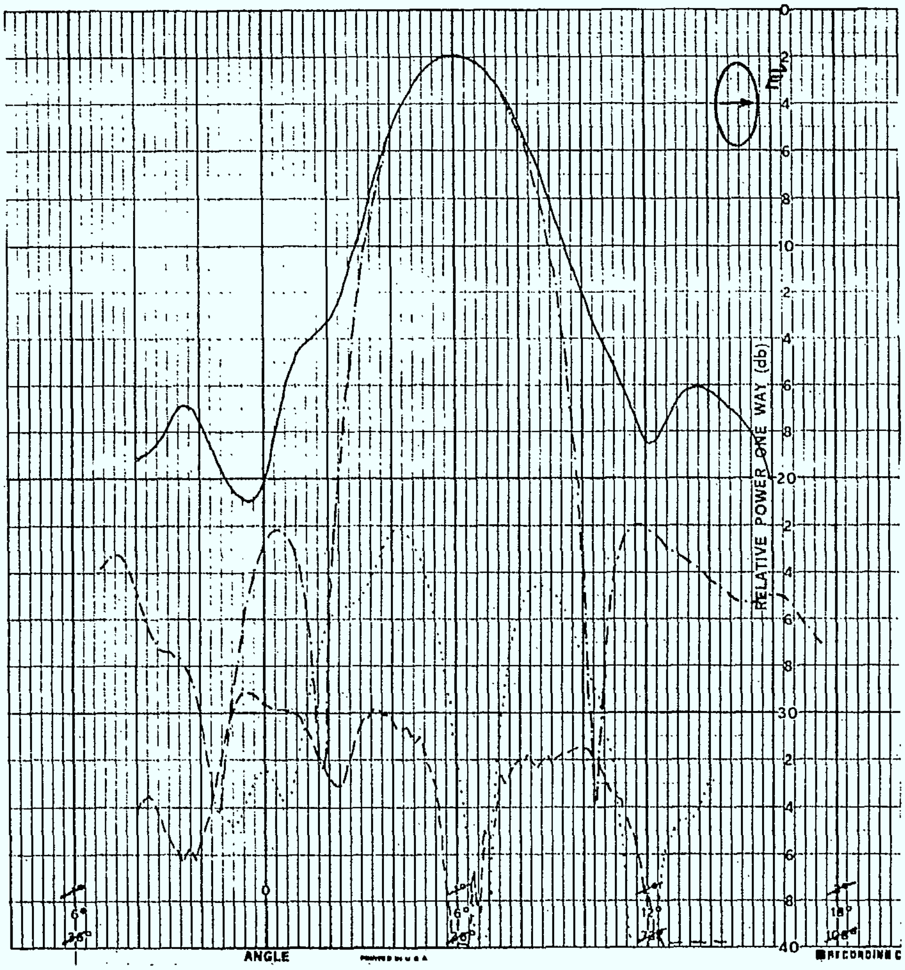

5.6d Measured scanning characteristics of a typical focal point fed, elliptical aperture, contour paraboloid (26 in. x 65 in. aperture dimensions) in the 4 GHz frequency band. (E-plane scan, H-plane patterns)

5.4 Linear Array of High Gain Horns

This method of synthesizing antenna beams is particularly rewarding for moderate gains and large aspect ratios.

The cost of horns in the 12 GHz frequency band is quite acceptable up to about a gain of 29   30 db. At 12 GHz this corresponds to the gain, a 10 in. square aperture with a TE_{10} mode excitement and approximately 90° quadratic phase error   50 in. length. Such a horn has about 6° beamwidth. 8 such horns forming a linear is capable of producing .75° x 6° beamwidth with an aspect ratio of 8. The network requires 7 hybrids for one polarization and an additional 7 hybrids and 7 orthogonalr couplers for dual polarizations, thus the feed circuit is identical to the one required for the 8 element feed array in the paraboloid, but it requires a longer feed line (a minimum of 40 inches plus the length of the hybrids) and associated loss.

The gain of such a system is equivalent to an approximately 7 ft. diameter paraboloid feed by the same element number array. Thus for the purpose of economic comparison the cost of the 7 ft. diameter paraboloid and 8 small horns has to be compared to the cost of the 8 horns with 10 in. square apertures and 50 in. length. It must be pointed out, that even if the cost of the two solutions is identical, which is probably the case, the single paraboloid solution is still better, because of the lower circuit loss (40 in. shorter waveguide). However, for larger aspect ratios the paraboloid can not provide a solution, thus for these cases the large horn approach is superior.

It may be mentioned that the number of horns can be reduced by increasing their length. For instnace a 10 in. x 15 in. aperture horn can be built with a 112 in. overall length for acceptable quadriatic phase error in their aperture and already 4 such horns can synthesize an aspect ratio of 6 with a 10 in. by 60 in. aperture resulting in a 1° x 6° beam. Such a system requires only 3 power divider hybrids.

5.5 Linear Array of Circular Paraboloids

The array systems discussed in the previous sections indicated that for aspect ratios up to 8, the Type 3 systems may not be able to compete economically with Type 1 or 2 systems for large gains. The reasons for this was the relatively large cost of long horns necessary for large horn gains.

This limitation can be easily removed by replacing the horn by a small paraboloid as soon as the element gain is exceeding about 30 db. From this point of view of gain (and cost) such systems can compete with the Type 1 and 2 systems but the basic limitation associated to the loss in the power divider waveguide remains a limitation of the configuration, particularly for low noise receivers.

6.0 MISCELLANEOUS TYPES OF ANTENNAS

6.1 Pillbox Fed Linear Horn (Array)

A pillbox fed by an orthocoupler and itself feeding a linear horn (Figure 6.1) forms a solid mechanical unit. The usefulness of such an antenna has also been evaluated for the present applications. Allowing a 90° quadratic phase error across the short dimension of the aperture the length of the horn should be

$$\frac{l}{\lambda} = 2\left(\frac{a}{\lambda}\right)^2$$

where 2a is the shorter aperture dimension.

Assuming a reasonable length of $l/\lambda = 50$ the short dimension of the aperture is $2a/\lambda = \sqrt{2l/\lambda} = 10$ resulting in a beamwidth of 6.8° for the polarization of Figure 6.2a and about 5° for case(b).

With a beam aspect ratio of 2, the beam cross-sections are $6.8^{\circ} \times 3.4^{\circ}$ and $5^{\circ} \times 2.5^{\circ}$ corresponding to on-axis gains of about 30.7 db and 33.3 db.

These gains fall short of the presently required gain of about 36.6 for an aspect ratio of 2.

It is possible to form an array of such structures to increase the gain. The increased weight and feed system complexity (4 hybrids and 3 orthocouplers) are probably still not prohibitive. Such a system could satisfy the requirements of the low gain low aspect ratio category of antennas. Its wide beamwidth could be about 2.3° and its narrow beamwidth depending on the size of the pillbox around 1.5° ($\sim 50\lambda$ long pillbox aperture). The calculated pattern in the plane of the long dimension is shown in Figure 6.3.

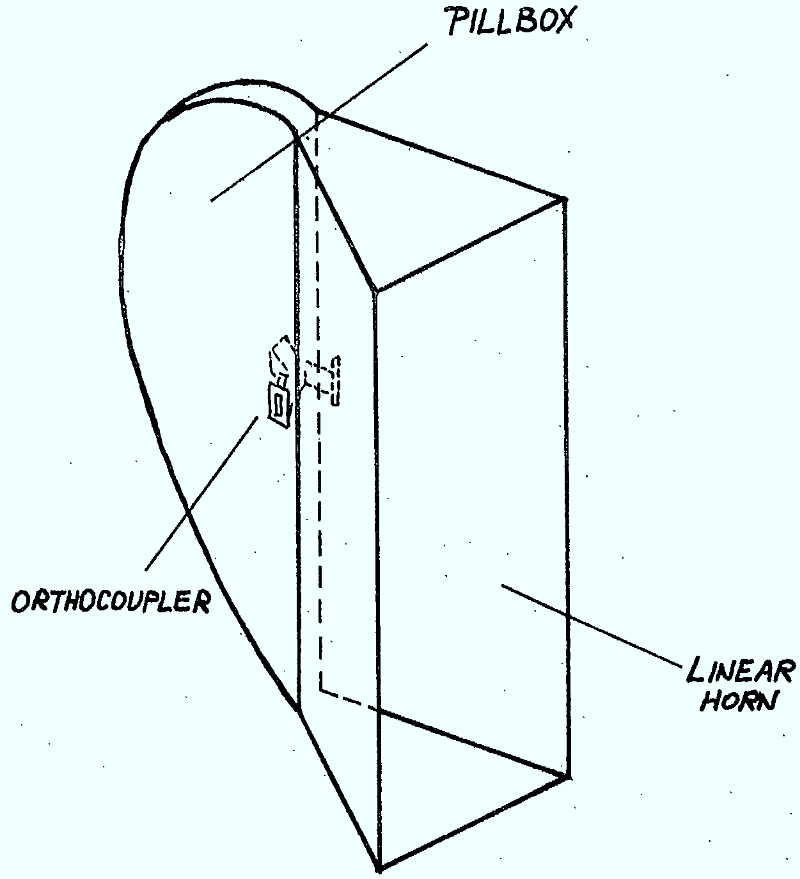

Fig. 6.1 Layout of the pillbox fed linear horn.

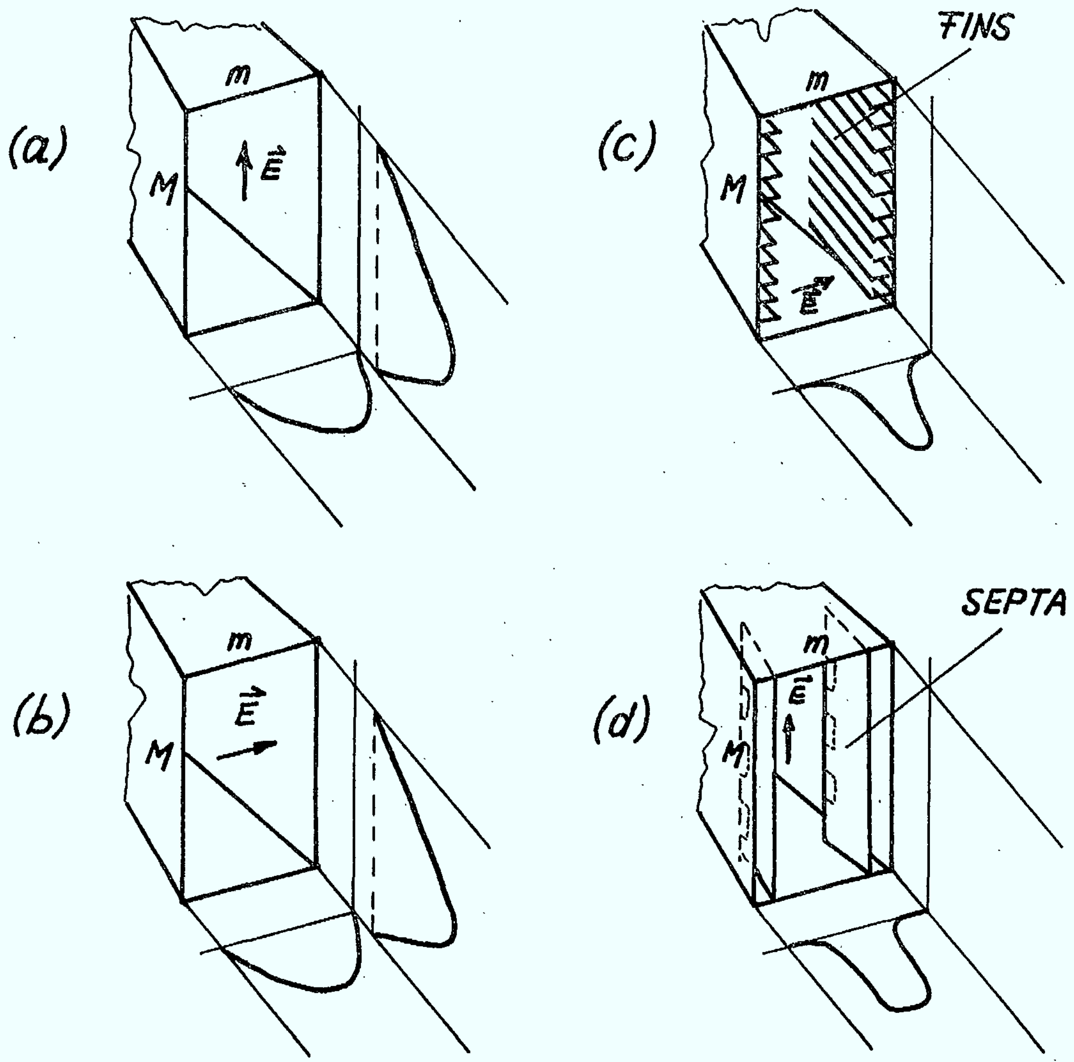

Fig. 6.2 Aperture distribution of the linear horn fed by a pillbox.

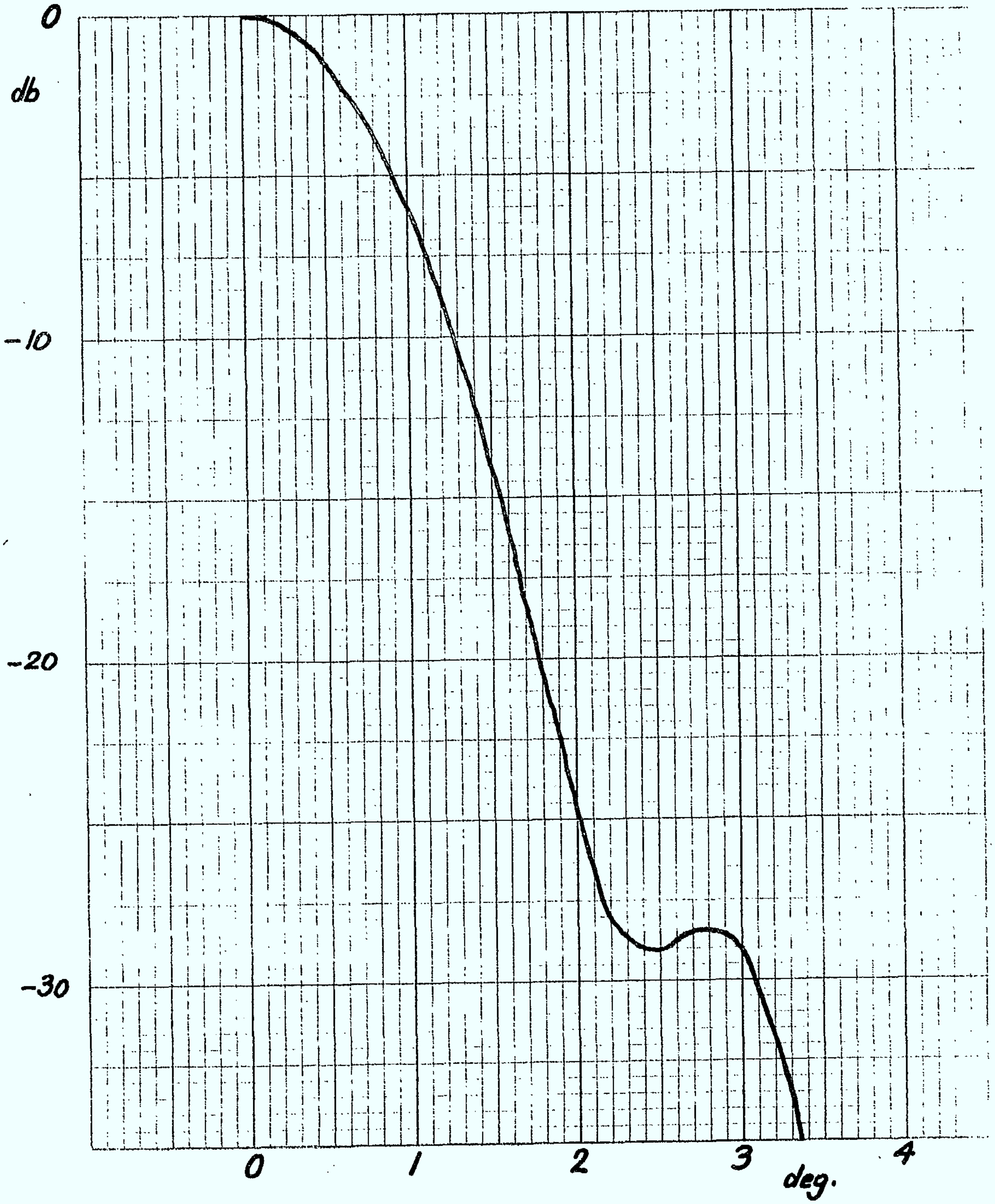

Fig. 6.3 Calculated pattern of a pillbox antenna.

7.0 THE BASIC DESIGN OF TWO ANTENNA CONFIGURATIONS

In this section, the basic configurations and estimated characteristics of two antenna designs are presented. They represent the possible realizations of antennas having recommended but considerably different beam characteristics. One belongs to the low aspect ratio, low gain category for the coverage of the $0.46^o \times 1.43^o$ satellite motion box (MB_1). The other is the medium gain, high aspect ratio antenna for the coverage of the $0.46^o \times 2.2^o$ motion box (MB_2). The low aspect ratio antenna with minor modifications is also suitable for the low gain coverage of MB_2.

7.1 Low Gain, Low Aspect Ratio Antenna

This antenna provides the coverage of MB_1 with an edge gain equivalent to the on-axis gain of a circular paraboloid of about 2.3 ft. diameter. It utilizes an elliptically contoured paraboloid reflector with an aperture area equal to that of a 3 ft. diameter circular paraboloid. Its major and minor axes are 44 in. and 29.4 in. It could be cut from a 4 ft. diameter commercially produced paraboloid. The reflector is fed by a rectangular aperture. A focal length of F = 42.2 in. is selected resulting in low cross-polarized levels and a larger feed aperture. The feed aperture dimensions normalized to wavelength are 3.0×1.44 for M-polarization and 2.0×2.16 for m-polarization. To avoid excessive blockage, the feed is offset in the M-plane by 11.0 inches (= M/4). The feed dimensions were selected for about 10 db feed pattern tapering at the edges of the reflector. The practical realization of this dual polarized feed may be achieved by a single rectangular horn with some fin loadings. Final details of the feed horn dimensions and configuration should be determined experimentally. The feed horn is fed through an orthocoupler providing the two isolated input ports. Assuming that the reflector would be cut from a circular paraboloid or using standard tooling for such, the diameter required will be larger because of the offset feed arrangement. For an offset of 11 inches, the diameter of the circular reflector (or mold) should be 44 + 2 (11) = 66 inches, i.e., 5.5 feet or the next standard size, 6 feet.

The dimensions of the antenna and some of its estimated characteristics are summarized in Table 7.1. The valuesare based on calculated and measured results.

7.2 Medium Gain, High Aspect Ratio Antenna

This antenna provides the coverage of MB_2. With a single feed, the increase in edge gain is attained at the expense of a high beam and aperture aspect ratio that is practically identical to that of MB_2. An elliptical paraboloidal reflector is used, fed by a rectangular aperture feed. The feed aperture dimensions expressed in terms of wavelength are $a_1 = .655$, $b_1 = 2.4$ for polarization along the narrow dimension of the reflector and $a_2 = 3.135$, $b_2 = .47$ for the

TABLE 7.1

Summary of Design Data and Characteristics of the Low Gain, Low Aspect Ratio Antenna

Polarization Direction	Reflector Dimensions (in.)		Aperture Area (ft.)^2	Aperture Aspect Ratio Ω_a	Offset (in.)	$\frac{F}{M}$	Highest Sidelobe (db)		G_o (db)	$G_{on\text{-}axis}$ (db)	G_{edge} (db)
	Major axis (M)	Minor axis (m)					E-plane	H-plane			
M	44	29.4	7.1	1.5	11	.96	24	20.5	41.2	38.65	37.55
m							20	18.0		38.15	37.05

Polarization Direction	Cross-polarized level db below peak		Pointing Error Sensitivity $\frac{db}{deg.}$	Feed Aperture Dimensions (λ)
	E-plane	H-plane		
M	35	26	2.8	$a_2 = 3$, $b_2 = 1.44$
m	> 30	30		$a_1 = 2$, $b_1 = 2.16$

polarization orthogonal to that. The feed aperture dimensions were selected for about 10 db feed pattern tapering at the edges of the reflector. Details of the feed horn dimensions and its design (it may be a fin loaded horn or a horn reflector) in general, could be determined best experimentally. A limited development effort to this end would also include considerations of reducing the distance between the phase centers for the two orthogonal polarizations and therefore, reduce gain loss due to quadratic phase error. The dimensions of this reflector are quite uncomfortable:
major diameter (M) = 144.4 in., minor diameter (m) = 30.2 in. Assuming that this reflector is cut from a commercially available circular paraboloid, its diameter must be 12 ft. Considering, for the present, paraboloids of fiber glass construction, the price doubles at every step in going from 10 to 12 to 15 ft. diameter. For offset feed, the required diameter increases with an amount twice the actual offset. To reduce the drop of edge gain due to beam squint resulting from an offset feed, the offset should be in the plane of the long dimension. An offset of 1.5 feet which is less than required would double the cost of the reflector. Based on this consideration, a center fed arrangement is suggested. It seems that the effects of higher blockage would be less disturbing than those associated with the offset feed and its associated very high reflector costs. Most commercially available reflectors have an $F/D \cong .4$. D in this case is M, thus our selected $F/M = .314$ is a realistic value. The feed is preceded by an orthocoupler which provides the isolated transmit and receive ports.

The estimated dimensions and major characteristics of the antenna described above are summarized in Table 7.2. The crosspolarized level is due to the reflector alone. The overall figure will be considerably worse if the contribution by the source is also taken into account. It is expected that the final figure will still be better than 20 db.

Considerable costs are involved in the production of this kind of antenna because of the high aspect ratio of the satellite motion box MB_2. If this MB_2 is going to be used an array type feed or an array of smaller circular reflectors, the types discussed in Chapter 5 could be considered. Their basic disadvantage is the complexity of the feed circuit which should be weighted against the relative simplicity of a limited tracking system. Moreover, an array type feed would still require the same length of the reflector, the dimension that essentially determines its cost.

TABLE 7.2

Summary of Design Data and Characteristics of the Medium Gain, High Aspect Ratio Antenna

Polarization Direction	Reflector Dimensions (in.) Major axis (M)	Minor axis (m)	Aperture Area $(ft.)^2$	Aperture Aspect Ratio Ω a	$\frac{F}{M}$	Highest Sidelobe (db) E-plane	H-plane	G_o (db)	$G_{on-axis}$ (db)	G_{edge} (db)
M	144.4	30.2	23.7	4.8	.314	23	18	46.5	44.9	41
m						24	19.5		43.9	40

Polarization Direction	Cross-polarized level below peak (db) 45° plane	Pointing Sensitivity in plane of M $\frac{db}{deg.}$	Gain loss due to phase error by feed	Ohmic Loss, Surface Error (db)	Feed Aperture Dimensions (λ)
M	38	4	.8 db	0.2	$a_2 = 3.135$, $b_2 = .47$
m	41				$a_1 = .655$, $b_1 = 2.4$

8.0 CONCLUSIONS

1. The usefulness of earth station antennas, which are continuously directed by their main beam maximum toward the satellite at the other end of the link, can be characterized by their G/T ratio for receive and gain for transmit purposes along a single direction, represented by the electrical axis of the antenna. In contrast, the usefulness of a non-tracking antenna is characterized by its receive G/T and transmit gain on a conical surface defined by the position of the antenna as the apex and the maximum excursions of the satellite. These most important antenna characteristics conveniently can be called as edge G/T and edge gain.

2. The influence of antenna design on edge G/T is dependent on the percentage of antenna noise temperature T_A in the total system noise temperature $T = T_A + T_R$, where T_R is the noise temperature of the receiver system. If $T_R \gg T_A$, then variations in T_A caused by internal antenna losses or ground radiation picked up via spillover radiation has little consequence on the system performance. Thus, for such cases, the optimization of the antenna gain for both the receive and transmit frequency band is the main governing problem and the design must produce a maximum gain over cost ratio, which in practice typically is proportional to the gain to weight ratio of the antenna.

   On the other hand, if $T_R \approx T_A$, which for the present medium gain application typically occurs when $C_R \approx C_A$, where C stands for the cost of the corresponding subsystems, then the provision of low antenna noise temperature becomes important. For such cases, the system has to be designed simultaneously for high edge G/T in the receive and high gain in the transmit band.

   From the above, it is obvious that an antenna optimization cannot be done independently from cost considerations, including the receiver and transmitter subsystems. However, since the scope of the present study did not include these subsystems, the antenna considerations had to be kept general, distinguishing only two types of receivers for which

   a) $T_R \approx T_A$

   or

   b) $T_R \gg T_A$

3. The frequency ratio between the highest transmit and lowest receive frequency is about 1.23:1. Since the presently considered antenna must be acceptable and efficient for the limiting case of edge of contour operation, one of the basic questions to be answered is: What shall the relationship be, between the angle represented by the edge of the satellite excursion contour and the 3 db beamwidth of the antenna.

   If the two are simply selected as equal, then for this limiting case of operation, the ideal antenna efficiency (for a perfect antenna) will be - 3 db and for a practical antenna, close to - 5 db. If the efficiency of the antenna is constant with frequency (- 2 db on beam axis), then this - 5 db edge efficiency will deteriorate by 1.53 db due to narrowing of the beam with frequency to - 6.53 db. This deterioration almost completely destroys the 1.8 db natural gain increase with frequency, yielding only .27 db edge gain increase with frequency. Thus, non-tracking antennas for the above described type of operation became less effective with increasing frequency and also produce an increasing amount of EIRP instability, due to wind effects.

   Alternatively, the antenna can be set up with frequency independent beamwidth. For such a case, the antenna efficiency on beam axis deteriorates with the square of the frequency, thus, if it had - 2 db efficiency at the low end of the band, it will have - 3.8 db efficiency at the high end. Such systems will have constant edge gain efficiency, no improvement in edge gain with frequency, but constant EIRP instability across the band which is probably a more valuable feature than the potentially available .27 db edge gain improvement.

4. The most basic tradeoff affecting the design of non-tracking antennas for a moving target is the compromise between available gain and coverage. While the gain of a point to point communicating antenna can be ideally arbitrarily selected, the gain of an antenna for an area coverage is given by the (angular) area. Under ideal (sector beam) conditions, the available edge gain is $4\pi/\Omega$, where Ω is the angular beam cross-section. In practice, the edge gain is 3 - 5 db below this value, depending on the sophistication of the antenna design. The higher edge efficiency is associated with sector beam, low spillover efficiency, low internal loss type of desings, while the poorer edge efficiencies are associated with more conventional antennas. Unfortunately, the higher the edge efficiency is, the lower the antenna efficiency becomes and the cost of such antennas rapidly overcomes the cost of converting the non-tracking antenna into a tracking antenna and achieve similar effective gain improvement.

Assuming none or only a moderate amount of sector beaming (with antenna efficiencies of $-2 \sim -5$ db and that the cost of the antenna is proportional to $D^{2.7}$, where D is the equivalent diameter of the antenna, the relationship between cost (C) and coverage angle (Ω) is

$$C \propto G^{1.35} = \left(\frac{4\pi}{\Omega}\right)^{1.35} = \frac{30.4}{\Omega^{1.35}}$$

Thus, the cost of the antenna is decreasing quite rapidly with coverage angle. For instance, if the coverage angle is increased by 2, the above formula predicts a cost reduction to 39%, thus, if the cost of the switch and connecting waveguide is negligible, then the two switched small antennas can provide the same edge gain for 78% of the cost, than a single larger antenna.

5. The next important tradeoff characteristic is the aspect ratio of the beam cross-section. Generally, the positions of a practical synchronous satellite as it appears from an earth station represents a figure of 8, which can be enveloped conveniently by an elliptical beam cross-section. The more elongated the apparent satellite trajectory is the larger the ideal aspect ratio for the earth station antenna for maximum edge gain.

   Typically, the antenna complexity increases and its efficiency decreases with increasing aspect ratio. Both of these effects increase the cost of the antenna for a given edge gain. Thus, for a given trajectory, an optimum edge gain to cost ratio can be calculated and the corresponding optimum aspect ratio is not necessarily identical to the aspect ratio of the envelope ellipse which can be constructed to the trajectory. In fact, generally, the optimum edge gain to cost ratio requires an aspect ratio which is smaller than the aspect ratio of the envelope ellipse.

6. For the practical situations represented by the possible operational conditions of the CTS satellite, the following ranges of parameters are interesting:

Angular coverage:	$.46^\circ \times \begin{cases} 1.43^\circ \\ 2.2^\circ \end{cases}$	$\Omega = .66\ (\text{deg})^2 \sim 1.0\ (\text{deg})^2$
Edge gain:	36.5 db - 42.4 db	
Antenna area:	7 Ft.^2 - 33 Ft.^2	
Aspect ratio:	1.5 - 4.8	

Due to the relationship between edge gain and coverage, the above variables are not independent. Still they represent quite a wide range of possible requirements, suggesting distinctly different forms of realizations. For the purpose of easy characterization, one can distinguish among small, medium and large antenna apertures and small, medium and large aspect ratios.

7. Due to the limited scope of the present report, it was impossible to make an exhaustive study of all the interesting, practical realizations for all the above combinations. However, the following tabulation lists all the antenna categories recommended for covering the two motion boxes. Those categories left empty do not represent required types. Detailed explanation follows the table.

ASPECT RATIOS

ANTENNA APERTURE AREAS	Small (~ 2)	Medium (~ 3)	Large (4 - 5)
Small	a) Elliptically contoured offset fed paraboloid with a rectangular horn. b) Horn refl. or pillbox fed par. cylinder $A = 7.06$ Ft.^{2} $a = 22.6$ in., $b = 45.1$ in. $b/a = 2$ $G_{edge}/\eta = 36.6$db, $\eta = 55\%$ (MB2)	4,1 Covered by small aspect ratio	Array of folded horns, for instance, 4 horns with 15 in. apertures. $A = 6.25$ Ft.^{2} $a = 15$ in, $b = 60$ in. $b/a = 4$ $G_{edge}/\eta = 37.1$ db, $\eta = 55\%$ (MB2)
Medium	Ellipically contoured off-set fed paraboloid fed with rectangular horn. $A = 17.3$ Ft.^{2} $a = 35.3$ in., $b = 70.6$ in. $b/a = 2$ $G_{edge}/\eta = 40.3$ db, $\eta = 55\%$ (MB1)	#2 #5 Covered by small aspect ratio for MB_1 Covered by large aspect ratio for MB_2	a) Elliptically contoured paraboloid with 1 or 2(rectangular) horn feeds. b) 2 element circular paraboloid array fed by 1 rect. horn each. $A = 23.7$ Ft.^{2} $a = 26.6$ in, $b=128$ in. $G_{edge}/\eta = 41.0$ db, $\eta = 55\%$ (MB2)
Large	Requires tracking #3	a) Circular paraboloid fed by 2 or 3 horn arrays. b) Elliptical paraboloid fed by rect. horn or dual horn arrays. $A = 33.2$ Ft.^{2} $G_{edge}/\eta = 42.4$ db, $\eta = 55\%$ (MB1)	Not practical

The cases tabulated are those categories that were found suitable to provide the beam characteristics recommended for the low and high gain coverage of the two motion boxes (See Table 2.5). The edge gain values refer to simple feeds. The numbers refer to the types indicated in Table 2.5. Small aperture area antennas cover both MB's with small aspect ratios, thus the medium aspect ratio was not filled in. (The large aspect ratio, low gain case was listed as a matter of interest.). Medium aperture area antennas cover MB_1 with small aspect ratio, and MB_2 with large aspect ratio. Thus, the medium aspect ratio case is not significant in this case. Finally, large aperture area small aspect ratio antenna has low edge gain that may be achieved by medium size antennas, and large aperture area, large aspect ratio antennas are not practical from the point of cost, operational difficulties and because of the effective edge gain they would provide, may be achieved with medium aspect ratio.

For most of the above listed antennas, the components (reflectors, feed horns, orthocouplers, combining hybrids) are available standard components or require scaling only from other frequency bands. Thus, the construction of these antennas represents essentially a packaging - integration task and a detailed testing to obtain the finer details of their characteristics.

For small aspect ratios, the optimum antennas tend to have a single radiating source, low internal loss and relatively small tolerance problems.

For large aspect ratios, some departure from the conventional paraboloid may be desirable either in the form of placing multiple feed horns into the optical system, removing part of the circular paraboloid and turning it into an elliptically shaped aperture, feeding such an aperture by an arrayed feed or arraying circular or elliptically contoured paraboloids.

The conversion of circular paraboloid into an elliptically contoured one helps to achieve a better control on beam cross-section and cuts down the wind load on the antenna. However, such methods generally increase the spillover radiation and noise temperature, particularly for arrayed feeds. Furthermore, the smaller reflector area (for small and mediux gains) does not reduce the reflector cost drastically, since they require the same tooling and they may even be cut out of a circular spinning.

The arrayed type of systems for large aspect ratios have the inherent advantage, that their hybrid power divider network can be replaced at low cost by a switching network, thus providing a larger gain associated with the switched beam steering. Thus, these systems have a built in growth capability for cases where the added sophistication associated with the switch operating logic is justified.

8. Actual cost analysis was not covered by the main part of this report. However, cost estimates for various applicable quantities can easily be developed for any or all of the listed cases in the previous table.

For the calculation of the cost of reflectors, it may be mentioned that spinning tools resulting a nominal .012 in. rms accuracy can be obtained for $2,800., up to 5 ft. diameters and for $7,000., up to 10 ft. diameters. The cost of actual spinnings are quantity dependent, but assuming Qty. 10 and the above sizes typically cost $300. and $800. respectively for the above sizes. The cost of backframes for the above accuracy typically cost about 3 - 4 times more than the spinning. For the accuracies required, the assembly time is typically equal to the cost of components.

Using the above model, the production cost of a low gain small aspect ratio antenna may be calculated as follows. Since it is cut from a 6 ft. diameter dish, the spinning tool for a .012 in. rms accuracy is $7,000. The cost of each spinning is $400. on a quantity 10 basis. Cost of backframe - $1,500. Assembly - $1,500. Thus, the production cost on a quantity 10 basis would be $4,100. The feed for dual polarization requires 1 horn, 1 orthocoupler and connecting waveguides and supports. Assuming an average of $600. for each of these components and the cost of the necessary connecting waveguides and supports, the feed system for such an antenna can be produced for approximately $1,600. Thus, a typical production cost of such an antenna will be about $5,700. without the supporting pedestal and not counting design costs and mark-up factors. If we assume that a standard spun reflector may be used and the tooling cost eliminated, the cost will be $5,000.

Considering a standard line 6 ft. diameter fiber glass reflector, it will cost about $500. It requires a simpler backframe and shorter assembly time. The cost of such a reflector could be approximately $1,500 on a quantity 10 basis. The feed costs being equal, the antenna may cost basically $3,100. It appears that the fibre glass construction has a cost advantage. If a standard type reflector cannot be used the special tooling required may cost as much as $5,000 for diameters up to 5 ft. and as much as $15,000 for diameters of 12 ft. On a quantity 10 basis, this will add about $750 to the cost, which will then be $3,850. At least, one manufacturer indicated, however, about a 6 - 8 month delivery for such special units.

9. The study program collected some background information for the understanding of non-tracking antennas for "tracking" slightly moving satellites. However, according to the scope of the present program, most of the study was restricted to survey and theoretical calculations. It seems to be desirable to carry the investigation from this point a step further to produce actual designs for one or more sets of specifications and verify these designs by more detailed calculations and measurements on experimental models. Such a program could take about 3 months and would cost about $25,000. (at cost). The results of the program would verify calculations and would provide the detailed characteristics of the feed and the antenna and would generally deal with the practical aspects of the construction of a breadboard model of a 3 ft. equivalent diameter antenna with low aspect ratio and an about 6 ft. equivalent diameter antenna with high aspect ratio if the satellite motion box MB_2 is to be considered or with a medium aspect ratio if coverage of MB_1 only is required. After the completion of such an effort, the specifications for such antenna models can be finalized and their implications on the overall CTS system can be accurately evaluated.

REFERENCES

1. Verbal Communication by CRC on May 1, 1973.

2. A.F. Sciambi, "The Effect of the Aperture Illumination on the Circular Aperture Antenna Pattern Characteristics," The Microwave Journal, August 1965.

3. J.W. Duncan, "Maximum Off-Axis Gain of Pencil Beams", Proc. of IEEE, October 1969.

4. J.W. Duncan, "Maximum Off-Axis Gain of Elliptical Beams," Proc. IEEE, Vol. 120, No. 4, April 1973.

5. S. Silver, Ed."Microwave Antenna Theory and Design", Dover, N.Y., 1965

6. J.A. Stovman and D. McClintock, "Final Report - An Investigation of Antenna Tracking Methods Suitable for Use With the Remote Ground Terminals Associated with CTS Communications Experiments", prepared under Contract No. PL 36001-1-3296, Serial No. OPLI -0182, November 1972.

APPENDIX

Program Listings

The following computer programs have been developed for evaluating the performance of parabolic cylinders. A short summary of their function preceeds their source lists.

Program EFIELD

This program computes source equations of desired taper, the beam direction for equal tapering in the aperture, the field distribution in the aperture, the field patterns in the principal planes resulting from longitudinally and transversally polarized sources, the on-axis gain and the efficiency.

The system is a parabolic cylinder reflector with a line source either centre fed or off-set fed.

Program PARCYT

This program computes the field pattern and source taper in the transverse plane, the maximum gain and the efficiency of a parabolic cylinder reflector with a centre fed uniform line source.

Program CHEESE

This program computes the field distribution in the aperture plane, the field patterns in the principal planes resulting from longitudinally and transversally polarized sources, the on-axis gain and the efficiency.

The system is a cheese type antenna centre fed by a rectangular horn.

```
PROGRAM PARCYT(INPUT,OUTPUT)
* PARABOLIC CYLINDER,TRANSVERSALLY POLARIZED
DIMENSION G(100),RO(100),PSI(100),PSID(100)
DIMENSION GDB(100)
COMPLEX CJ,CON2,SUMPSI,A,E
*
FOD=.5
P=1.
ALAM=0.989*0.0254
AL=52.49*0.0254
R=1000.
D=10.97*0.0254
PO=20
PI=3.14159265
UPSI=2.* ATAN(1./(4.*FOD))
UPSID=UPSI*57.3
PRINT,UPSID
AK=2.* PI/ALAM
CJ=CMPLX(0.,1.)
CON1=(D/4.)*(1./TAN(UPSI/2.))
CON2=(376.7/(ALAM*R))*CEXP(-CJ*AK*R)*SQRT(P/(PI*AL*376.7))
SUMX=AL
A=CON2*SUMX
NPSI=61
ANPSI=FLOAT(NPSI)
*
DPSI=(2.*UPSI/ANPSI)
PSI(1)=-UPSI+DPSI/2.
PSID(1)=PSI(1)*57.3
NMAX=PO/2.
BB=1.
AN=2.
DO 111 NN=1,NMAX
BB=BB* AN/(AN-1.)
AN=AN+2.
111 CONTINUE
RO(1)=CON1*(1./(COS(PSI(1)/2.))**2)
G(1)=(COS(PSI(1)/2.))**PO
G(1)=BB* G(1)
GDB(1)=10.*ALOG10(G(1))
*
DO 50 I=2,NPSI
IM1=I-1
PSI(I)=PSI(IM1)+ DPSI
PSID(I)=PSI(I)*57.3
RO(I)=CON1*(1./(COS(PSI(I)/2.))**2)
G(I)=(COS(PSI(I)/2.))**PO
G(I)=BB*G(I)
GDB(I)=10.* ALOG10(G(I))
50 CONTINUE
*
```

```
DUTH=.4/57.3
UTH=-DUTH
JUT=0
100 UTH=UTH+ DUTH
UTHD=UTH*57.3
JUT=JUT+1
IF(UTHD.GT.9.2) GO TO 1000
*
SUMPSI=0.
JP=0
200 JP=JP+1
IF(JP.GT.NPSI) GO TO 300
SUMPSI=SUMPSI+ SQRT(RO(JP)*G(JP))*CEXP(-CJ*AK*RO(JP)*
+(1.+ COS(PSI(JP)-UTH)))*DPSI*(COS(UTH)+SIN(UTH)*TAN(PSI(JP)/2.))
GO TO 200
*
300 E=-CJ* A*SUMPSI
EMAG=CABS(E)
IF(JUT.EQ.1)EMAX=EMAG
EMAG=EMAG/EMAX
EMDB=20.*ALOG10(EMAG)
EPHD=57.3* ATAN2(AIMAG(E),REAL(E))
PRINT 9,UTHD,EMAG,EMDB,EPHD
9 FORMAT(5X,4F8.3)
GO TO 100
*
1000 CONTINUE
NNPSI=NPSI/2+1
IF((NNPSI/2)*2.EQ.NNPSI) NNPSI=NNPSI-1
DO 250 I=1,NNPSI,2
GG=G(I)/G(NNPSI)
GGDB=GDB(I)-GDB(NNPSI)
PRINT 10, PSID(I),RO(I),GG,GGDB
10 FORMAT(5X,4F8.3)
250 CONTINUE
* GAIN CALCULATION
PIN=0.
XIN=AL
JP=0
400 JP=JP+1
IF(JP.GT.NPSI) GO TO 500
PIN=PIN+SQRT(G(JP))*DPSI/COS(0.5*PSI(JP))
GO TO 400
500 GM=D*AL/TAN(0.5*UPSI)/2./ALAM**2*PIN**2*(XIN/AL)**2
GMD=10.* ALOG10(GM)
GO=(4.*PI*D* AL)/ALAM**2
GOD=10.* ALOG10(GO)
GFACT=GM/GO
PRINT 15, GM,GMD,GO,GOD,GFACT
15 FORMAT(1H0,1P5E12.4)
STOP
END
```

```
PROGRAM EFIELD(INPUT,OUTPUT)
EXTERNAL FYZ,FXZ,FG,GYZL,GYZT,GXZ
EXTERNAL COSM
COMPLEX FYZ,FXZ,FG,GYZL,GYZT,GXZ
COMPLEX QFYZ,QFXZ,QFG,QGYZL,QGYZT,QGXZ
EXTERNAL GYZTM,GYZLM
COMPLEX GYZLM,GYZTM,QGYZLM,QGYZTM
COMPLEX COSM,ANS
COMMON /CONS/ AL,D,AK,ANG,CPSIO,F,A,B,C,M,N
SCALE=12.*0.0254
RATIO=57.2958
AL=3.963327
AL=AL* SCALE
D=AL/5.
F=0.5* D
DAMLA=0.02511
CPSI=2.* ATAN(0.25*D/F)
AL2=AL/2.
AK=6.283185/DAMLA
CPSI1=0.
CPSI2=2.* ATAN(0.5*D/F+ TAN(0.5*CPSI1))
TPSI2=(TAN(CPSI2/2.))**2
TPSI1=(TAN(CPSI1/2.))**2
DANG=0.1/RATIO
ANG=0.
ANGD=0.
DBX=10.
DBPSI=10.
CALL ABC(DBX,DBPSI,0.5*(CPSI2-CPSI1),A,C,M)
N=1
CALL QG8(-AL2,AL2,COSM,ANS)
B=AL/CABS(ANS)
PRINT 12,A,B,C,M
12 FORMAT(6X,3 F8.3,I5)
11 FORMAT(6X,6F10.4)
IF(CPSI1+ CPSI2.NE.0.) GO TO 89
CPSIO=0.
PSIC=0.
GO TO 35
89 CONTINUE
AA=(COS(CPSI1/2.)/COS(CPSI2/2.))**(2./FLOAT(M))
YO=(AA* COS(CPSI1/2.)-COS(CPSI2/2.))/(SIN(CPSI2/2.)-AA*SIN(CPSI1/
+   2.))
CPSIO=2.*ATAN(YO)
TPSIC=(SQRT((1.+2./M)**2+8.*YO*YO/M)-(1.+2./M))/(4.*YO/M)
34 PSIC=ATAN(TPSIC)
DPSIC=PSIC*RATIO*2.
DCPSI=CPSI*RATIO
35 PRINT 11,DPSIC,DCPSI
DPSI=(CPSI2-CPSI1)/20.
PSI=CPSI1
REF=M*10.*ALOG10(COS(PSIC-CPSIO/2.))+20.*ALOG10(COS(PSIC))
DO 25 I=1,21
ATT=M*10.* ALOG10(COS((PSI-CPSIO)/2.))+20.*ALOG10(COS(PSI/2.))
ATT=ATT-REF
```

```
ATTO=M*10.*ALOG10(CCOS((PSI-CPSIO)*0.5))
YYY=2.* F* TAN(PSI/2.)
DDPSI=PSI*RATIO
PRINT 11,DDPSI,ATT,YYY,ATTO
25 PSI=PSI+DPSI
PRINT 11,AL,D,F,DAMLA
DCPSI1=CPSI1*RATIO
DCPSI2=CPSI2* RATIO
DCPSIO=CPSIO* RATIO
PRINT 11,DCPSI1,DCPSI2,DCPSIO
FK=2.* F/DAMLA
XK=2.* AL/DAMLA
N=1
CALL QG8(-AL2,AL2,FYZ,QFYZ)
TT2=TPSI2-TPSI1
TT1=SQRT(TPSI2)-SQRT(TPSI1)
K=1
KK=0
DO 10 I=1,91
IF(K.NE.1) GO TO 29
NP=ABS(FK*((1.-COS(ANG))*TT2-2.*SIN(ANG)*TT1))
NM=ABS(FK*((1.-COS(ANG))*TT2+2.*SIN(ANG)*TT1))
N=NP+1
CALL QG8(CPSI1,CPSI2,GYZL,QGYZL)
N=NM+1
CALL QG8(CPSI1,CPSI2,GYZLM,QGYZLM)
N=NP+1
CALL QG8(CPSI1,CPSI2,GYZT,QGYZT)
N=NM+1
CALL QG8(CPSI1,CPSI2,GYZTM,QGYZTM)
EYZL=CABS(QFYZ*QGYZL)
EYZLM=CABS(QFYZ*QGYZLM)
EYZT=CABS(QFYZ*QGYZT)
EYZTM=CABS(QFYZ*QGYZTM)
29 N=1.+ XK*SIN(ANG)
IF(KK.NE.0) GO TO 9
CALL QG8(-AL2,AL2,FXZ,QFXZ)
N=1.+ FK*(1.-COS(ANG))*TPSI2*2
CALL QG8(CPSI1,CPSI2,GXZ,QGXZ)
EXZ=CABS(QFXZ*QGXZ)
IF(I.NE.1) GO TO 9
YZLM=EYZL
YZTM=EYZT
XZM=EXZ
EYZL=0.
EYZT=0.
EXZ=0.
EYZLM=0.
EYZTM=0.
GO TO 19
9 IF(K.NE.1) GO TO 21
EYZL=20.* ALOG10(EYZL/YZLM)
EYZLM=20.* ALOG10(EYZLM/YZLM)
EYZT=20.* ALOG10(EYZT/YZTM)
EYZTM=20.* ALOG10(EYZTM/YZTM)
21 IF(KK.NE.0) GO TO 19
EXZ=20.* ALOG10(EXZ/XZM)
IF(K.EQ.1) GO TO 19
```

```
PRINT 11,ANGD,EXZ
GO TO 23
19 PRINT 11,ANGD,EXZ,EYZL,EYZLM,EYZT,EYZTM
23 ANG=ANG+ DANG
ANGD=ANGD+0.1
K=K+1
IF(K.EQ.6) K=1
IF(I.LT.51) GO TO 10
K=1
KK=1
ANG=ANG+4.* DANG
ANGD=ANGD+0.4
10 CONTINUE
N=1
CALL QG8(CPSI1,CPSI2,FG,QFG)
GCONS=CABS((QFYZ*QFG/AL)**2)/TAN(CPSI/2.)
GMAX=AL* D* GCONS/2./DAMLA/DAMLA
GEFF=GCONS/8./3.14159
GMAX=10.* ALOG10(GMAX)
PRINT 11,GMAX,GEFF
STOP
END
COMPLEX FUNCTION FYZ(X)
COMMON /CONS/ AL,D,AK,ANG,CPSIO,F,A,B,C,M,N
FYZ=(1.,0.)* SQRT(B*(COS(3.14159*X/A/AL))**M)
RETURN
END
COMPLEX FUNCTION FXZ(X)
COMMON /CONS/ AL,D,AK,ANG,CPSIO,F,A,B,C,M,N
COMPLEX FYZ
FXZ=FYZ(X)*CEXP((0.,1.)* AK*X*SIN(ANG))
RETURN
END
COMPLEX FUNCTION FG(PSI)
COMMON /CONS/ AL,D,AK,ANG,CPSIO,F,A,B,C,M,N
DPSI=(PSI-CPSIO)/2.
FG=(1.,0.)* SQRT(C*(COS(DPSI))** M)/COS(PSI/2.)
RETURN
END
COMPLEX FUNCTION GYZL(PSI)
COMMON /CONS/ AL,D,AK,ANG,CPSIO,F,A,B,C,M,N
COMPLEX FG
GYZL=CEXP((0.,-1.)*AK*F*(1.+COS(PSI+ANG))/(COS(PSI/2.))**2)
+    * FG(PSI)
RETURN
END
COMPLEX FUNCTION GYZT(PSI)
COMMON /CONS/ AL,D,AK,ANG,CPSIO,F,A,B,C,M,N
COMPLEX FG,GYZL
PSI2=PSI/2.
GYZT=GYZL(PSI)*COS(ANG+PSI2)/COS(PSI2)
RETURN
END
COMPLEX FUNCTION GXZ(PSI)
COMMON /CONS/ AL,D,AK,ANG,CPSIO,F,A,B,C,M,N
COMPLEX FG
GXZ=CEXP((0.,-1.)* AK*(1.+COS(ANG)*COS(PSI))/(COS(PSI/2.))**2)
+    * FG(PSI)
RETURN
END
```

```
SUBROUTINE QG(XL,XU,FCT,Y)
COMPLEX FCT,Y
A=0.5*(XL+XU)
B=XU-XL
C=0.4869533*B
Y=0.03333567*(FCT(A+C)+ FCT(A-C))
C=0.4325317*B
Y=Y+0.07472567*(FCT(A+C)+FCT(A-C))
C=0.3397048*B
Y=Y+0.1095432*(FCT(A+C)+FCT(A-C))
C=0.2166977*B
Y=Y+0.1346334*(FCT(A+C)+FCT(A-C))
C=0.0744371 7*B
Y=B*(Y+0.1477621*(FCT(A+C)+FCT(A-C)))
RETURN
END
COMPLEX FUNCTION GYZLM(PSI)
COMMON /CONS/ AL,D,AK,ANG,CPSIO,F,A,B,C,M,N
COMPLEX FG
GYZLM=CEXP((0.,-1.)*AK*F*(1.+COS(PSI-ANG))/(COS(PSI/2.))**2)
+   * FG(PSI)
RETURN
END
COMPLEX FUNCTION GYZTM(PSI)
COMMON /CONS/ AL,D,AK,ANG,CPSIO,F,A,B,C,M,N
COMPLEX FG,GYZLM
PSI2=PSI/2.
GYZTM=GYZLM(PSI)*COS(PSI2-ANG)/COS(PSI2)
RETURN
END
SUBROUTINE ABC(DBX,DBPSI,PSI,A,C,M)
M=-DBPSI/10./ALOG10(COS(PSI/2.))-2.+0.5
A=1.5708/ACOS(10.**(-DBX/10./M))
II=M/2
COSM=1.
AN=M
DO 10 I=1,II
COSM=COSM*(AN-1.)/AN
10 AN=AN-2.
IF(II*2.EQ.M) COSM=COSM*1.5708
C=1.5708/COSM
RETURN
END
SUBROUTINE QG8(XL,XU,FCT,Y)
COMPLEX FCT,Y,YY
COMMON /CONS/ AL,D,AK,ANG,CPSIO,F,A,B,C,MM,N
XD=(XU-XL)/N
XXL=XL
XXU=XXL+ XD
Y=(0.,0.)
DO 20 I=1,N
CALL QG(XXL,XXU,FCT,YY)
Y=Y+ YY
XXL=XXL+ XD
XXU=XXU+ XD
20 CONTINUE
RETURN
END
READY.
```

```
PROGRAM CHEESE(INPUT,OUTPUT)
EXTERNAL FYZ,FXZ,FG,GYZL,GYZT,GXZ
EXTERNAL COSM
COMPLEX FYZ,FXZ,FG,GYZL,GYZT,GXZ
COMPLEX QFYZ,QFXZ,QFG,QGYZL,QGYZT,QGXZ

COMPLEX COSM,ANS
COMMON /CONS/ AL,D,AK,ANG,CPSIO,F,A,B,C,M,N
SCALE=12.*0.0254
RATIO=57.2958
AL=0.792665
AL=AL* SCALE
D=5.* AL
F=0.25*D
DAMLA=0.02511
CPSI=2.* ATAN(0.25*D/F)
AL2=AL/2.
AK=6.283185/DAMLA
CPSI1=-CPSI
CPSI2=2.* ATAN(0.5*D/F+ TAN(0.5*CPSI1))
TPSI2=(TAN(CPSI2/2.))**2
TPSI1=(TAN(CPSI1/2.))**2
DANG=0.1/RATIO
ANG=0.
ANGD=0.
DBX=15.
DBPSI=15.
CALL ABC(DBX,DBPSI,0.5*(CPSI2-CPSI1),A,C,M)
N=1
CALL QGS(-AL2,AL2,COSM,ANS)
B=AL/CABS(ANS)

PRINT 12,A,B,C,M
12 FORMAT(6X,3 F8.3,I5)
11 FORMAT(3F9.3)
33 FORMAT(F9.3,6X,2F9.3)
IF(CPSI1+ CPSI2.NE.0.) GO TO 89
CPSIO=0.
PSIC=0.
GO TO 35
89 CONTINUE
AA=(COS(CPSI1/2.)/COS(CPSI2/2.))**(2./FLOAT(M))
YO=(AA*COS(CPSI1/2.)-COS(CPSI2/2.))/(SIN(CPSI2/2.)-AA*SIN(CPSI1/
+   2.))
CPSIO=2.*ATAN(YO)
TPSIC=(SQRT((1.+2./M)**2+8.*YO*YO/M)-(1.+2./M))/(4.*YO/M)
34 PSIC=ATAN(TPSIC)
DPSIC=PSIC*RATIO
DCPSI=CPSI*RATIO
35 PRINT 11,DPSIC,DCPSI
DPSI=(CPSI2-CPSI1)/20.
PSI=CPSI1
REF=M*10.* ALOG10(COS(PSIC-CPSIO/2.))+20.*ALOG10(COS(PSIC))
```

```
DO 25 I=1,21
ATT=M*10.* ALOG10(COS((PSI-CPSIO)/2.))+20.*ALOG10(COS(PSI/2.))
ATT=ATT-REF
ATTO=M*10.* ALOG10(CCOS((PSI-CPSIO)*0.5))
YYY=F* TAN(PSI/2.)*2.
DDPSI=PSI* RATIO
PRINT 11,DDPSI,ATT,YYY,ATTO
25 PSI=PSI+DPSI
PRINT 11,AL,D,F,DAMLA
DCPSI1=CPSI1*RATIO
DCPSI2=CPSI2*RATIO
DCPSIO=CPSIO* RATIO
PRINT 11,DCPSI1,DCPSI2,DCPSIO
FK=2.* F/DAMLA
XK=2.* AL/DAMLA
N=1
CALL QG8(-AL2,AL2,FYZ,QFYZ)
TT2=TPSI2-TPSI1
TT1=SQRT(TPSI2)-SQRT(TPSI1)
K=1
KK=0
U=3.14159* AL/DAMLA
DO 10 I=1,81
IF(KK.EQ.1) GO TO 29
NP=ABS(FK*((1.-COS(ANG))*TT2-2.*SIN(ANG)*TT1))
N=NP+1
CALL QG8(CPSI1,CPSI2,GYZL,QGYZL)
CALL QG8(CPSI1,CPSI2,GYZT,QGYZT)
EYZL=CABS(QGYZL)
EYZT=CABS(QGYZT)
IF(K.NE.1) GO TO 9
29 N=1.+ XK*SIN(ANG)
CALL QG8(-AL2,AL2,FXZ,QFXZ)
N=1.+ FK*(1.-COS(ANG))*TPSI2*2
CALL QG8(CPSI1,CPSI2,GXZ,QGXZ)
EXZ=CABS(QFXZ*QGXZ)
IF(I.EQ.1) EXZL=AL*CABS(QGXZ)
IF(I.NE.1) EXZL=AL*CABS(QGXZ)*SIN(U*SIN(ANG))/SIN(ANG)/U
EXZL=ABS(EXZL)
IF(I.NE.1) GO TO 9
YZLM=EYZL
YZTM=EYZT
XZM=EXZ
XZLM=EXZL
EYZL=0.
EYZT=0.
EXZ=0.
EXZL=0.
GO TO 10
9 CONTINUE
IF(KK.EQ.1) GO TO 21
EYZL=20.*ALOG10(EYZL/YZLM)
EYZT=20.*ALOG10(EYZT/YZTM)
21 IF(K.NE.1) GO TO 39
EXZ=20.*ALOG10(EXZ/XZM)
EXZL=20.*ALOG10(EXZL/XZLM)
39 CONTINUE
```

```
      IF(KK.EQ.1) GO TO 78
      IF(K.EQ.1) GO TO 19
      PRINT 11, ANGD,FYZL,FYZT
      GO TO 23
   19 PRINT 11,ANGD,FYZL,EYZT,EXZL,FXZ
   23 ANG=ANG+DANG
      ANGD=ANGD+Ø.1
      K=K+1
      IF(K.EQ.6) K=1
      IF(I.LT.51) GO TO 10
      K=1
      KK=1
      ANG=ANG+4.*DANG
      ANGD=ANGD+Ø.4
      GO TO 1Ø
   78 PRINT 33,ANGD,EXZL,EXZ
      ANG=ANG+5.* DANG
      ANGD=ANGD+Ø.5
   1Ø CONTINUE
      N=1
      CALL QG8(CPSI1,CPSI2,FG,QFG)
      GCONS=CABS((QFYZ*QFG/AL)**2)/TAN(CPSI/2.)
      GMAX=AL*D*GCONS/2./DAMLA/DAMLA
      GEFF=GCONS/8./3.14159
      DIFF=(ABS(QFYZ)/AL)**2
      GMAX1=GMAX/DIFF
      GMAX=1Ø.* ALOG1Ø(GMAX)
      GEFF1=GEFF/DIFF
      GMAX1=1Ø.* ALOG1Ø(GMAX1)
      PRINT 11,GMAX,GEFF,GMAX1,GEFF1
      STOP
      END
      COMPLEX FUNCTION FYZ(X)
      COMMON /CONS/ AL,D,AK,ANG,CPSIO,F,A,B,C,M,N
      FYZ=(1.414,Ø.)*COS(3.14159*X/AL)
      RETURN
      END
      COMPLEX FUNCTION FXZ(X)
      COMMON /CONS/ AL,D,AK ANG,CPSIO,F,A,B,C,M,N
      COMPLEX FYZ
      FXZ=FYZ(X)*CEXP((Ø.,1.)*AK*X*SIN(ANG))
      RETURN
      END
      COMPLEX FUNCTION FG(PSI)
      COMMON /CONS/ AL,D,AK,ANG,CPSIO,F,A,B,C,M,N
      DPSI=(PSI-CPSIO)/2.
      FG=(1.,Ø.)*SQRT(C*(COS(DPSI))**M)/COS(PSI/2.)
      RETURN
      END
      COMPLEX FUNCTION GYZL(PSI)
      COMMON /CONS/ AL,D,AK,ANG,CPSIO,F,A,B,C,M,N
      COMPLEX FG
      GYZL=CEXP((Ø.,-1.)*AK*F*(1.+COS(PSI+ANG))/(COS(PSI/2.))**2)
     +     * FG(PSI)
      RETURN
      END
      COMPLEX FUNCTION GYZT(PSI)
      COMMON /CONS/ AL,D,AK ANG,CPSIO,F,A,B,C,M,N
      COMPLEX FG,GYZL
```

```
      PSI2=PSI/2.
      GYZT=GYZL(PSI)*COS(ANG+PSI2)/COS(PSI2)
      RETURN
      END
      COMPLEX FUNCTION GXZ(PSI)
      COMMON /CONS/ AL,D,AK,ANG,CPSIO,F,A,B,C,M,N
      COMPLEX FG
      GXZ=CEXP((0.,-1.)*AK*(1.+COS(ANG)*COS(PSI))/(COS(PSI/2.))**2)
     +  * FG(PSI)
      RETURN
      END
      SUBROUTINE QG(XL,XU,FCT,Y)
      COMPLEX FCT,Y
      A=0.5*(XL+XU)
      B=XU-XL
      C=0.4869533*B
      Y=0.03333567*(FCT(A+C)+FCT(A-C))
      C=0.4325317*B
      Y=Y+0.07472567*(FCT(A+C)+FCT(A-C))
      C=0.3397048*B
      Y=Y+0.1095432*(FCT(A+C)+ FCT(A-C))
      C=0.2166977*B
      Y=Y+0.1346334*(FCT(A+C)+ FCT(A-C))
      C=0.07443717*B
      Y=B*(Y+0.1477621*(FCT(A+C)+FCT(A-C)))
      RETURN
      END
      COMPLEX FUNCTION COSM(X)
      COMMON /CONS/ AL,D,AK,ANG,CPSIO,F,A,B,C,M,N
      COSM=(COS(3.14159*X/A/AL))**M
      RETURN
      END
      SUBROUTINE ABC(DBX,DBPSI,PSI,A,C,M)
      M=-DBPSI/10./ALOG10(COS(PSI/2.))-2.+0.5
      A=1.5708/ACOS(10.**(-DBX/10./M))
      II=M/2
      COSM=1.
      AN=M
      DO 10 I=1,II
      COSM=COSM*(AN-1.)/AN
   10 AN=AN-2.
      IF(II*2.EQ.M) COSM=COSM*1.5708
      C=1.5708/COSM
      RETURN
      END
      SUBROUTINE QG8(XL,XU,FCT,Y)
      COMPLEX FCT,Y,YY
      COMMON /CONS/ AL,D,AK,ANG,CPSIO,F,A,B,C,MN,N
      XD=(XU-XL)/N
      XXL=XL
      XXU=XXL+XD
      Y=(0.,0.)
      DO 20 I=1,N
      CALL QG(XXL,XXU,FCT,YY)
      Y=Y+YY
      XXL=XXL+XD
      XXU=XXU+XD
   20 CONTINUE
      RETURN
      END
```